

# Microbial symbionts buffer hosts from the demographic costs of environmental stochasticity

Joshua C. Fowler<sup>1,2\*</sup>, Shaun Ziegler<sup>3</sup>, Kenneth D. Whitney<sup>3</sup>,  
Jennifer A. Rudgers<sup>3</sup>, Tom E.X. Miller<sup>1</sup>

<sup>1</sup>\*Department of BioSciences, Rice University, Houston, 77005, TX, USA.

<sup>2</sup>Department of Biology, University of Miami, Miami, 33146, FL, USA.

<sup>3</sup>Department of Biology, University of New Mexico, Albuquerque, 87131, NM, USA.

\*Corresponding author(s). E-mail(s): [jcf221@miami.edu](mailto:jcf221@miami.edu);

Contributing authors: [shaun.ziegler@gmail.com](mailto:shaun.ziegler@gmail.com); [whitneyk@unm.edu](mailto:whitneyk@unm.edu);

[jrudgers@unm.edu](mailto:jrudgers@unm.edu); [tom.miller@rice.edu](mailto:tom.miller@rice.edu);

Phone: 719-359-2960

## Author Contributions

J.C.F. contributed to data collection, data analysis, and led manuscript drafting. S.Z. contributed to data collection and manuscript revisions. K.D.W. contributed to research conception, data collection, and manuscript revisions. J.A.R. established transplant plots, contributed to research conception, data collection, and manuscript revisions. T.E.X.M. contributed to research conception, data collection, data analysis, and manuscript revisions.

## Data and Code Accessibility

Data will be made accessible as an Environmental Data Initiative package online  
**DOI:** [updated here when available](#). Code for all analysis is available through  
<https://github.com/joshuacfowler/Grass-Endophyte-Stochastic-Demography>

**Article Type:** Letter

**Running Title:** Symbiont-mediated demographic buffering

**Keywords:** stochastic demography, plant-microbe interactions, environmental variability, symbiosis, mutualism, long-term data, life history, Epichloë, Poaceae

**This file contains:** Abstract ( 150 words), Main Text (5397 words), Figures (1-4); Supporting Information - Supplemental Methods, Supplemental Figures A1-A28, Supplemental Tables S1-S3, References (66)

047

**Abstract**

048

Species' persistence in increasingly variable climates will depend on resilience  
049 against the fitness costs of environmental stochasticity. Most organisms host  
050 microbiota that shield against stressors. Here, we test the hypothesis that, by  
051 limiting exposure to environmental extremes, microbial symbionts reduce hosts'  
052 demographic variance. We parameterized stochastic models using data from a  
053 14-year symbiont-removal experiment including seven grass species that host  
054 *Epichloë* fungal endophytes. Endophytes reduced variance in fitness by > 10%, on  
055 average. Hosts with "fast" life history traits that lacked longevity as an intrinsic  
056 buffer benefited most from symbiont-mediated variance buffering. Under current  
057 climate conditions, contributions of variance buffering were modest compared to  
058 symbiont benefits to mean fitness. However, simulations of increased stochasticity  
059 amplified benefits of variance buffering and made it the more important pathway  
060 of host-symbiont mutualism than elevated mean fitness. Microbial-mediated  
061 variance buffering is likely an important, yet cryptic, mechanism of resilience in  
062 an increasingly variable world.

063

064

065

066

067

068

069

070

071

072

073

074

075

076

077

078

079

080

081

082

083

084

085

086

087

088

089

090

091

092

<b>Introduction</b>	093
Global climate change involves heterogenous changes in environmental variability, including increases in frequency of extreme weather events and in frequency of “whiplash events” that alternate between climate extremes [1–3]. <sup>1</sup> Yet, the ecological consequences of changing variability are less well understood than those of changing climate means, such as long-term warming or drying. Incorporating environmental variability into forecasts of population dynamics can improve predictions of the future [4].	094
Classic theory predicts that long-term population growth rates (equivalently, population mean fitness) will decline under increased environmental stochasticity because the costs of bad years outweigh the benefits of good years – a consequence of nonlinear averaging [5, 6]. For example, in unstructured populations, the long-term stochastic growth rate in a fluctuating environment ( $\lambda_s$ ) will always be lower than the arithmetic mean growth rate ( $\bar{\lambda}$ ) by an amount proportional to the environmental variance ( $\sigma^2$ ):	095
$\log(\lambda_s) \approx \log(\bar{\lambda}) - \frac{\sigma^2}{2\bar{\lambda}^2}$	(1)
Populations structured by size or stage similarly experience costs of temporal variability [7, 8]. There are accordingly two pathways to increase population viability in a variable environment: increase the arithmetic mean growth rate and/or dampen temporal fluctuation in growth rates, also called “demographic buffering”.	100
Both inherent characteristics of species and properties of the environments they experience can buffer demographic fluctuations. Inherent characteristics include life history traits [9], trade-offs among vital rates [10], and transient shifts in population structure [11]. For example, theory predicts that long-lived species, those on the slow end of the slow-fast life history continuum, will be less sensitive to environmental variability than short-lived species [12], a pattern which has empirical support across plants [13, 14] and animals [15, 16]. Demographic variance is also determined by external abiotic factors, such as the magnitude of environmental variability [17] or the degree of environmental autocorrelation [18, 19]. The complex interplay of these factors determines the risks of extinction faced by populations [20] and underlies management strategies promoting ecosystem resilience [21]. Yet, little is known about how inter-specific interactions influence demographic variability or contribute to demographic buffering [22].	101
Most multicellular organisms host symbiotic microbes that affect growth and performance [25, 26], and many of these are vertically transmitted from maternal hosts to offspring [27]. Vertical transmission links the fitness of hosts and symbionts in a feedback loop that selects for mutual benefits [28]. Many vertically-transmitted microbes are mutualistic and protect hosts from stressful environmental conditions including drought, extreme temperatures, or natural enemies [29, 30]. Some of the best studied examples include bacterial symbionts of insects that provide their hosts with thermal tolerance through the production of heat-shock proteins [31], and fungal symbionts of	102
<hr/>	103
<sup>1</sup> Add citation – <a href="https://www.nature.com/articles/s41558-018-0140-y">https://www.nature.com/articles/s41558-018-0140-y</a>	104
	105
	106
	107
	108
	109
	110
	111
	112
	113
	114
	115
	116
	117
	118
	119
	120
	121
	122
	123
	124
	125
	126
	127
	128
	129
	130
	131
	132
	133
	134
	135
	136
	137
	138

139 plants that produce anti-herbivore and drought-protective compounds [32–34]. How-  
140 ever, these diverse protective symbioses are context-dependent: the magnitude of  
141 benefits depends on environmental conditions [35, 36] and thus will vary temporally  
142 in a stochastic environment [37]. We hypothesized that context-dependent benefits  
143 from symbionts may buffer hosts against variability through strong benefits during  
144 harsh periods and neutral or even costly outcomes during benign periods, reducing  
145 the impacts of host exposure to extremes and dampening inter-annual variance rela-  
146 tive to non-symbiotic hosts (Fig. ??<sup>2</sup>). Variance buffering is a previously unexplored  
147 mechanism by which symbionts may benefit their hosts instead of or in addition to  
148 elevating average fitness (Fig. ??<sup>3</sup>), the focus of most previous research.

149 To test the hypothesis that context-dependent benefits of symbiosis buffer hosts  
150 from the fitness costs of temporal environmental stochasticity, we used a combination  
151 of long-term field experiments and stochastic demographic modeling. We used cool-  
152 season grasses and *Epichloë* fungal endophytes as a tractable experimental model in  
153 which non-symbiotic plants can be derived from naturally symbiotic plants through  
154 heat treatment, providing a contrast of symbiont effects that controls for the con-  
155 founding influence of host genetic background. *Epichloë* endophytes are specialized  
156 symbionts growing intercellularly in the aboveground tissue of ~ 30% of *C<sub>3</sub>* grass  
157 species [38]. These fungi are primarily transmitted vertically from maternal plants  
158 through seeds [39]. They produce a variety of alkaloids that can protect host plants  
159 from natural enemies [40] and drought stress [41].

160 Over 14 years (2007–2021), we collected longitudinal demographic data on the  
161 survival, growth, reproduction, and recruitment of all plants within replicated  
162 endophyte-symbiotic and endophyte-free populations at our field site in southern Indi-  
163 ana, USA. Through taxonomic replication (seven host-symbiont species pairs) we  
164 aimed to understand whether host life history traits could explain inter-specific vari-  
165 ation in the magnitude of demographic buffering through symbiosis. We used this  
166 long-term data to parameterize stochastic population projection models in a hierar-  
167 chical Bayesian framework. Specifically, we (1) quantified the effect of symbiosis on  
168 the mean and variance of host vital rates (survival, growth and reproduction) and fit-  
169 ness, (2) evaluated the relationship between host life history traits and the magnitude  
170 of symbiont-mediated variance buffering, (3) determined the relative contributions of  
171 symbiont-mediated mean and variance effects to host fitness, and (4) projected how  
172 increased environmental stochasticity (expected under future climates) changes the  
173 importance of variance buffering as a pathway of host-symbiont mutualism.

## 174 175 Materials and Methods

### 176 177 Study site and species

178 This study was conducted at Indiana University’s Lilly-Dickey Woods Research and  
179 Teaching Preserve (39.238533, -86.218150) in Brown County, Indiana, USA. This site  
180 is part of the Eastern broadleaf forests of southern Indiana, where the ranges of many  
181 understory cool-season grass species overlap. The experiment focused on seven of these

183  
184 <sup>2</sup>Reference new figure  
<sup>3</sup>Reference new figure

grasses (*Agrostis perennans*, *Elymus villosus*, *Elymus virginicus*, *Festuca subverticillata*, *Lolium arundinaceum*, *Poa alsodes*, and *Poa sylvestris*), each of which hosts a unique species of *Epichloë* endophyte (Table S1). All are native to eastern North America except the Eurasian species *L. arundinaceum*. 185  
186  
187  
188  
189  
190

## Endophyte removal, plant propagation, and field set-up

Seeds from naturally symbiotic populations of the seven focal host species were collected during summer-fall 2006 from Lilly-Dickey Woods and the nearby Bayles Road Teaching and Research Preserve (39.220167, -86.542683). To generate symbiotic (S+) and symbiont-free (S-) plants from the same genetic lineages, seeds from each species were disinfected with a heat treatment described in Table S1 or left untreated. The heat treatment created symbiont-free plants by warming seeds to temperatures at which the fungus becomes inviable but the host seeds can still germinate. Both heat-treated and untreated seeds were surface sterilized with bleach to remove epiphyllous microbes, cold stratified for up to 4 weeks, then germinated in a growth chamber before transfer to the greenhouse at Indiana University where they grew for ~ 8 weeks. We confirmed endophyte status by staining thin sections of inner leaf sheath with aniline blue and examining tissue for fungal hyphae at 200X magnification [42]. We established experimental populations with vegetatively propagated clones of similar sizes (ranging from one to six tillers). By starting the experiment with plants of similar sizes and the same number of unique genotypes, we aimed to limit any potential effects of heat treatments on initial plant growth [43].<sup>4</sup> 191  
192  
193  
194  
195  
196  
197  
198  
199  
200  
201  
202  
203  
204  
205  
206  
207  
208  
209  
210  
211  
212  
213  
214  
215  
216  
217  
218  
219  
220  
221  
222  
223  
224  
225  
226  
227  
228  
229  
230

## Long-term demographic data collection

Each summer (2008–2021) we censused all individuals in each plot for survival, growth and reproduction, and added new recruits to the census. Plots contained 13.3 individuals/m<sup>2</sup> on average over the course of the experiment. Each census year was a sample of inter-annual climatic variation (n = 14 years, comprising 13 demographic transition years). We censused each species during its peak fruiting stage (May: *Poa alsodes*, *Poa sylvestris*; June: *Festuca subverticillata*; July: *Elymus villosus*, *Elymus virginicus*, *Lolium arundinaceum*; September: *Agrostis perennans*), such that the censuses were pre-breeding and new recruits came from the previous years' seed production<sup>5</sup>. Leaf litter was cleared out of each plot prior to the census, to aid in locating plants. For each plant remaining from the previous year, we determined survival, measured its size as a count of tillers, and collected reproductive data as counts of reproductive

---

<sup>4</sup>I don't remember if this was always here but it actually makes no sense to me, and I think (?) a reviewer said something similar. I think nothing is lost if we cut this sentence.

<sup>5</sup>Could reference life cycle figure here.

231 tillers and seed-bearing spikelets on all reproductive tillers to a maximum of three. We  
232 also tagged all unmarked individuals that were recruits from the previous years' seed  
233 production and collected the same demographic data. New recruits typically had one  
234 tiller and were non-reproductive. In 2008 through 2010, we took additional counts of  
235 seeds per inflorescence for all reproducing individuals in the plots to relate inflorescence  
236 and spikelet counts to seed production. In 2018, we stopped collecting data for the  
237 exotic *L. arundinaceum*, which had very high survival and low recruitment, and conse-  
238 quently very low variation across years. In total across 14 years, the dataset included  
239 demographic information for 16,789 individual host-plants and 31,216 transition-year  
240 observations.

241 We expected plots to maintain their endophyte status (S+ or S-) because these  
242 fungal symbionts are almost exclusively vertically transmitted, and plots were spaced  
243 a minimum of 5 m apart, limiting seed dispersal or horizontal transmission of the  
244 symbiont between plots. We regularly confirmed endophyte treatment throughout the  
245 lifetime of the experiment by opportunistically taking subsets of seeds from repro-  
246 ductive individuals and scoring them for their endophyte status with microscopy as  
247 above. Overall, these scores reflected 98% faithfulness of recruits to their expected  
248 endophyte status across species and plots (Fig. S23; Supplement data). Additionally,  
249 we have rarely observed fungal stromata, the fruiting bodies by which *Epichloë* are  
250 potentially transmitted horizontally, provided the fly vector is also present [44]. For  
251 *A. perennans*, *F. subverticillata*, *L. arundinaceum*, and *P. alsodes*, we never observed  
252 stromata. We observed stromata only infrequently for *E. villosus*, and even more rarely  
253 for *E. virginicus* and *P. sylvestris* (Table S2). For these species, stromata have only  
254 been observed irregularly across years on 35, 4, and 6 plants respectively, making up  
255 < 0.3% of all censused plants.

256

## 257 **Vital rate modeling**

258 Equipped with these demographic data, we fit statistical models for adult survival,  
259 seedling survival, adult growth, seedling growth, reproductive status (flowering or  
260 vegetative), fertility of flowering plants (number of inflorescences), production of seed-  
261 bearing spikelets (number per inflorescence), the average number of seeds per spikelet,  
262 and the recruitment of seedlings from the preceding year's seed production. We fit these  
263 vital rates as generalized linear mixed models in a hierarchical Bayesian framework  
264 using RStan [45] which allowed us to isolate endophyte effects on vital rate means and  
265 variances, borrow strength across species for some variance components, and propagate  
266 uncertainty from the individual-level vital rates to population projection models [46].  
267 Each size-structured vital rate model included year effects specific to each species and  
268 endophyte status as well as random plot variance shared across species. All models  
269 included the same linear predictor, including two key parameters for each species: one  
270 which described the effect of endophyte symbiosis on the mean of that vital rate, and  
271 another which described the inter-annual variance in the vital rate for symbiotic and  
272 symbiont-free plants. The species- and endophyte status-specific random year effects  
273 allowed us to quantify the effect of endophytes on inter-annual variance for each vital  
274 rate. Other parameters accounted for size structure in the data (defined as the number  
275 of tillers) as well as the difference between originally transplanted plants (raised in a  
276

greenhouse) and those which recruited naturally into the plots. Preliminary analyses indicated similar model fits between models including linear and quadratic terms, and so we proceeded with only linear effects. Full details of the vital rate modeling are included in the *Supporting Information Supplemental Methods*. All parameters were given vague priors [47]. We ran each vital rate model for 2500 warm-up and 2500 MCMC sampling iterations with three chains. We assessed model convergence with trace plots of posterior chains and checked for  $\hat{R}$  values less than 1.01, indicating low within- and between-chain variation [48, 49]. For those models that showed poor convergence, we extended the MCMC sampling to include 5000 warm-up and 5000 sampling iterations, which was only necessary for seedling growth. We graphically checked vital rate model fit with posterior predictive checks comparing simulated and observed data (Fig. S29-S39).

## Stochastic population model

We parameterized a stochastic matrix projection model for each host species using the fitted statistical vital rate models. Each matrix projection model included two state variables:  $r_t$  (the number of newly recruited individuals in year  $t$  which we assume to be non-reproductive), and  $\mathbf{n}_t$  (a vector including all non-seedling individuals of sizes  $x \in \{1, 2, \dots, U\}$  ranging from one to the maximum number of tillers  $U$ ). We use these two state variables to avoid having to assume demographic equivalence between seedling and non-seedling one-tiller plants. We used the same model structure, corresponding to a pre-breeding census, for each species and endophyte status (not shown in model notation for readability). See Fig. S21 for a generalized life cycle graph.

The number of recruits in year  $t + 1$  is given by:

$$r_{t+1} = \sum_{x=1}^U P(x; \boldsymbol{\tau}_P) F(x; \boldsymbol{\tau}_F) K(x; \boldsymbol{\tau}_K) DR(\boldsymbol{\tau}_R) n_t^x \quad (2)$$

The total number of seeds produced by a maternal plant of size  $x$  is the product of the size-specific probability of flowering  $P$ , the number of inflorescences conditional on flowering  $F$ , the number of spikelets per inflorescence  $K$ , and the number of seeds per spikelet  $D$ . Multiplying by the probability of transitioning from seed to seedling  $R$  gives a per-capita rate of seedling production, which is multiplied by the number of plants of size  $x$  ( $n_t^x$ , the  $x^{\text{th}}$  element of  $\mathbf{n}_t$ ) and summed over all sizes. Each function also depends on the species- and endophyte-specific year random effects for that vital rate ( $\boldsymbol{\tau}$ , a vector of year-specific values derived from the statistical models).

The number of  $y$ -sized plants in year  $t + 1$  is given by:

$$n_{t+1}^y = Z(y; \boldsymbol{\tau}_Z) B(\boldsymbol{\tau}_B) r_t + \sum_{x=1}^U S(x; \boldsymbol{\tau}_S) G(x, y; \boldsymbol{\tau}_G) n_t^x \quad (3)$$

where  $n_{t+1}^y$  is the  $y^{\text{th}}$  element of vector  $\mathbf{n}_{t+1}$ . The first term on the right hand side of Eqn. 3 represents growth ( $Z$ ) and survival ( $B$ ) of seedling recruits. The second term includes the survival of previously  $x$ -sized plants and the growth of survivors from size  $x$  to  $y$ , summed over all  $x$ . To avoid predictions of unrealistic growth outside of the

323 observed size distribution, we set a ceiling on the growth function for plants at the  
324 97.5<sup>th</sup> percentile of observed sizes for each host species [50].

325 Each of the vital rate functions in Eqns. 2 and 3 have separate intercepts and year  
326 random effects for symbiotic and symbiont-free populations, allowing us to calculate  
327 the effect of endophyte symbiosis on the mean, variance, and coefficient of variation  
328 (CV) of  $\lambda$ , the dominant eigenvalue of the year- and endophyte-specific projection  
329 matrix. This model treats climate drivers implicitly through year-specific random  
330 effects. We also developed a climate-explicit version with the addition of parameters  
331 defining the relationship between either annual or growing season drought index and  
332 each vital rate. A full description of climate-explicit methods can be found in the  
333 *Supporting Information Supplemental Methods*.

334 To calculate stochastic population growth rates ( $\lambda_s$ ) for each host species and endo-  
335 phyte status we simulated population dynamics for 1000 years by randomly sampling  
336 from the 13 annual transition matrices, discarding the first 100 years to minimize the  
337 influence of initial conditions. Sampling observed transition matrices (rather than inde-  
338 pendently sampling regression coefficients) produces models that realistically capture  
339 inter-annual variation by preserving correlations between vital rates [56]. We tallied  
340 the total population size at each time step as  $N_t = r_t + \sum_{x=1}^U n_t^x$  and calculated the  
341 stochastic growth rate as  $\log(\lambda_s) = E[\log(\frac{N_t}{N_{t+1}})]$  [57, 58]. We calculated the total  
342 effect of endophyte symbiosis as the difference in  $\lambda_s$  between S+ and S- populations.  
343 We propagated uncertainty from the vital rate models to the calculation of  $\lambda_s$  using  
344 500 draws from the posterior distribution of model parameters.

345

## 346 Life History Analysis

347

348 We collected metrics describing each host species' life history to test the relationship  
349 between pace of life and variance buffering (Table S2). Using the Rage package [51],  
350 we calculated  $R_0$ , longevity, generation time, Keyfitz entropy, and Demetrius entropy  
351 from the mean transition matrix for symbiont-free populations.<sup>6</sup> We recorded seed size  
352 as the average lemma length from the Flora of North America [52]. We also calculated  
353 the 99th percentile of maximum observed age for symbiont-free plants from the census  
354 data for each species. Next, we fit Bayesian phylogenetic mixed-effects models using  
355 the brms package [53] to test the relationship between each life history trait and the  
356 effect of symbiosis on the CV of  $\lambda$  (a measure of variance buffering) while controlling  
357 for phylogenetic non-independence between host and symbiont species. We pruned  
358 species-level phylogenies of plants [54] and *Epichloë* fungi [55] to include the focal  
359 species. *Agrostis perennans* was not included in the tree, and so we used the congener  
360 *A. hyemalis*. We defined separate phylogenetic covariance matrices for each pruned  
361 tree. We propagated uncertainty in the estimated variance buffering effect  $V$  with a  
362 measurement error model:

363

364

365  $V_{MEAN,h} \sim Normal(V_{EST,h}, V_{SD,h})$  (4a)

366

---

367 <sup>6</sup>I think a brief description of each of these is necessary, especially the two entropies, which most readers  
368 will not have seen before.

$V_{EST,h} \sim Normal(\mu_h, \sigma)$	(4b)	369
$\mu = \alpha + \beta * trait + \pi_j$	(4c)	370
$\alpha \sim Normal(0, .5)$	(4d)	371
$\beta \sim Normal(0, .1)$	(4e)	372
$\sigma \sim Half - Normal(.04, .01)$	(4f)	373
$\pi_h \sim MVN(0, \sigma_\pi \mathbf{A})$	(4g)	374
$\sigma_\pi \sim Half - Normal(0, .1)$	(4h)	375
		376
		377
		378
		379
		380
		381
		382
		383
		384
		385
		386
		387
		388
		389
		390
		391
		392

Here,  $V_{EST}$  is the variance buffering effect for host species  $h$ , estimated from the posterior mean ( $V_{MEAN}$ ) and standard deviation ( $V_{SD}$ ), propagating uncertainty associated with the effect of symbiosis. The model includes an intercept ( $\alpha$ ) and a slope ( $\beta$ ) defining the relationship between the variance buffering effect and the life history trait. The residual standard deviation is given by ( $\sigma$ ). We used weakly informative priors to aid model convergence. Each prior was centered at zero, except for the residual standard deviation, which we centered at the standard deviation of the estimated variance buffering effect, .04. The phylogenetic random effect ( $\pi$ ), which is modeled as a multivariate normal distribution, has a between-species standard deviation ( $\sigma_\pi$ ) structured by the phylogenetic covariance matrix  $\mathbf{A}$ . We ran each MCMC sampling chain for 8000 warmup iterations and 2000 sampling iterations. We assessed model convergence as described for the vital rate models.

## Mean-variance decomposition

We decomposed the total endophyte effect on  $\lambda_s$  into contributions from effects on vital rate means, variances, and their interaction. Specifically, we repeated the calculation of S+ and S-  $\lambda_s$  described above for two additional “treatments”: (1) endophyte effects on mean vital rates only, with inter-annual variances shared between S+ and S- at the S- reference level for all vital rates, and (2) endophyte effects on vital rate variances only, with vital rate means shared between S+ and S- at the S- reference level. The combination of all four  $\lambda_s$  treatments (S+ vital rate means and variances, S- means and variances, S+ means with S- variances, S- means with S+ variances) allowed us to quantify to what extent the overall effect of symbiosis derives from changes in vital rates means, variances, and their interaction. The interaction occurs because the variance penalty to stochastic growth is proportional to the arithmetic mean of annual growth rates (as in Eq. 1, for example) such that variance is more detrimental for populations with lower average growth rates. To quantify how mean and variance effects of symbionts arise through effects on different vital rates, we performed an additional decomposition described in the *Supporting Information Supplemental Methods* that isolates symbiont effects on growth and survival from their effects on fertility and recruitment.

We simulated scenarios of increased variance relative to that observed during the study period by sampling subsets of the 13 observed annual transition matrices. We created two scenarios of increased environmental variance by sampling the transition matrices associated with the set of either six or two most extreme  $\lambda$  values. These

415 extreme  $\lambda$  values represent the best and worst years for S- populations, the reference  
416 condition. By sampling away from an average year in both directions, the six- and two-  
417 years scenarios increased the standard deviation of annual host growth rates by 1.3  
418 and 2.1 times, respectively, without changing mean growth rates (< 2.3% difference  
419 in  $\bar{\lambda}$  between simulation treatments, Fig. S50). We performed the same mean-variance  
420 decomposition for these scenarios as for the ambient conditions (all 13 years sampled)  
421 for all host species described above.

422

## 423 Results

424

### 425 Symbionts buffer host demographic variance

426

427 Across the 14 census years, endophytes reduced inter-annual variance for 66% (37/56)  
428 of host species-vital rate combinations (average Cohen's D for effects on vital rate  
429 standard deviation: -0.15) (Fig. 2A; Fig. S6 - Fig. S18). Endophytes also increased  
430 mean vital rates for the majority (36/56) of host species-vital rate combinations (aver-  
431 age Cohen's D for effects on vital rate mean: 0.15), and benefits were particularly  
432 strong for host survival, plant growth and recruitment (Fig. 2A; Fig. S1 - Fig. S5).  
433 The magnitude of mean and variance effects differed among host species and vital  
434 rates. Symbiont effects on vital rate variance were as large and even exceeded effects  
435 on vital rate means for certain species. For example, endophytes modestly increased  
436 mean adult survival (Fig. 2C) and strongly reduced variance in survival (Fig. 2D)  
437 for *Festuca subverticillata*, while for *Poa alsodes*, variance buffering was more appar-  
438 ent in seedling growth and inflorescence production (Fig 2E). Additionally, some vital  
439 rates showed costs of endophyte symbiosis. Symbiotic individuals of *A. perennans*  
440 grew larger than those without endophytes (Fig. 2B), yet endophytes also reduced  
441 this species' mean recruitment rates (Fig. 2A). Similarly, endophytes increased vari-  
442 ance for certain species' vital rates, such as in seedling growth for *Elymus villosus* and  
443 *Festuca subverticillata* (Fig. 2A).

444 Because not all vital rates contribute equally to fitness, we used stochastic matrix  
445 models to integrate the diverse effects on vital rates described above into comprehen-  
446 sive measures for the arithmetic mean and variance of year-to-year fitness ( $\lambda_t$ ).<sup>7</sup> On  
447 average across host species, the mean fitness of S+ populations increased by more than  
448 10% ( $> 92\%$  confidence that endophytes increased  $\bar{\lambda}$ ) and inter-annual variability in  
449 fitness was 26% lower ( $> 86\%$  confidence that endophytes decreased the coefficient  
450 of variation of  $\lambda_t$ ) than S- populations (Fig. 3). For some host species, the CV of  $\lambda_t$   
451 declined by more than 62% (*P. alsodes*, *F. subverticillata*), while for others, endophyte  
452 effects on variance were substantially smaller (5% lower for *E. villosus*, 13% lower for  
453 *A. perennans*), or even positive (37% increase for *E. virginicus*).

454

---

455 <sup>7</sup>The methods and results sections are inconsistent in their use of  $\lambda$  vs  $\lambda_t$ . I think we could use either  
456 but either way tighten this up.

457

458

459

460

<b>Faster life histories predict stronger symbiont-mediated variance buffering</b>	461
	462
	463
	464
	465
	466
	467
	468
	469
	470
	471
	472
	473
	474
	475
	476
	477
	478
	479
	480
	481
	482
	483
	484
	485
	486
	487
	488
	489
	490
	491
	492
	493
	494
	495
	496
	497
	498
	499
	500
	501
	502
	503
	504
	505
	506

## Contributions from variance buffering are weak relative to mean effects

To evaluate the relative importance of mean fitness benefits and variance buffering as alternative pathways of mutualism, we decomposed the overall effect of the symbiosis on the stochastic growth rate  $\lambda_S$  using simulations that included either the full symbiosis effect (both mean and variance buffering effects), mean effects alone, variance effects alone, or neither mean nor variance effects. Overall, the full effect of symbiosis on  $\lambda_S$ , averaged across host species, provided strong evidence of grass-endophyte mutualism (99% certainty of a positive total effect on  $\lambda_s$ ) (Fig. 5; see Fig. S52 for individual host species). Contributions to this full effect derived from both mean and variance buffering effects, as well as a slightly negative interaction (i.e., the combined influence of mean and variance effects was smaller than the sum of their individual effects). Endophytes' contributions to  $\lambda_S$  from mean effects were four times greater, averaged across species, than contributions from variance buffering (Fig. 5), suggesting that, under the regime of environmental variability represented by our 14-year study, dampened fluctuations in fitness via variance buffering was a far less important element of the benefits of symbiosis than increased mean fitness. Decomposing this result further into contributions through endophytes effects on different vital rates demonstrated that demographic buffering arose primarily from symbionts' effects on host survival and growth, rather than from effects on reproduction (Fig. S53). Results for individual host species were largely consistent with the cross-species trends (Fig S22). The full effect of symbiosis on  $\lambda_S$  was positive for seven out of eight host species, with statistical confidence ranging from 66% to > 99% certainty. The one exception

---

<sup>8</sup>This last sentence feels discussiony, though I am not sure if there is a natural place to put it there.

507 was the host species *P. sylvestris*, for which our analysis indicated that fungal endo-  
508 phytes were effectively neutral in their overall fitness effect (45% and 55% posterior  
509 probability of positive and negative effects; Fig S22).

510

## 511 **Variance buffering strengthens under increased environmental 512 variability**

513

514 To simulate increased variability, we repeated the decomposition of  $\lambda_S$  for two alterna-  
515 tive forecast scenarios, randomly sampling transition matrices that represented either  
516 the six or two most extreme years, subsets of the thirteen transition matrices across  
517 the 14-year study period. Increased variability elicited stronger mutualistic benefits  
518 of endophyte symbiosis than ambient variability (Fig. 5; overall effect of the symbio-  
519 sis increased by > 130%, a 2.3 fold increase). This increase was driven by increased  
520 contributions from the variance buffering mechanism (from a 24% contribution in the  
521 ambient scenario to a 66% contribution in the most variable scenario) rather than  
522 from greater mean effects. In the most variable scenario, the relative importance of  
523 mean and variance effects reversed, with variance buffering contributions that were 1.5  
524 times greater than contributions from mean benefits, averaged across species (Fig. 5).

525

## 526 **Discussion**

527

528 Across seven host species, eight vital rates, 14 years, and 16,789 individual plants,  
529 our analysis provided the first empirical evidence of demographic buffering conferred  
530 by microbial symbionts. Our analysis of taxonomically-replicated, long-term field  
531 experiments that manipulated the presence/absence of fungal symbionts in plants  
532 demonstrated that heritable microbes can commonly benefit hosts not only through  
533 improved mean fitness – the focus of most previous research – but also through buffer-  
534 ing against environmental variance. When mean and variance effects of symbionts were  
535 considered together, none of the host-symbiont pairings were antagonistic (i.e., with  
536 endophytes that both decreased mean fitness and increased variance) (Fig. 3C), sug-  
537 gesting that variation across host species and vital rates in mean and variance effects  
538 may reflect alternative strategies that yield similar net benefits of endophyte symbiosis.  
539 These alternative strategies may explain the long-term stability of these mutualisms

540 Symbiont-mediated demographic buffering is a potential target of selection for  
541 improved holobiont fitness [59]. Our results show that by partnering with context-  
542 dependent symbionts in variable environments, hosts can supplement their inherent  
543 life-history strategy. We found support for the prediction that hosts with fast life cycles  
544 that produce many small offspring with low per-capita chance of success benefit from  
545 the variance buffering effects of the symbiosis [60, 61]. Considering fungal life history  
546 traits, the three host species for which the net mutualism benefit was weakest (*Ely-  
547 mus villosus*, *Elymus virginicus*, and *Poa sylvestris*) (Fig. 2C) were the only hosts for  
548 which we observed fungal stromata, fruiting bodies capable of horizontal (contagious)  
549 transmission (Table S2). This result supports the theoretical expectation that strict  
550 vertical transmission drives the evolution of strong host-symbiont mutualism [28, 62].  
551 For example, variation in the benefits of host-symbiont mutualism introduces a poten-  
552 tial feedback driving the evolution of horizontal transmission under conditions where

the interaction benefits are weak or costly [63]. Additionally, imperfect transmission, the production of symbiont-free offspring from a symbiotic maternal individual, occurs in this system (Table S2) and raises interesting questions about how symbiosis may influence evolutionary bet-hedging. Variation in offspring type potentially improves the chances that at least some individuals perform well in any given year [64] which could be explored by loosening the assumption in our analysis of perfect vertical transmission. For *Epichloë* hosts, this offspring variation likely would occur primarily through the production of symbiotic or symbiont-free offspring, as individual hosts are typically home to single haplotypes of asexually reproducing symbionts [65], but across host-microbe systems the diversity of the microbiome may be an important key to expanding phenotypic variance [66]. Our understanding of how life history variation modulates the fitness consequences of microbial symbiosis would profit from tests across a wider span of taxonomic groups [67].<sup>9</sup>

553  
554  
555  
556  
557  
558  
559  
560  
561  
562  
563  
564  
565

Work remains to be done to connect endophyte effects on mean and variance to realistic forecasts of host-symbiont dynamics under global change. Our simulations of increased environmental variability indicated that mutualism with microbial symbionts, and their variance buffering effects in particular, will take on increased importance for hosts under a more variable future climate. However, our analyses treated certain important aspects determining stochastic population growth rates implicitly. First, we amplified interannual variance in yearly fitness rather than realistically connecting the most important climate drivers to each vital rate [68, 69]. Reduced sensitivity to drought, as has been reported for some *Epichloë* symbioses [41], is a candidate mechanism that could generate a signature of variance buffering: drought conditions may have weaker fitness costs for S+ hosts, reducing fluctuations in fitness through time. We performed a climate-explicit analysis that indicated that symbionts reduced sensitivity to annual or growing season drought indices for five of seven host taxa (Supporting Information Text; Fig. S24-S25; Table S3). However, we did not find a strong relationship between the magnitude of variance buffering and relative drought sensitivities, suggesting that other climatic factors or other temporally-varying aspects of the environment may elicit benefits of endophyte symbiosis, including documented resistance to herbivory for six of these host taxa [70, 71]. Identifying the type and timescale of relevant drivers would allow more direct connections between demographic models and outputs from global climate models. The magnitude and autocorrelation of climate variability are likely to impact future population projections [72]. Second, climate-demography relationships may change unpredictably under global climate change. For example, interacting effects of multiple climate drivers and shifting cost-benefits between hosts and symbionts may alter vital rate correlations. Increased positive correlations between vital rates could amplify demographic variance [8, 73], negating demographic buffering provided by symbionts. Finally, the limits of extrapolating spatially and temporally beyond the experimental plots are unknown. While commonly used to build inference about ecological processes and environmental variables, space-for-time substitutions can be misleading [74]. Environmental variability is spatially heterogeneous and is expected to both increase and decrease across the

566  
567  
568  
569  
570  
571  
572  
573  
574  
575  
576  
577  
578  
579  
580  
581  
582  
583  
584  
585  
586  
587  
588  
589  
590  
591  
592  
593  
594  
595  
596  
597  
598

---

<sup>9</sup>*Is it worth talking about demographic lability anywhere?*

599 broad ranges of our focal species [2]. Locally adapted populations may have divergent  
600 responses, making it difficult to predict the fate of the symbiosis.

601

## 602 Conclusion

603

604 Ecologists increasingly recognize the importance of symbiotic microbes for host organ-  
605 isms and the populations, communities, and ecosystems in which their hosts reside  
606 [75–78]. Despite awareness of these ubiquitous interactions, long-term studies of micro-  
607 bial symbiosis are very rare. Our results provide an important advance to improve  
608 forecasts of the responses of populations (and symbiota) to increasing environmental  
609 stochasticity under global change, suggesting that, for some host species, microbial  
610 symbiosis may compensate for the lack of intrinsic tolerance of variability conferred by  
611 “slow” life history traits. We found that, relative to mean fitness benefits, symbiont-  
612 mediated variance buffering made weak contributions to host-symbiont mutualism  
613 under the current regime of environmental variability. However, demographic buffer-  
614 ing is likely to become the dominant benefit that fungal endophytes confer to grass  
615 hosts in more variable future environments. Thus, demographic buffering – a cryptic  
616 microbial influence that manifests only over long time scales – is poised to become  
617 the dominant way in which grasses benefit from symbiosis with fungal endophytes in  
618 more variable climates of the future. This result emerges from the context-dependent  
619 nature of grass-endophyte interactions, combined with the observation that environ-  
620 mental stochasticity generates fluctuation in context. These key ingredients, and thus  
621 the potential for symbiont-mediated variance buffering, similarly apply to the diverse  
622 host-microbe symbioses across the tree of life.

623

624

625

626

627

628

629

630

631

632

633

634

635

636

637

638

639

640

641

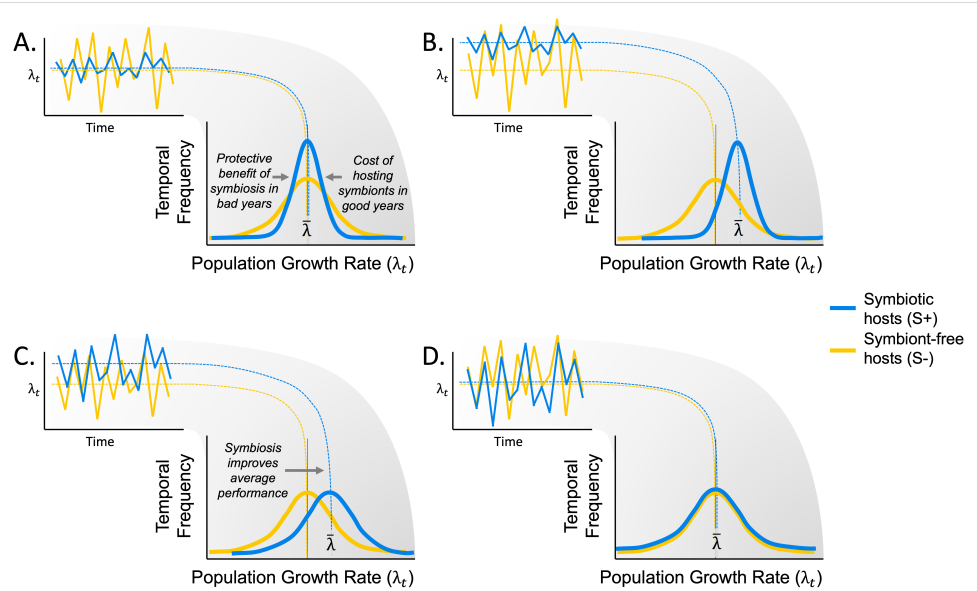
642

643

644

<b>Acknowledgments.</b> We thank Mark Sheehan, Ali Campbell, Kyle Dickens, Blaise Willis, and Sar Lindner for contributions to field data collection. We also thank Volker Rudolf, Daniel Kowal, Lydia Beaudrot and Judie Bronstein for helpful comments on and discussion of this project. This research was supported by the National Science Foundation (grants 1754468 and 2208857).	645 646 647 648 649 650 651 652 653 654 655 656 657 658 659 660 661 662 663 664 665 666 667 668 669 670 671 672 673 674 675 676 677 678 679 680 681 682 683 684 685 686 687 688 689 690
<b>Supplementary information.</b> Supplementary information for this paper includes Supplementary Methods, Figs. A1 to A28, and Tables A1 to A3.	

691 **Figures**



714 **Fig. 1** Hypothesized effects of symbiosis on the mean and variance of annual population growth  
 715 rates. (A) Context-dependent symbiosis may provide benefits to hosts during harsh years while being  
 716 neutral or costly during benign years. Temporal variance in populations growth rates of symbiotic  
 717 host populations (S+; blue lines) is expected to decrease relative to symbiont-free hosts (S-; yellow  
 718 lines). (B) Symbiosis may improve average performance across years in addition to reducing temporal  
 719 variance. (C) Consistent benefits of symbiosis could improve average performance across years with  
 720 no influence on temporal variance. (D) Symbiosis may have an effectively neutral effect on population  
 721 growth rates.

737  
 738  
 739  
 740  
 741  
 742  
 743  
 744  
 745  
 746  
 747  
 748  
 749  
 750  
 751  
 752  
 753  
 754  
 755  
 756  
 757  
 758  
 759  
 760  
 761  
 762  
 763  
 764  
 765  
 766  
 767  
 768  
 769  
 770  
 771  
 772  
 773  
 774  
 775  
 776  
 777  
 778  
 779  
 780  
 781  
 782

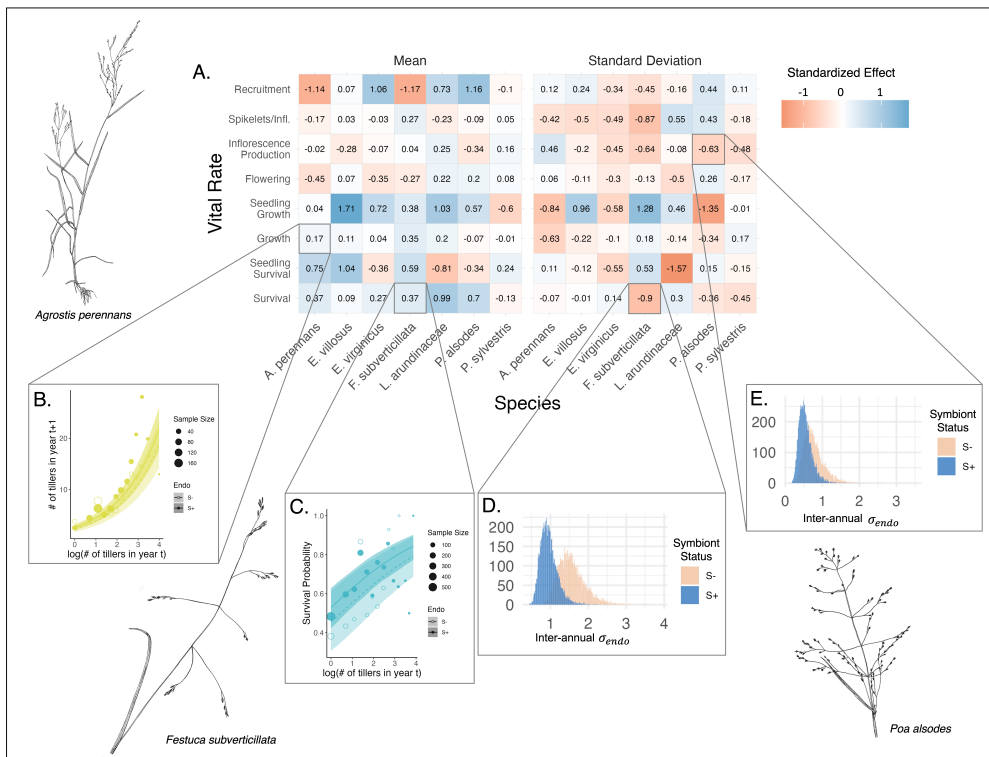


**Fig. 2** Endophyte symbiosis altered host vital rates.(A) Shading represents the posterior mean standardized effect size (Cohen's D) of endophyte symbiosis on mean or standard deviation of host vital rates (blue indicates that symbiosis increased the mean or standard deviation and red indicates a reduction). Endophytes' diverse vital rate effects include increased (B) mean growth of *A. perennans* and (C) mean survival probability of *F. subverticillata*. Endophyte presence also reduced inter-annual standard deviation in (D) the survival of *F. subverticillata* and (E) the fertility of *P. alsodes*. In panels B-C, mean vital rate estimates are shown with 80% credibles along with data binned by size for symbiotic (S+) and symbiont-free (S-) plants, while panels D-E show estimated posterior distributions of endophyte-status specific inter-annual standard deviation ( $\sigma_{e,h}^2$ ) for each vital rate for S+ (blue) and S- (beige) populations. Organism silhouettes modified from "Festuca subverticillata" by Cindy Roché and "Agrostis hyemalis" and "Poa alsodes" by Sandy Long ©Utah State University.

783

784

785

786

787

788

789

790

791

792

793

794

795

796

797

798

799

800

**Fig. 3** Mean and variance-buffering effects on fitness. Black circles indicate the average effect of endophytes along with 500 posterior draws (smaller colored circles) on the (A) mean and (B) coefficient of variation in  $\lambda$  for each host species as well as a cross species mean. (C) For all hosts, endophytes either reduce variance, increase the mean, or both, and consequently when considering stochastic environments, the interactions are always at least potentially mutualistic.

801

802

803

804

805

806

807

808

809

810

811

812

813

814

815

816

817

818

819

820

821

**Fig. 4** Host species with faster life history traits experience stronger effects of symbiont-mediated

822 variance buffering. Regressions between life history traits describing the fast-slow life history continuum ((A) 99th percentile maximum age observed during long term censuses in years; (B) Seed size)

823 and the effect of endophyte symbiosis on the coefficient of variation in population growth rate ( $\lambda$ ).

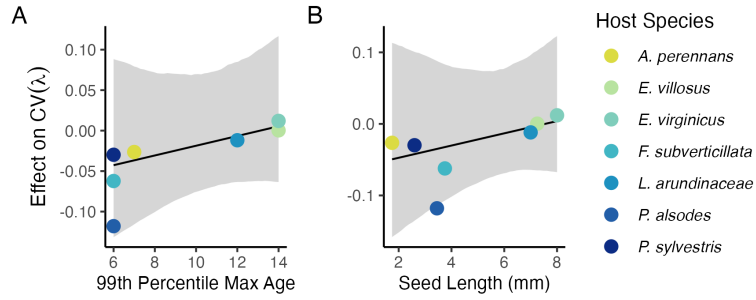
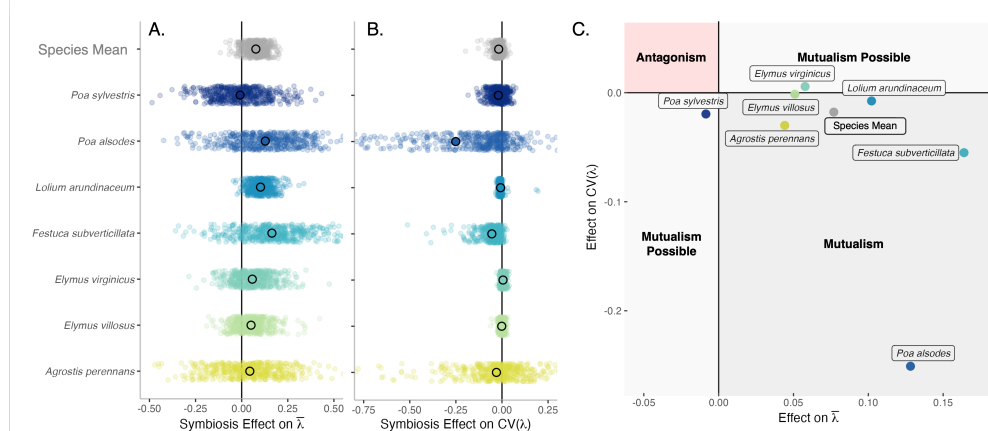
824 Each panel shows the fitted mean relationship (line) along with the 95% credible interval.

825

826

827

828



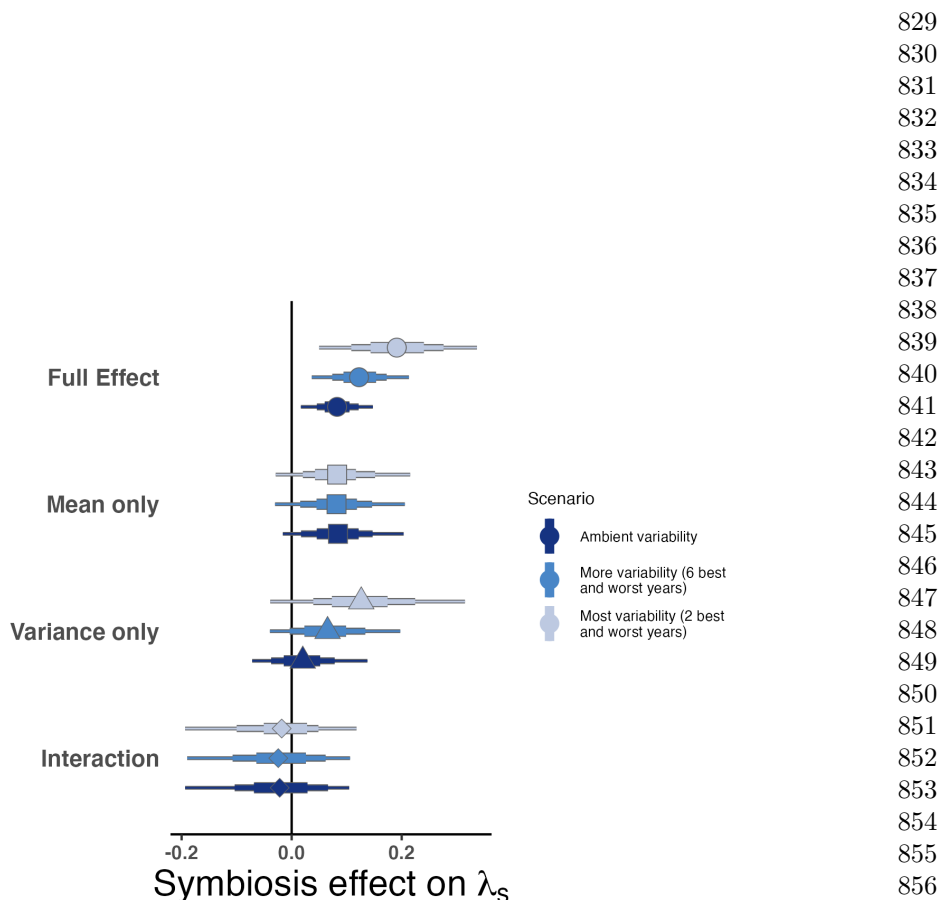


**Fig. 5** Cross-species average endophyte contributions to stochastic growth rates under observed and elevated variance. Endophyte symbiosis contributes to the total effect of mutualism on  $\lambda_S$  through benefits to mean growth rates and through variance buffering as well as the interaction between mean and variance effects. Shapes indicate the posterior mean of each contribution averaged across the seven focal symbiota, along with bars for the 50, 75 and 95% credible intervals. The full effect of the symbiosis (circles) becomes more mutualistic under scenarios of increased variance (represented by color shading). Relative to the ambient scenario sampling transition matrices for all 13 transition years during the study period, simulations increased variance by sampling the most extreme six or two years years, leading to increased contributions from variance buffering effects (triangles) and a constant contribution from mean effects (squares).

875 **Supporting Information**

876

877 **Supplemental Methods**

878 **Detailed vital rate modeling**

879  
880 We fit vital rates models in a Bayesian hierarchical framework. Statistical models for  
881 adult survival, seedling survival, adult growth, seedling growth, flowering (yes or no),  
882 fertility of flowering plants (number of flowering tillers), production of seed-bearing  
883 spikelets (number per inflorescence), the average number of seeds per spikelet, and the  
884 recruitment of seedlings from the preceding year's seed production, were constructed  
885 as follows:

886 *Survival* - We modeled survival as a Bernoulli process, where the survival ( $S$ ) of  
887 an individual  $i$  in plot  $p$  and census year  $t$  was predicted by the plot-level endophyte  
888 status ( $e$ ), host species ( $h$ ), size in the preceding census, and the plant's origin status  
889 (whether it was initially transplanted or naturally recruited into the plot).

890

891

892 
$$S_{i,p,e,h,t} \sim Bernoulli(\hat{S}_{i,p,e,h,t}) \quad (1a)$$

893 
$$\text{logit}(\hat{S}_{i,p,e,h,t}) = \beta_{0_h} + \beta_1 * \text{origin}_i \quad (1b)$$

894 
$$+ \beta_{2_h} * \text{endo}_e + \beta_{3_h} * \text{size}_{i,t-1} + \tau_{e,h,t} + \rho_p \quad (1c)$$

895 
$$\tau_{e,h,t} \sim \text{Normal}(0, \sigma_{\tau_{e,h}}^2) \quad (1d)$$

896 
$$\rho_p \sim \text{Normal}(0, \sigma_\rho^2) \quad (1e)$$

897

898

899 Here,  $\hat{S}$  is the survival probability,  $\beta_{0_h}$  is an intercept specific to each host species,  
900  $\beta_1$  is the effect of the plant's recruitment origin,  $\beta_{2_h}$  is the endophyte effect,  $\beta_{3_h}$  is the  
901 size effect,  $\tau_{e,h,t}$  is a normally distributed year effect for each species and endophyte  
902 status with variance  $\sigma_{\tau_{e,h}}^2$ , and  $\rho_p$  is a normally distributed plot effect with variance  
903  $\sigma_\rho^2$  ( $p(e)$  indicates that plot identity is uniquely associated with an endophyte status).  
904 We assume that origin effect  $\beta_1$  and plot-to-plot variance  $\sigma_\rho^2$  are shared across host  
905 species, allowing us to "borrow strength" across the multi-species dataset; other model  
906 parameters are unique to host species. We separately modeled the survival of newly  
907 recruited seedlings with a similar model but omitting previous size dependence and  
908 origin status.

909 *Growth* - We modeled plant size in census year  $t$  ( $G$ ) with the same linear pre-  
910 dictor for the mean as described for survival. Because we measured size as positive  
911 integer-valued counts of tillers, we modeled it with a zero-truncated Poisson-inverse  
912 Gaussian distribution. This distribution includes a shape parameter  $\lambda_G$  to account for  
913 overdispersion in the data. We additionally modeled the growth of newly recruited  
914 seedlings separately with a Poisson-inverse Gaussian model omitting size structure  
915 and the plants' origin status as with seedling survival.

916 *Flowering* - We modeled whether or not a plant was flowering during the census ( $P$ )  
917 as a Bernoulli process, with the same linear predictor for the mean as described above  
918 for survival except that size dependence for reproductive vital rates was determined  
919

920

by the individual's size during the same census year as opposed to its size during the previous year.	921
	922
<i>Fertility</i> - For a plant that was flowering during the census, its fertility was the number of reproductive tillers produced ( $F$ ), which we modeled as a function of size in the same census period with a zero-truncated Poisson-Inverse Gaussian distribution, with the same linear predictor for the mean as described above.	923
	924
	925
	926
<i>Spikelets per Inflorescence</i> - Spikelet production ( $K$ ) was recorded as integer counts on up to three inflorescences per reproducing plant. We modeled these data with a negative binomial distribution, with the same linear predictor for the mean as described above.	927
	928
	929
	930
<i>Seed Production per Spikelet</i> - For individuals with recorded counts of seed production, we calculated the number of seeds per spikelet from our counts of seeds and spikelets per inflorescence, and then modeled seeds per spikelet ( $D$ ) as means of a Gaussian distribution for each species and endophyte status. Because we had less detailed data across years and plants for seed production than for other reproductive vital rates, we omitted both plot and year random effects.	931
	932
	933
	934
	935
	936
<i>Seedling Recruitment</i> - We used a binomial distribution to model the recruitment of new seedlings ( $R$ ) into the plots from seeds produced in the preceding year, assuming no long-lived seed bank. We included an intercept specific to each host and endophyte status and the same random effects structure as in other models. We estimated the number of seeds per plot in the preceding year by multiplying the total number of reproductive tillers per plant by the mean number of spikelets per inflorescence and mean number of seeds per spikelet ( $D$ ). For plants with missing fertility or spikelet data, we used the expected number of reproductive tillers ( $F$ ) or of spikelets per inflorescence from ( $K$ ), drawing from the full posteriors of our models. We rounded this value to get the estimated seed production for each individual, and finally summed across all reproductive plants in each year and plot to get the total number of seeds produced.	937
	938
	939
	940
	941
	942
	943
	944
	945
	946
	947
	948
	949
<b>Estimating climate drivers of environmental context-dependence</b>	950
To connect the variance buffering effects of endophytes with inter-annual variability in climate, we built climate-explicit stochastic matrix population models from the vital rate data in addition to the climate-implicit model described in the main text. Identifying the potentially complex relationships between vital rates and environmental drivers remains a key challenge for accurate forecasts of the ecological impacts of environmental stochasticity [79]. We first downloaded temperature and precipitation data from a weather station in Bloomington, IN, approx. 27 km from our study site, using the rnoaa package [80]. Compared to other weather stations in the area, the measurements from Bloomington contain the most complete climate record across the study period and are correlated with more local measurements from Nashville, IN for years in which local data are available (total daily precipitation: $R^2 = .76$ ; mean daily temperature: $R^2 = .94$ ). The mean annual temperature across the study period was $11.9 C^\circ$ (SD: $1.05 C^\circ$ ) and the average annual precipitation was 1237.9 mm/year (SD: 204.89 mm/year) (Fig. S24). Given the known role of endophytes in promoting host drought tolerance, we calculated the Standardised Precipitation-Evapotranspiration	951
	952
	953
	954
	955
	956
	957
	958
	959
	960
	961
	962
	963
	964
	965
	966

967 Index (SPEI) for 3 and 12 months preceding each annual censuses, reflecting drought  
968 during the growing season and across the year [81]. To calculate SPEI, we used the  
969 Thornthwaite equation to model potential evapotranspiration as implemented in the  
970 SPEI R package [82]

971 We repeated the process of fitting statistical models for each vital rate as described  
972 in **Materials and Methods** with the inclusion of a parameter describing the influ-  
973 ence of SPEI. We fit separate vital rate models incorporating either the growing season  
974 or annual drought index for each vital rate, except for the model describing the mean  
975 number of seeds per inflorescence. This model was fit without climate effects because  
976 the data came from only a few years. Initial analyses indicated similar fits for models  
977 including only a linear term and those with both linear and quadratic terms describ-  
978 ing the relationship between the climate driver and the vital rate response, and so  
979 we proceeded with models including only the linear term. We expected that includ-  
980 ing climate predictors into the models would explain some inter-annual variance in  
981 vital rates, shrinking the variance associated with the fitted year random effects. We  
982 assessed model fit with graphic posterior predictive checks and convergence diagnostics  
983 as described for the climate-implicit analysis. Finally, we next built matrix projec-  
984 tion models incorporating the climate-dependent vital rate functions to assess the  
985 response of symbiotic (S+) vs symbiont-free (S-) populations to drought. The model  
986 is as described in **Materials and Methods** with the inclusion of parameters describ-  
987 ing the slope of the relationship with SPEI. We compared the sensitivity of  $\lambda$  to either  
988 annual or seasonal SPEI of S+ populations ( $\frac{\Delta\lambda^+}{\Delta SPEI}$ ) with those of S- populations  
989 ( $\frac{\Delta\lambda^-}{\Delta SPEI}$ )(Fig. S25; Table S).

990 Most species were slightly more responsive to growing season rather than annual  
991 drought conditions, and for most species symbiotic populations were less sensitive to  
992 SPEI than symbiont-free populations (Fig. S25; Table S3). However, these drought  
993 indices did not explain the full extent of inter-annual variability in demographic  
994 vital rates. For example, flowering in *A. perennans* had one of the strongest climate  
995 signals (82% probability of a positive relationship with SPEI), yet the estimated inter-  
996 annual variance  $\sigma_{\tau_P}^2$  for symbiont-free plants shrank from 6.7 to 6.1 after including  
997 3-month SPEI as a covariate, suggesting that other factors contribute to inter-annual  
998 variability.  
999

## 1000 **Vital rate mean-variance decomposition**

1001

1002 We repeated the mean-variance decomposition to quantify the extent that mean and  
1003 variance effects on stochastic population growth rates arise through different vital  
1004 rates. Specifically, we repeated the calculation of  $\lambda_s$  as described in the main text  
1005 for symbiotic populations as well as symbiont-free populations, as well as for four  
1006 additional “treatments”. These treatments differentiate between mortality and growth  
1007 related vital rates (adult survival, adult growth, seedling survival, and seedling growth)  
1008 and reproductive vital rates (probability of flowering, inflorescence production, spikelet  
1009 production, seed production, and recruitment). Each treatment held vital rate mean  
1010 and interannual variances at the S- reference level across vital rates while introducing  
1011 (1) endophyte effects on the vital rate means for survival and growth vital rates only,  
1012 (2) endophyte effects on the vital rate variances for survival and growth vital rates

only, (3) endophyte effects on the vital rate means for reproductive vital rates only, and (4) endophyte effects on the vital rate variances for reproductive vital rates only.

The combination of all six  $\lambda_s$  treatments allowed us to quantify to what extent the overall effect of symbiosis derives from changes in mean and variance of mortality and growth versus in reproductive vital rates. To explore how these contributions could be expected to change under increased variability relative to that observed during the study period, we repeated this decomposition under the scenarios of increased variance described in the main text, sampling transition matrices associated with the set of either six or two most extreme  $\lambda$  values.

This analysis revealed that both mean and variance buffering effects are driven primarily by symbiont effects on survival and growth rather than on reproduction (Fig S53).

1059 Supplemental Figures S1-S28

1060

1061

1062

1063

**Adult Survival**  
Data from Original plants only

1064

1065

1066

1067

1068

1069

1070

1071

1072

1073

1074

1075

1076

1077

1078

1079

1080

1081

1082

1083

1084

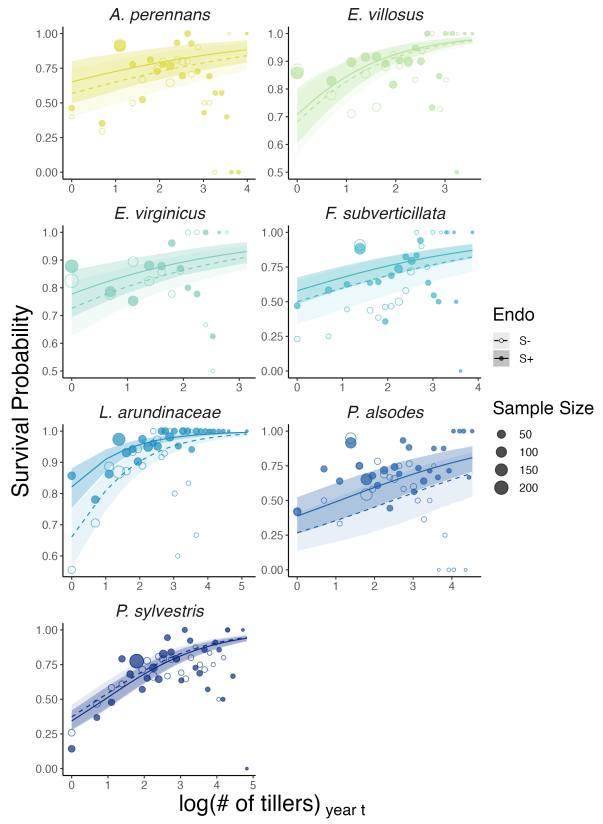
1085

1086

1087

1088

1089



1090 **Fig. S1** Effect of endophyte symbiosis on mean adult survival. Fitted curves represent the size-  
1091 specific mean survival probability for original plants along with data binned by size shown as open  
1092 circles with a dashed line for symbiont-free (S-) plants, while the solid line and filled circles represent  
1093 symbiotic (S+) plants. 80% credible intervals are shown with dark shading for S+, or light shading  
1094 for S-.

1095

1096

1097

1098

1099

1100

1101

1102

1103

1104

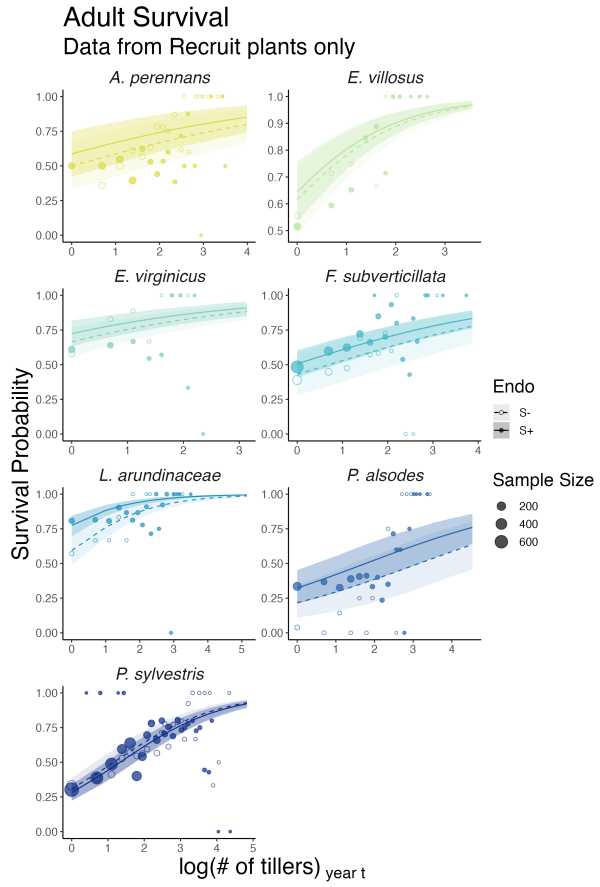
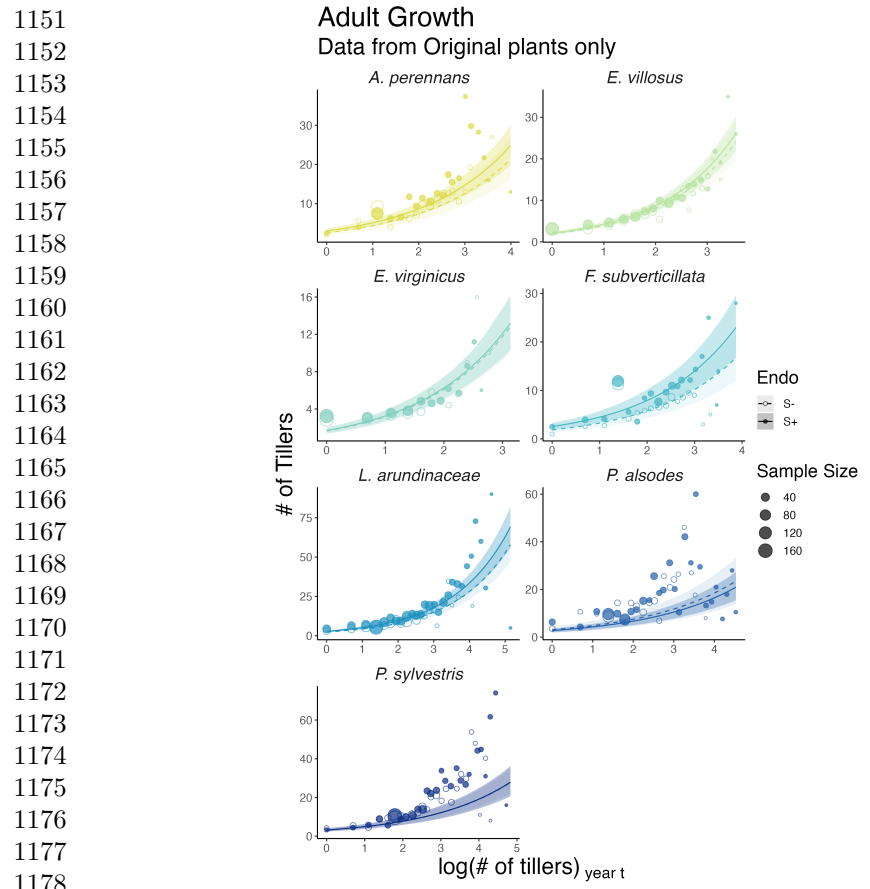


**Fig. S2** Effect of endophyte symbiosis on mean adult survival. Fitted curves represent the size-specific mean survival probability for recruited plants along with data binned by size shown as open circles with a dashed line for symbiont-free (S-) plants, while the solid line and filled circles represent symbiotic (S+) plants. 80% credible intervals are shown with dark shading for S+, or light shading for S-.

1105  
1106  
1107  
1108  
1109  
1110  
1111  
1112  
1113  
1114  
1115  
1116  
1117  
1118  
1119  
1120  
1121  
1122  
1123  
1124  
1125  
1126  
1127  
1128  
1129  
1130  
1131  
1132  
1133  
1134  
1135  
1136  
1137  
1138  
1139  
1140  
1141  
1142  
1143  
1144  
1145  
1146  
1147  
1148  
1149  
1150



1179 **Fig. S3** Effect of endophyte symbiosis on mean adult growth. Fitted curves represent the size-specific  
1180 mean expected plant size for original plants along with data binned by size shown as open circles with  
1181 a dashed line for symbiont-free (S-) plants, while the solid line and filled circles represent symbiotic  
1182 (S+) plants. 80% credible intervals are shown with dark shading for S+, or light shading for S-.  
1183  
1184  
1185  
1186  
1187  
1188  
1189  
1190  
1191  
1192  
1193  
1194  
1195  
1196

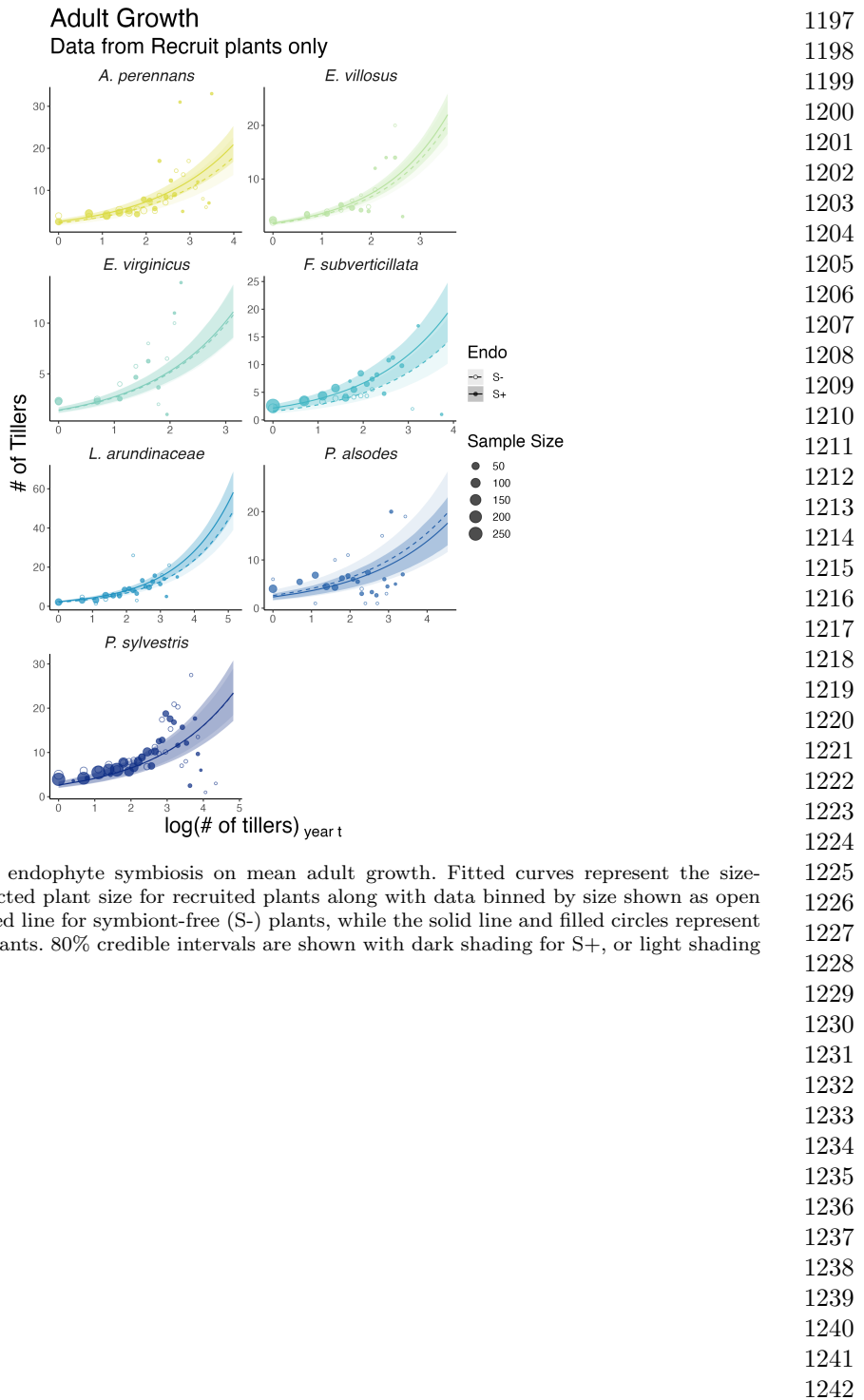
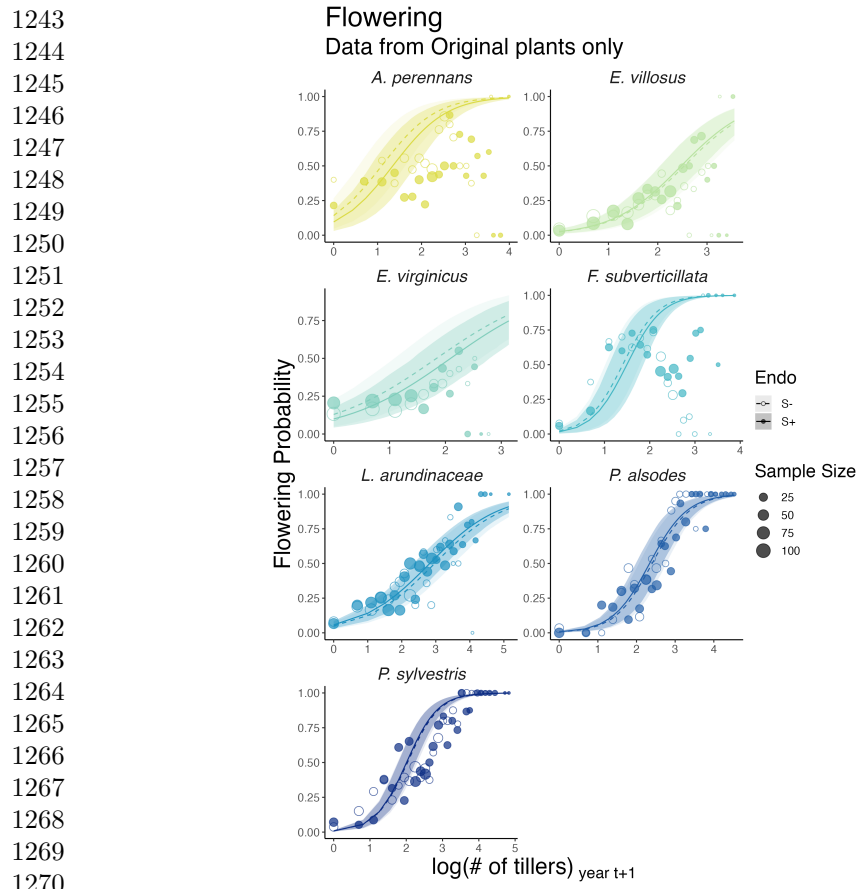


**Fig. S4** Effect of endophyte symbiosis on mean adult growth. Fitted curves represent the size-specific mean expected plant size for recruited plants along with data binned by size shown as open circles with a dashed line for symbiont-free (S-) plants, while the solid line and filled circles represent symbiotic (S+) plants. 80% credible intervals are shown with dark shading for S+, or light shading for S-.



1271 **Fig. S5** Effect of endophyte symbiosis on mean flowering. Fitted curves represent the size-specific  
 1272 mean flowering probability for original plants along with data binned by size shown as open circles with  
 1273 a dashed line for symbiont-free (S-) plants, while the solid line and filled circles represent symbiotic  
 1274 (S+) plants. 80% credible intervals are shown with dark shading for S+, or light shading for S-.  
 1275  
 1276  
 1277  
 1278  
 1279  
 1280  
 1281  
 1282  
 1283  
 1284  
 1285  
 1286  
 1287  
 1288

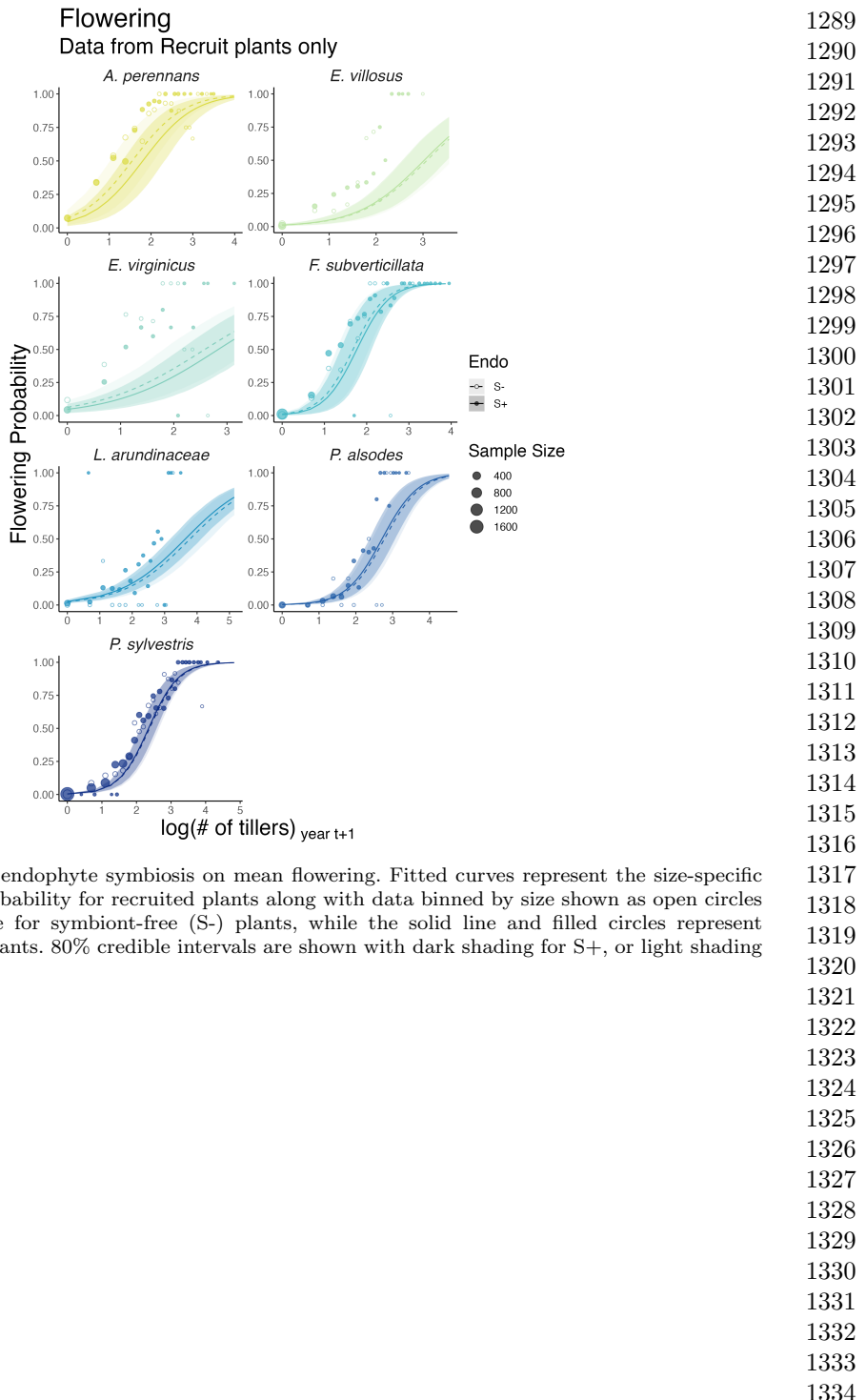
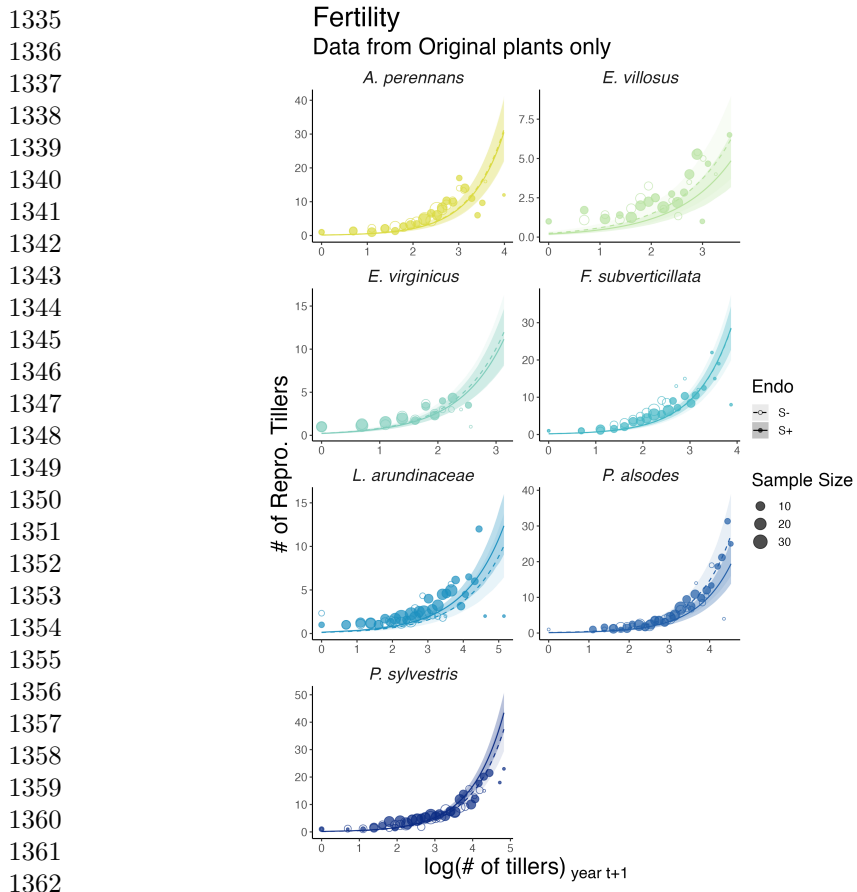


**Fig. S6** Effect of endophyte symbiosis on mean flowering. Fitted curves represent the size-specific mean flowering probability for recruited plants along with data binned by size shown as open circles with a dashed line for symbiont-free (S-) plants, while the solid line and filled circles represent symbiotic (S+) plants. 80% credible intervals are shown with dark shading for S+, or light shading for S-.



1363 **Fig. S7** Effect of endophyte symbiosis on mean fertility. Fitted curves represent the size-specific  
 1364 mean expected number of flowering tillers for original plants along with data binned by size shown  
 1365 as open circles with a dashed line for symbiont-free (S-) plants, while the solid line and filled circles  
 1366 represent symbiotic (S+) plants. 80% credible intervals are shown with dark shading for S+, or light  
 1367 shading for S-.

1368  
 1369  
 1370  
 1371  
 1372  
 1373  
 1374  
 1375  
 1376  
 1377  
 1378  
 1379  
 1380

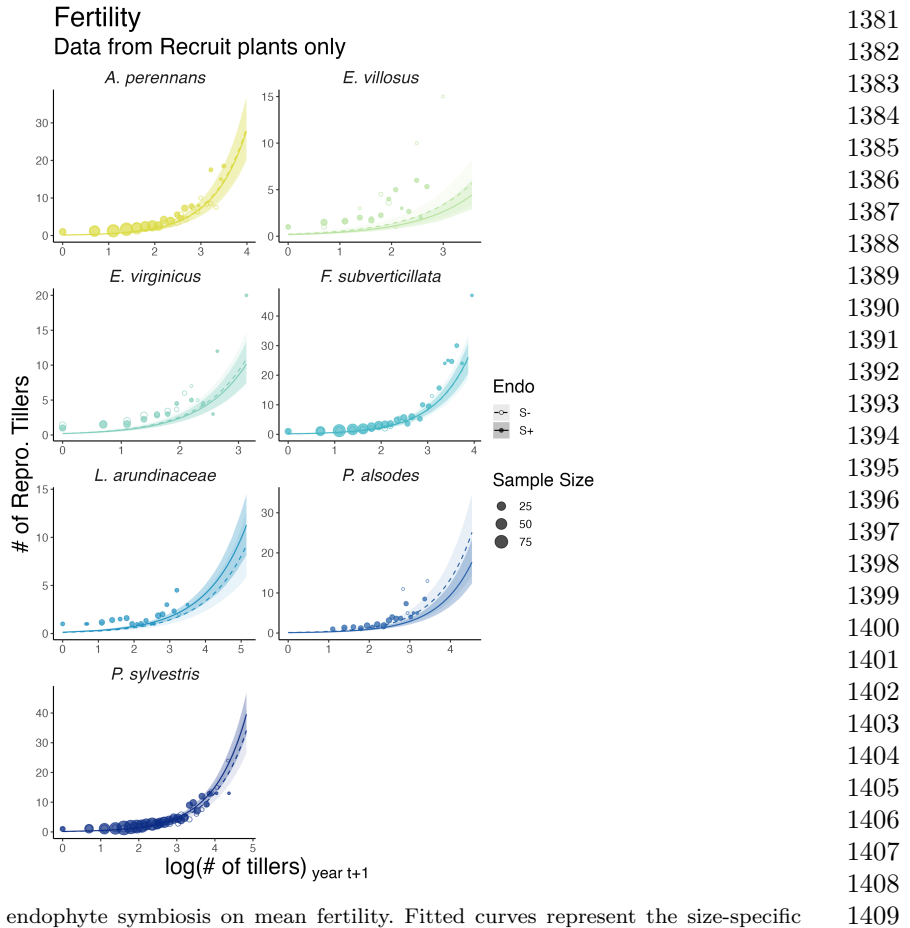
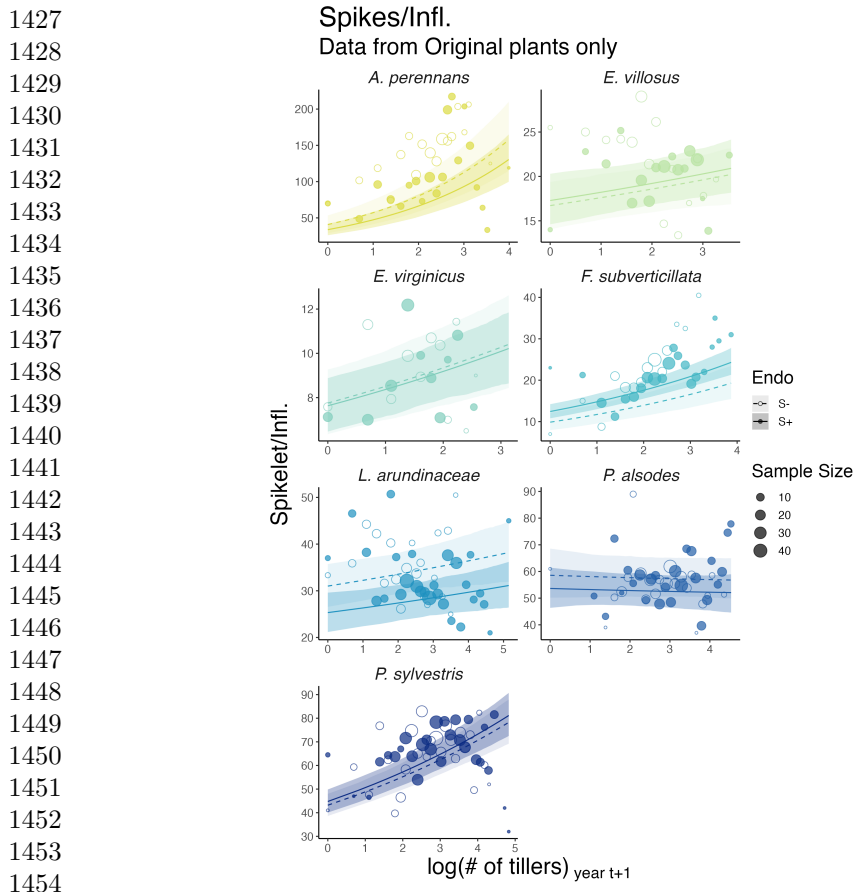


**Fig. S8** Effect of endophyte symbiosis on mean fertility. Fitted curves represent the size-specific mean expected number of flowering tillers for recruited plants along with data binned by size shown as open circles with a dashed line for symbiont-free (S-) plants, while the solid line and filled circles represent symbiotic (S+) plants. 80% credible intervals are shown with dark shading for S+, or light shading for S-.



1455 **Fig. S9** Effect of endophyte symbiosis on mean spikelet production. Fitted curves represent the  
1456 size-specific mean expected number of spikelets per inflorescence for original plants along with data  
1457 binned by size shown as open circles with a dashed line for symbiont-free (S-) plants, while the solid  
1458 line and filled circles represent symbiotic (S+) plants. 80% credible intervals are shown with dark  
1459 shading for S+, or light shading for S-.

1460  
1461  
1462  
1463  
1464  
1465  
1466  
1467  
1468  
1469  
1470  
1471  
1472

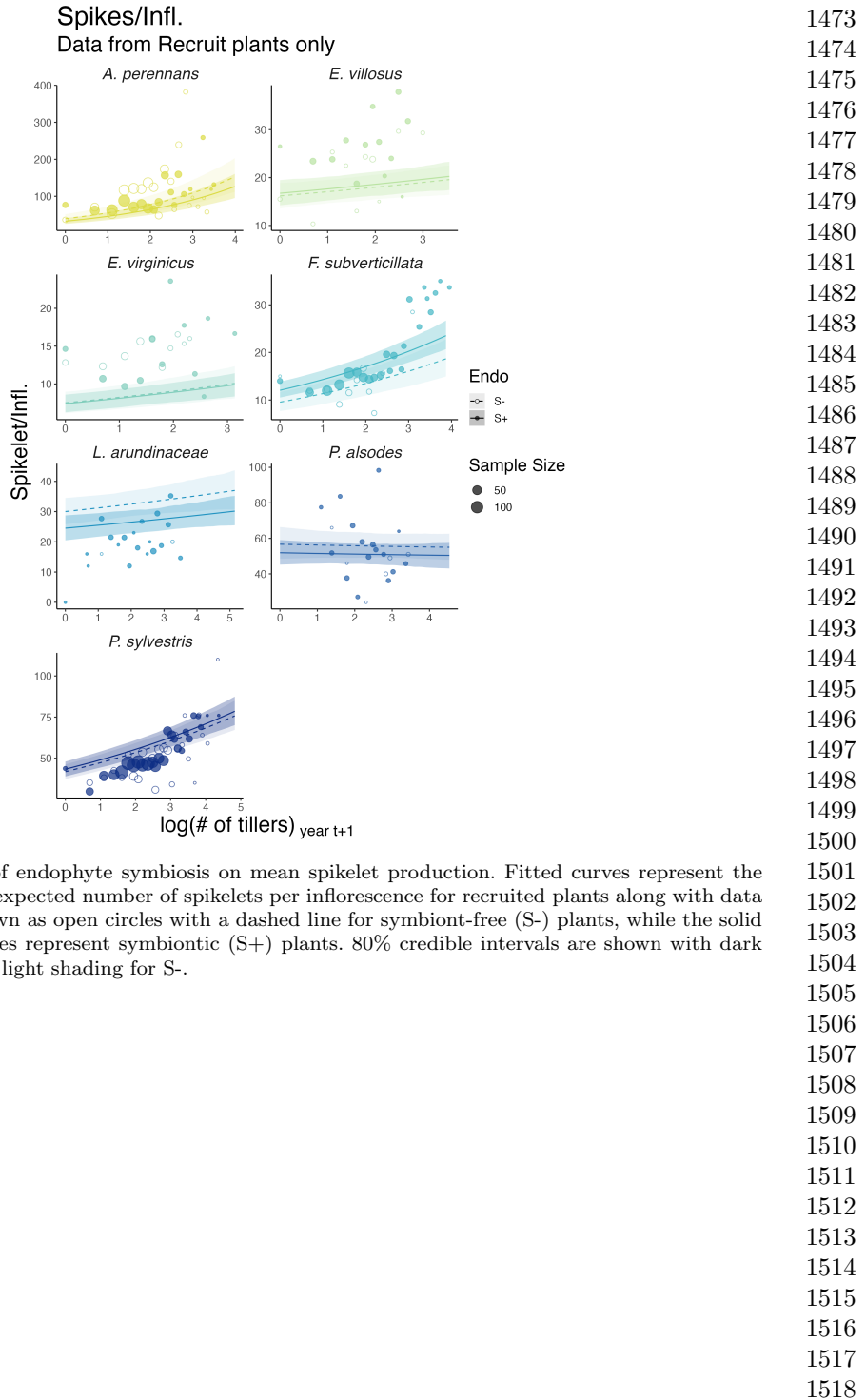
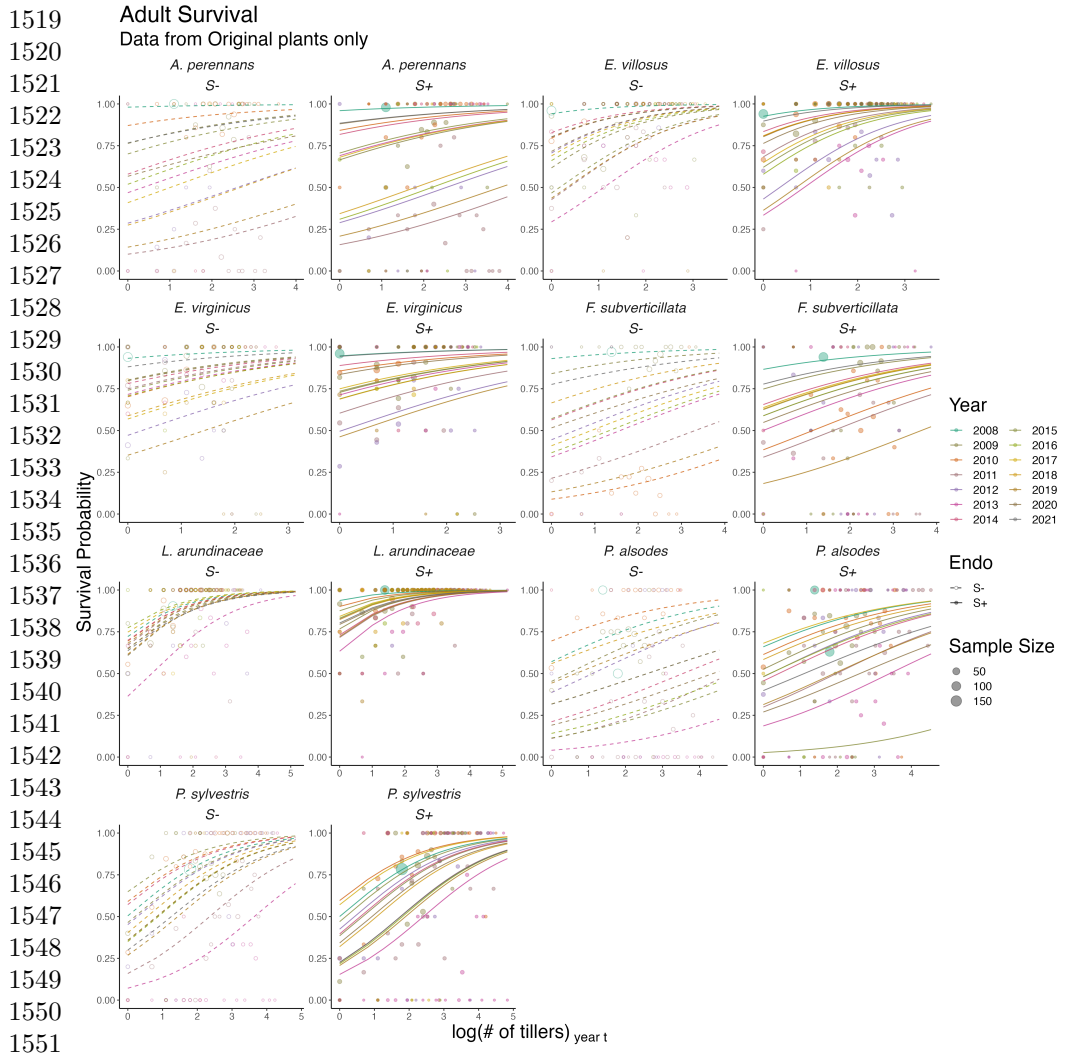
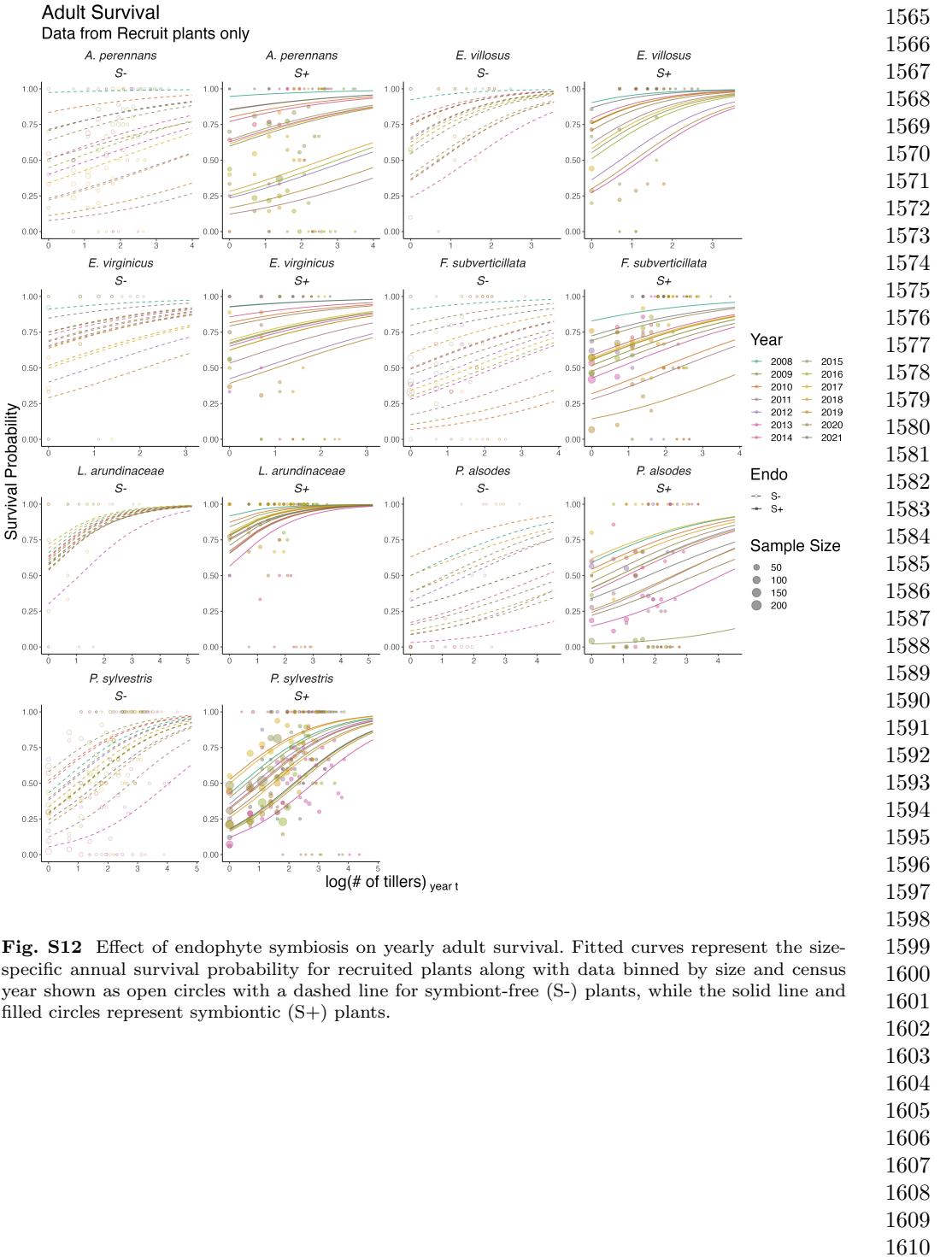


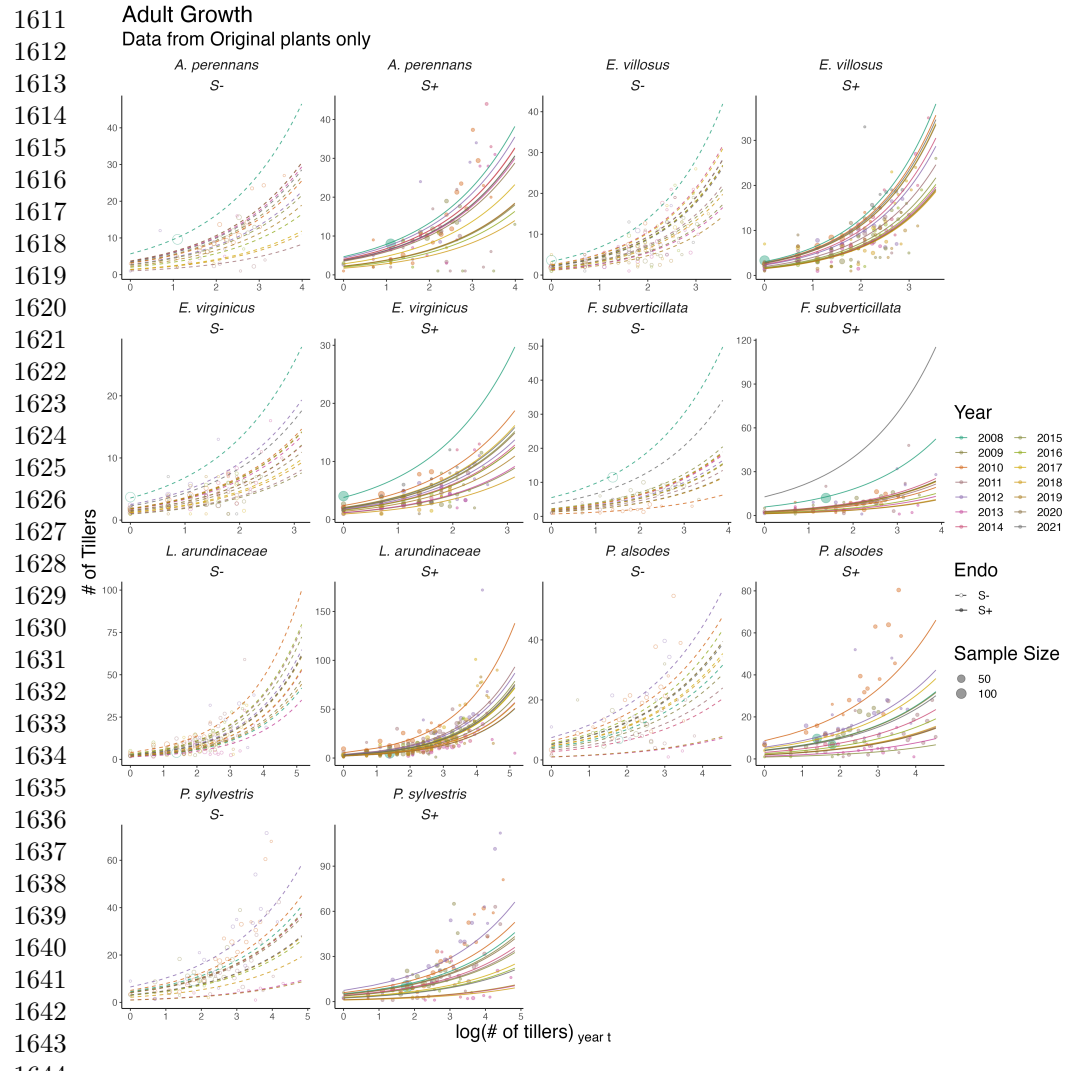
**Fig. S10** Effect of endophyte symbiosis on mean spikelet production. Fitted curves represent the size-specific mean expected number of spikelets per inflorescence for recruited plants along with data binned by size shown as open circles with a dashed line for symbiont-free (S-) plants, while the solid line and filled circles represent symbiotic (S+) plants. 80% credible intervals are shown with dark shading for S+, or light shading for S-.



1553 **Fig. S11** Effect of endophyte symbiosis on yearly adult survival. Fitted curves represent the size-  
1554 specific annual survival probability for original plants along with data binned by size and census year  
1555 shown as open circles with a dashed line for symbiont-free (S-) plants, while the solid line and filled  
1556 circles represent symbiotic (S+) plants.

1556  
1557  
1558  
1559  
1560  
1561  
1562  
1563  
1564





1645 **Fig. S13** Effect of endophyte symbiosis on yearly adult growth. Fitted curves represent the size-  
1646 specific annual expected plant size for original plants along with data binned by size and census year  
1647 shown as open circles with a dashed line for symbiont-free (S-) plants, while the solid line and filled  
1648 circles represent symbiotic (S+) plants.

1648  
1649  
1650  
1651  
1652  
1653  
1654  
1655  
1656

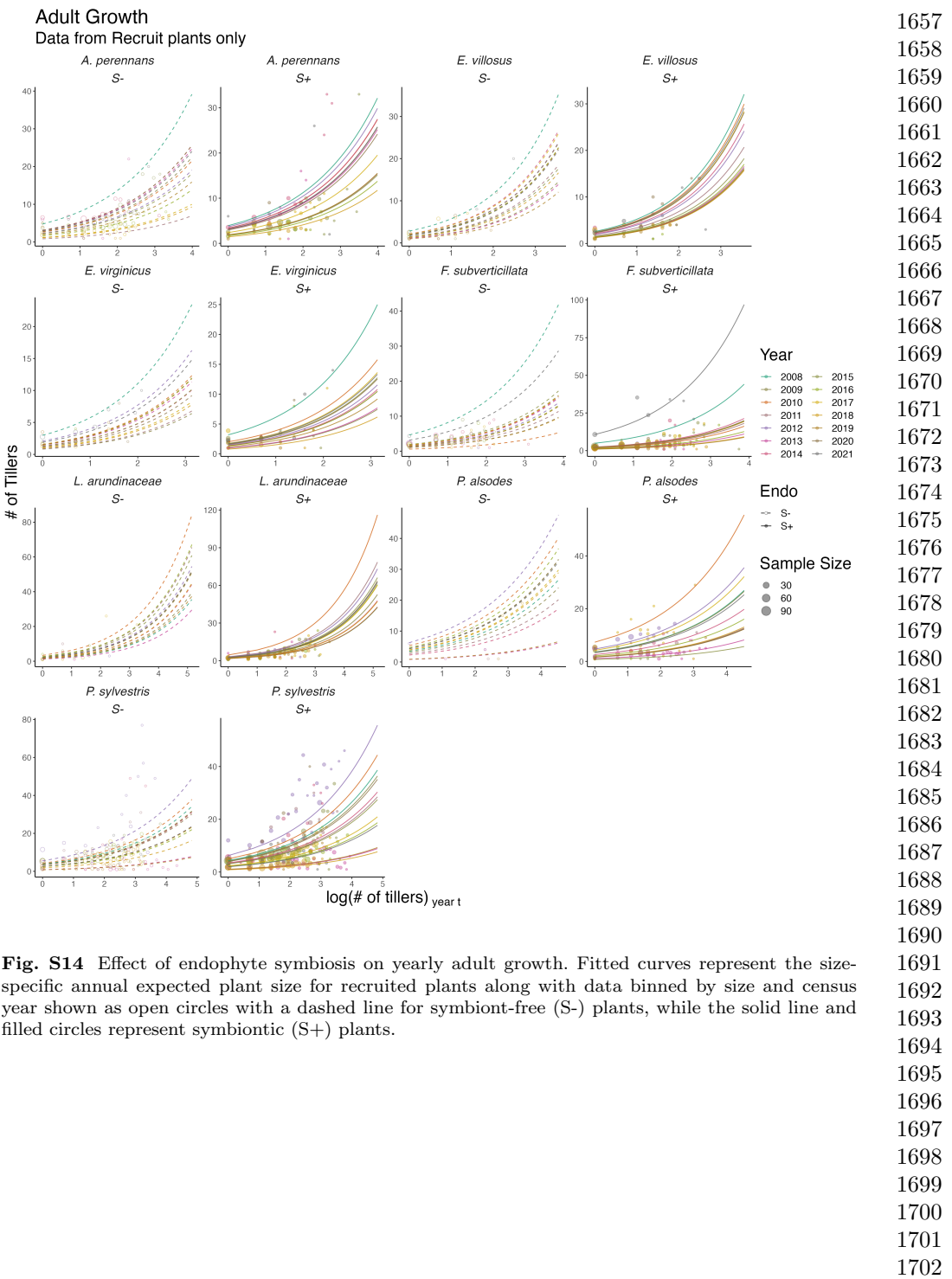
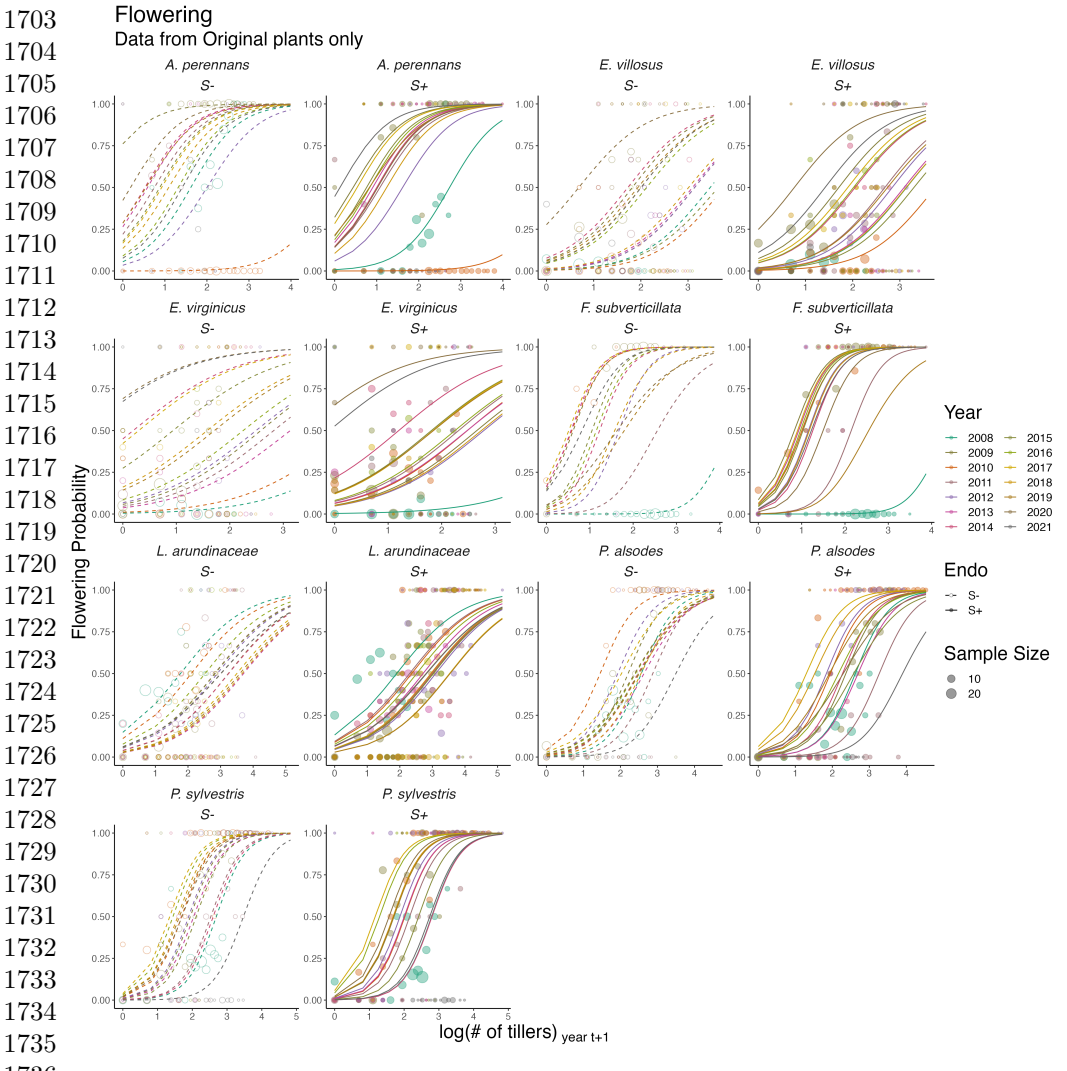


**Fig. S14** Effect of endophyte symbiosis on yearly adult growth. Fitted curves represent the size-specific annual expected plant size for recruited plants along with data binned by size and census year shown as open circles with a dashed line for symbiont-free (S-) plants, while the solid line and filled circles represent symbiotic (S+) plants.



1737 **Fig. S15** Effect of endophyte symbiosis on yearly flowering. Fitted curves represent the size-specific  
1738 annual flowering probability for original plants along with data binned by size and census year shown  
1739 as open circles with a dashed line for symbiont-free (S-) plants, while the solid line and filled circles  
1740 represent symbiotic (S+) plants.

1741  
1742  
1743  
1744  
1745  
1746  
1747  
1748

Flowering  
Data from Recruit plants only

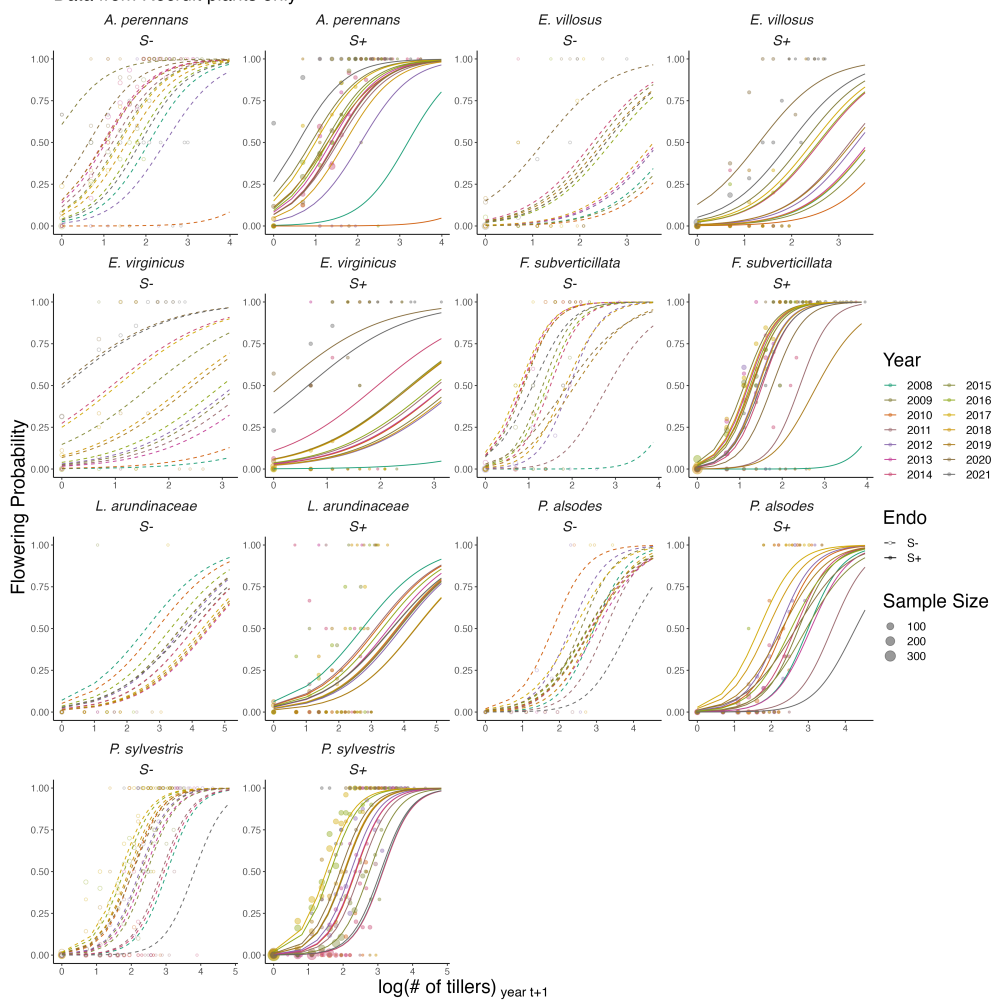
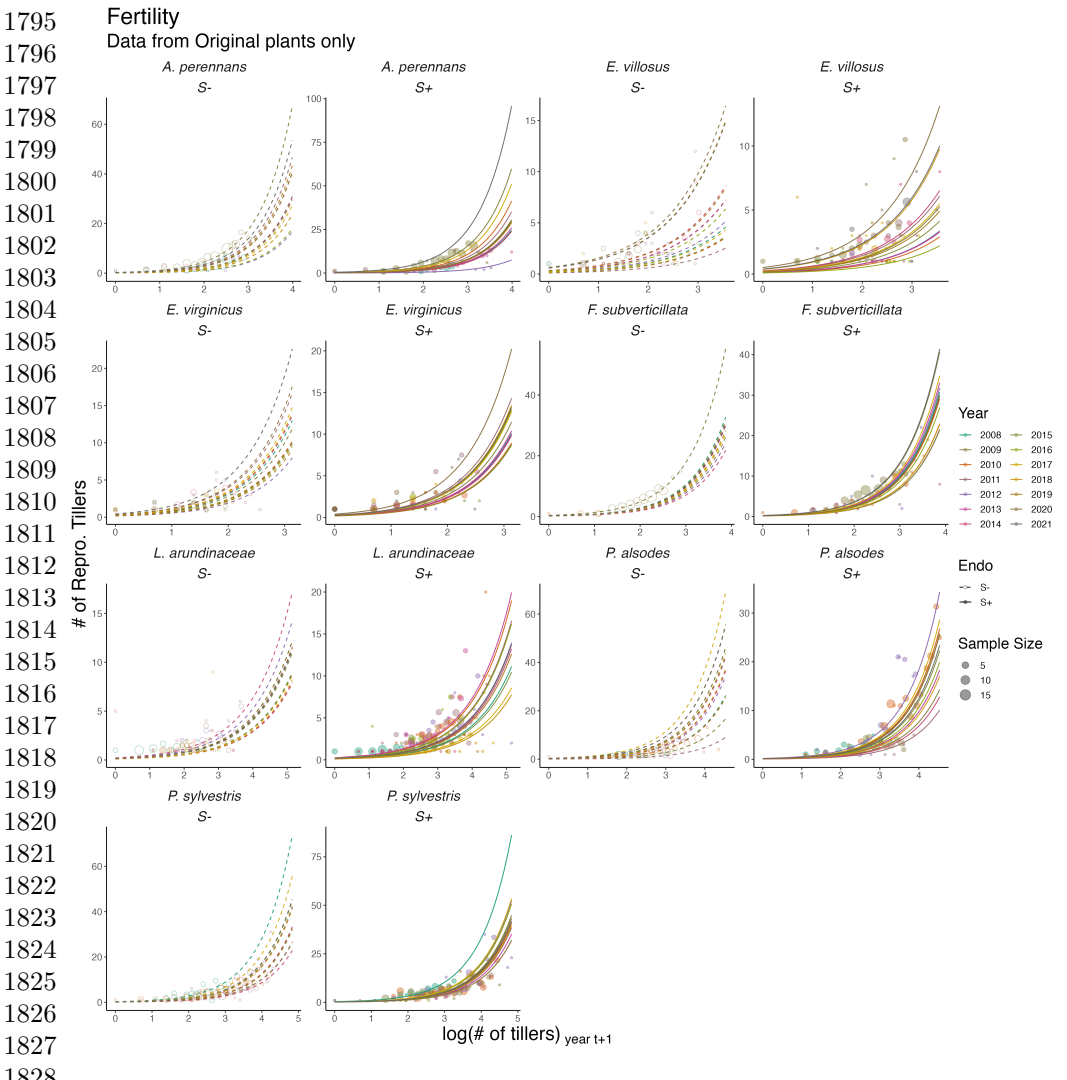


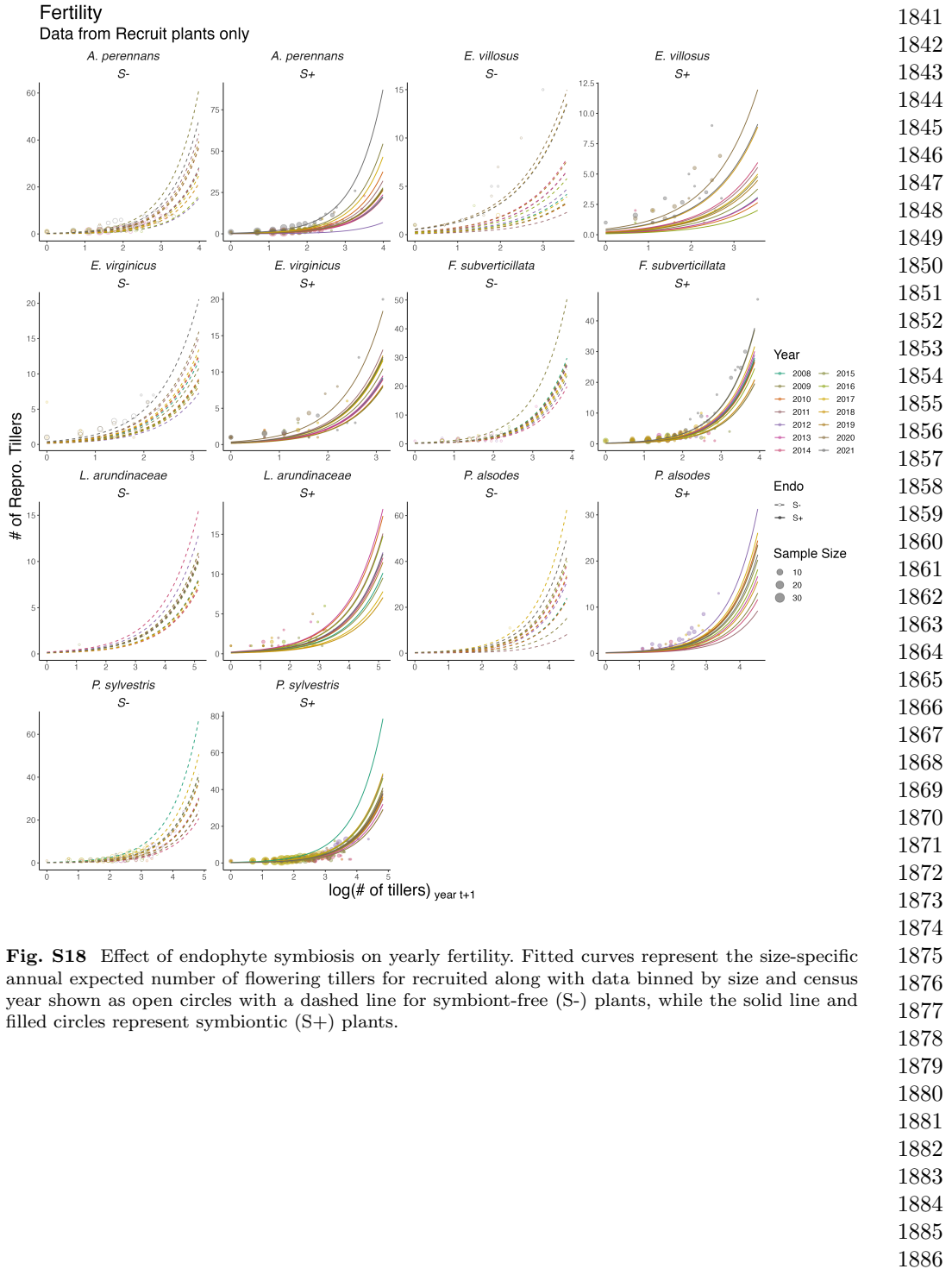
**Fig. S16** Effect of endophyte symbiosis on yearly flowering. Fitted curves represent the size-specific annual flowering probability for recruited plants along with data binned by size and census year shown as open circles with a dashed line for symbiont-free (S-) plants, while the solid line and filled circles represent symbiotic (S+) plants.

1749  
1750  
1751  
1752  
1753  
1754  
1755  
1756  
1757  
1758  
1759  
1760  
1761  
1762  
1763  
1764  
1765  
1766  
1767  
1768  
1769  
1770  
1771  
1772  
1773  
1774  
1775  
1776  
1777  
1778  
1779  
1780  
1781  
1782  
1783  
1784  
1785  
1786  
1787  
1788  
1789  
1790  
1791  
1792  
1793  
1794

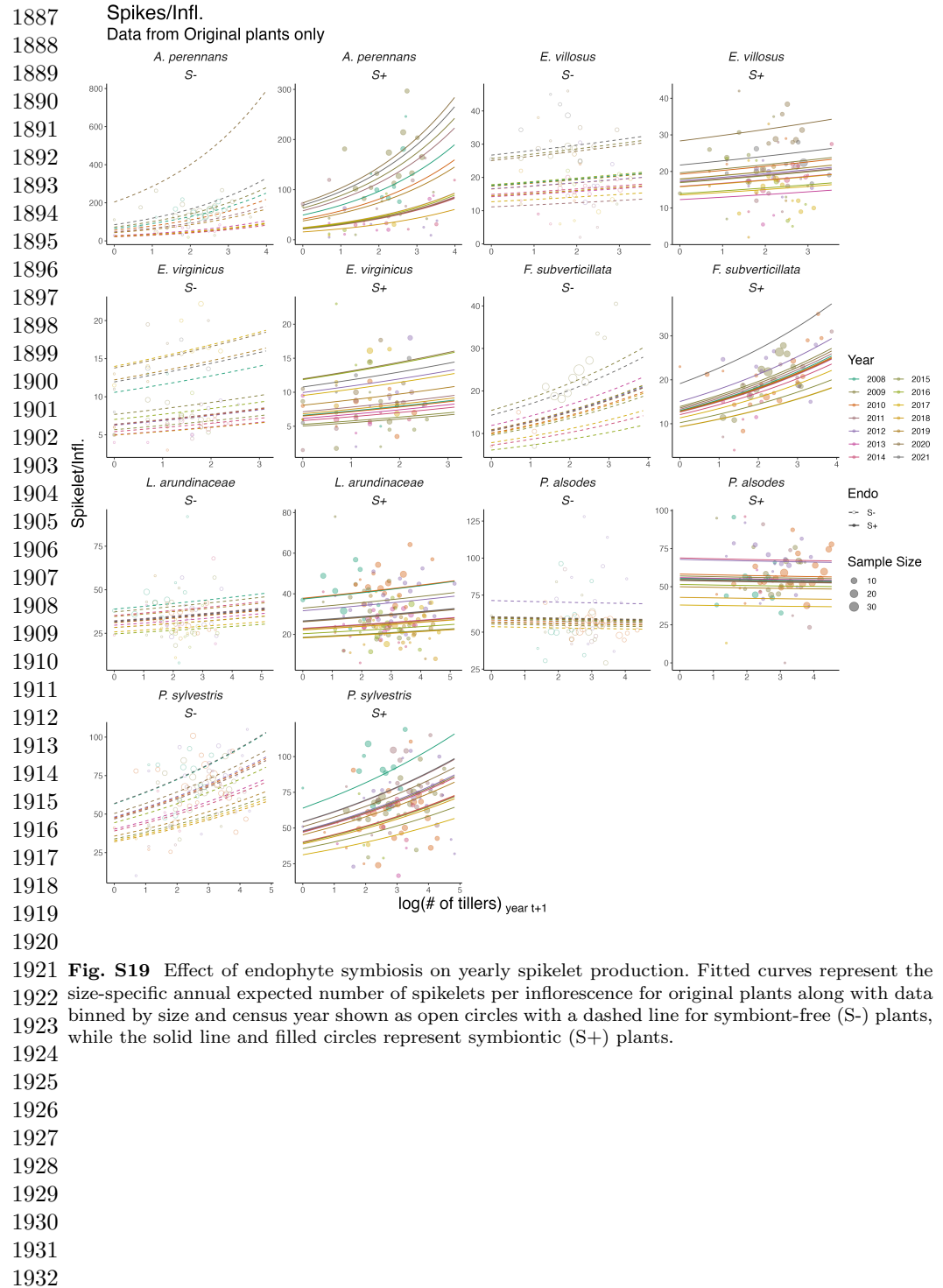


1829 **Fig. S17** Effect of endophyte symbiosis on yearly fertility. Fitted curves represent the size-specific  
 1830 annual expected number of flowering tillers for original plants along with data binned by size and  
 1831 census year shown as open circles with a dashed line for symbiont-free (S-) plants, while the solid line  
 1832 and filled circles represent symbiotic (S+) plants.

1833  
 1834  
 1835  
 1836  
 1837  
 1838  
 1839  
 1840



**Fig. S18** Effect of endophyte symbiosis on yearly fertility. Fitted curves represent the size-specific annual expected number of flowering tillers for recruited along with data binned by size and census year shown as open circles with a dashed line for symbiont-free (S-) plants, while the solid line and filled circles represent symbiotic (S+) plants.



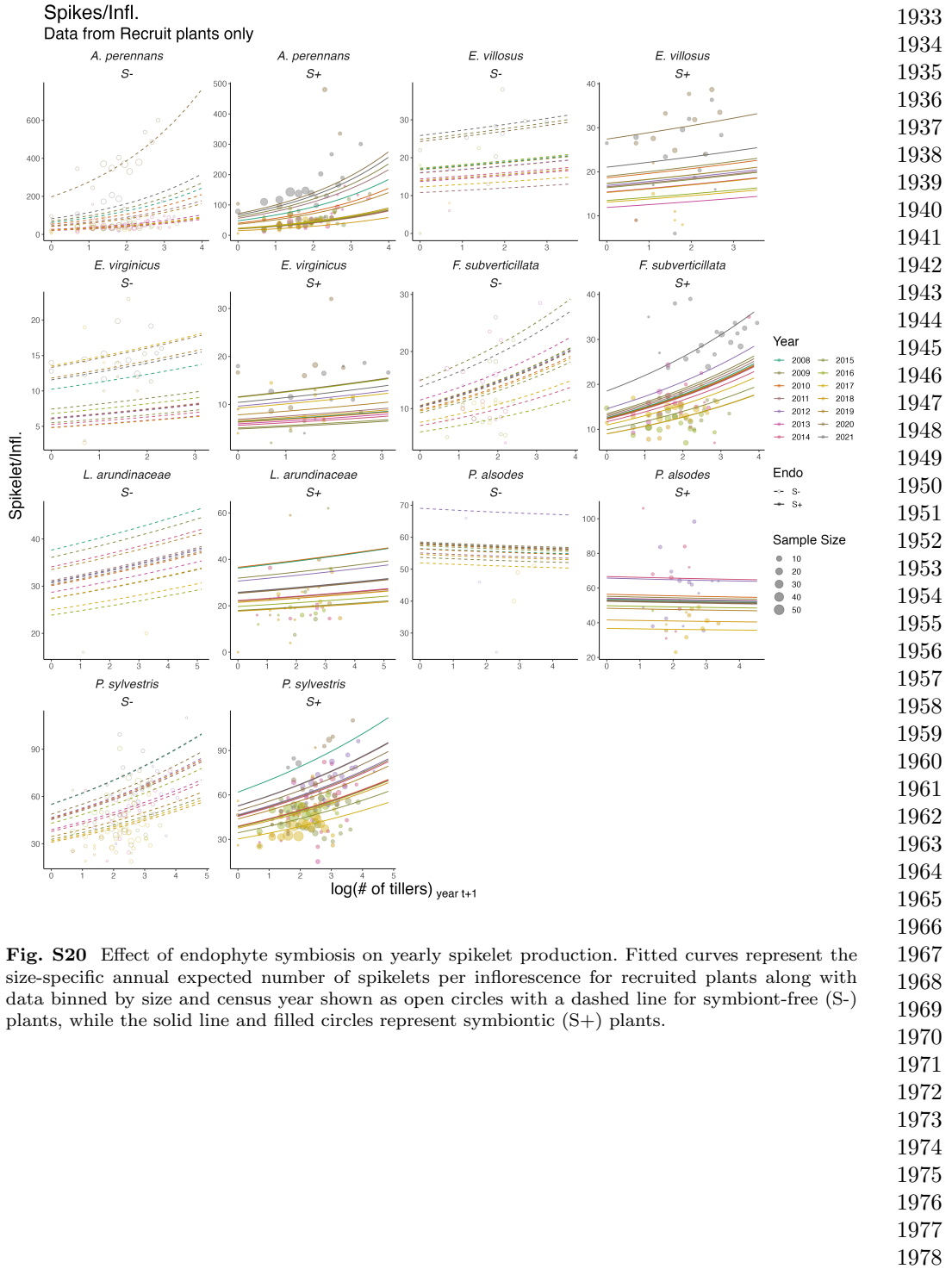
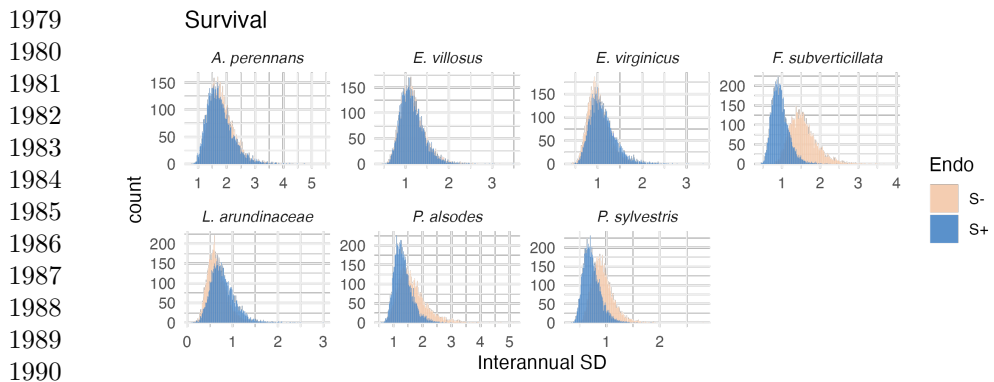


**Fig. S20** Effect of endophyte symbiosis on yearly spikelet production. Fitted curves represent the size-specific annual expected number of spikelets per inflorescence for recruited plants along with data binned by size and census year shown as open circles with a dashed line for symbiont-free (S-) plants, while the solid line and filled circles represent symbiotic (S+) plants.



1991 **Fig. S21** Posterior distributions of the standard deviations of inter-annual year effects for survival.

1992 Histograms include 7500 post-warmup MCMC samples for symbiotic (S+; blue) and symbiont-free

1993 (S-; tan) plants from fitted vital rate model.

1994

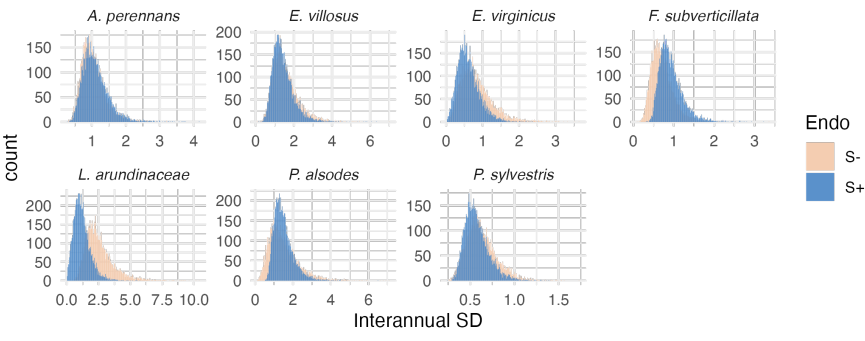
1995

1996

1997

### Seedling Survival

1998



2009 **Fig. S22** Posterior distributions of the standard deviations of inter-annual year effects for seedling survival.

2010 Histograms include 7500 post-warmup MCMC samples for symbiotic (S+; blue) and symbiont-free

2011 (S-; tan) plants from fitted vital rate model.

2012

2013

2014

2015

2016

2017

2018

2019

2020

2021

2022

2023

2024

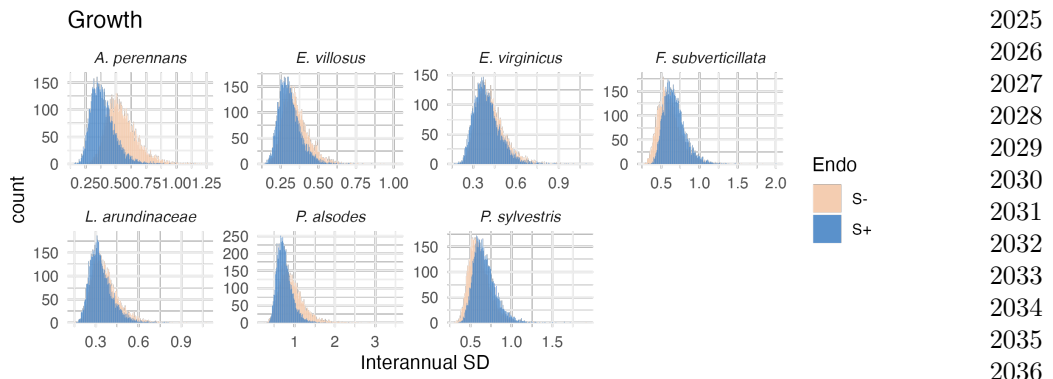


**Fig. S23** Posterior distributions of the standard deviations of inter-annual year effects for growth. Histograms include 7500 post-warmup MCMC samples for symbiotic (S+; blue) and symbiont-free (S-; tan) plants from fitted vital rate model.

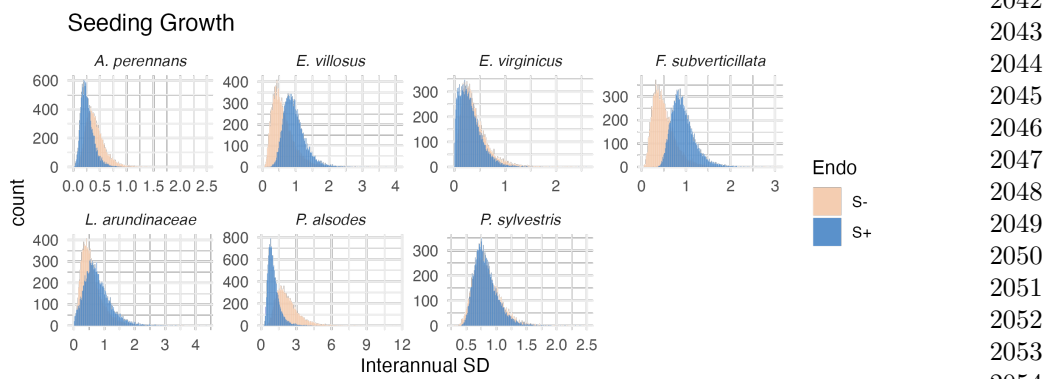
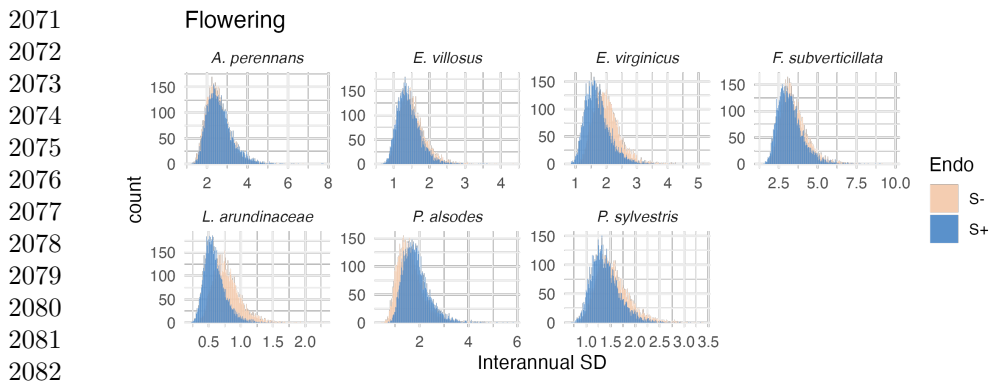
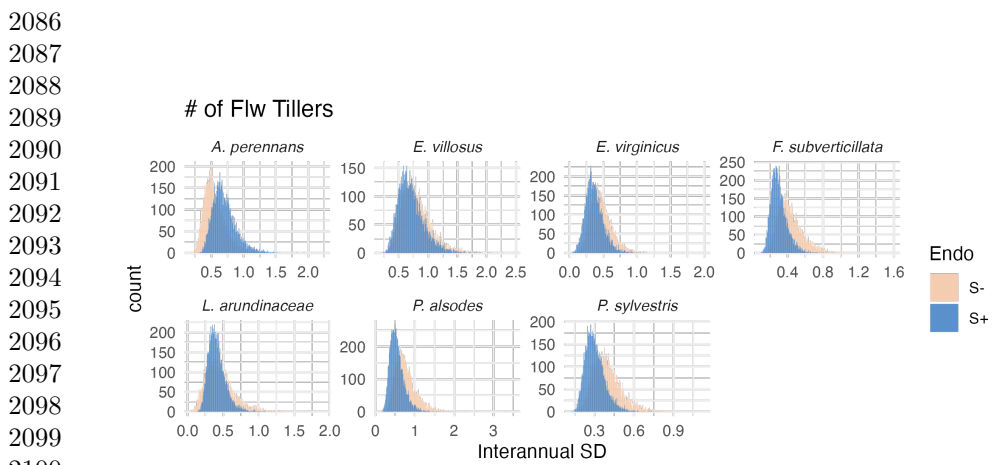


**Fig. S24** Posterior distributions of the standard deviations of inter-annual year effects for seedling growth. Histograms include 7500 post-warmup MCMC samples for symbiotic (S+; blue) and symbiont-free (S-; tan) plants from fitted vital rate model.

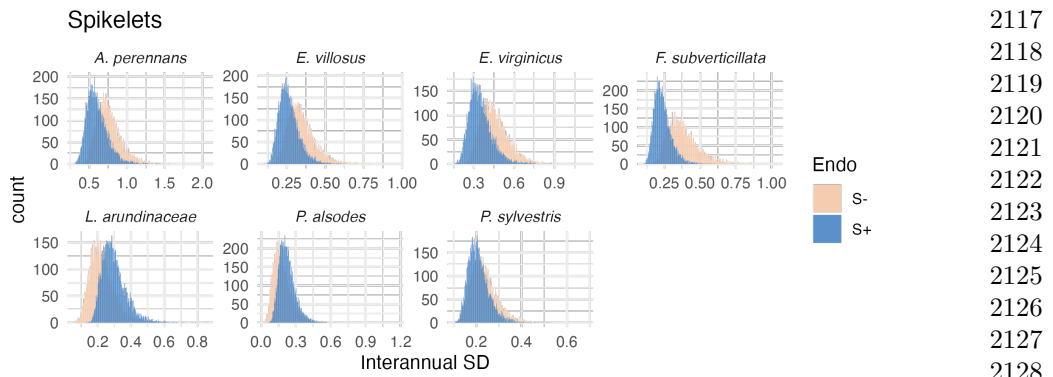
2025  
2026  
2027  
2028  
2029  
2030  
2031  
2032  
2033  
2034  
2035  
2036  
2037  
2038  
2039  
2040  
2041  
2042  
2043  
2044  
2045  
2046  
2047  
2048  
2049  
2050  
2051  
2052  
2053  
2054  
2055  
2056  
2057  
2058  
2059  
2060  
2061  
2062  
2063  
2064  
2065  
2066  
2067  
2068  
2069  
2070



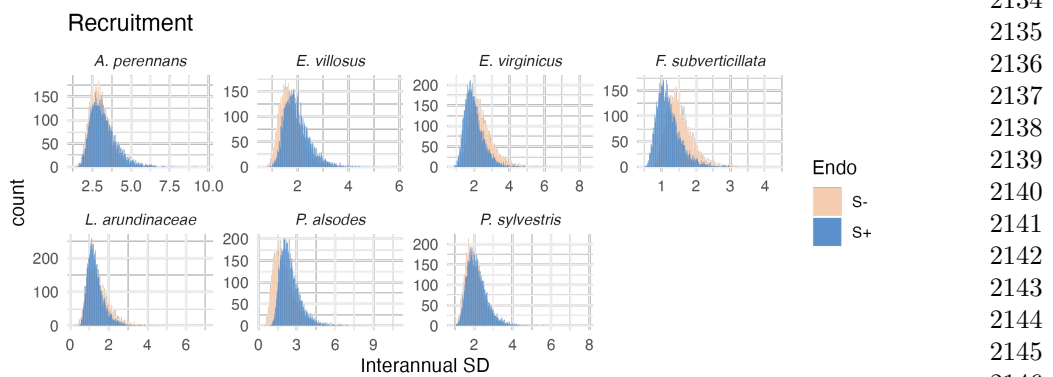
2083 **Fig. S25** Posterior distributions of the standard deviations of inter-annual year effects for flowering  
 2084 probability. Histograms include 7500 post-warmup MCMC samples for symbiotic (S+; blue) and  
 2085 symbiont-free (S-; tan) plants from fitted vital rate model.



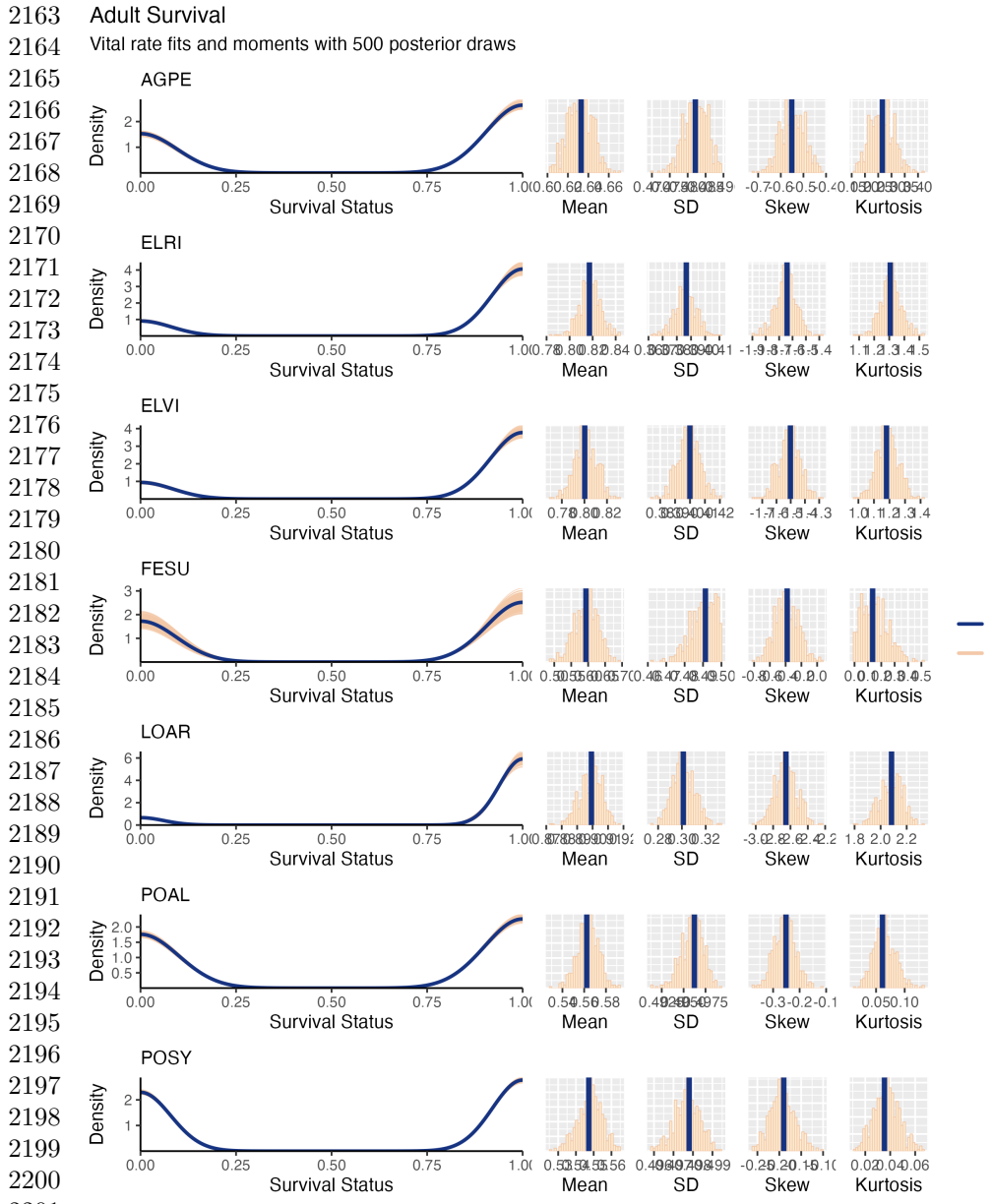
**Fig. S26** Posterior distributions of the standard deviations of inter-annual year effects for fertility (no. of flowering tillers). Histograms include 7500 post-warmup MCMC samples for symbiotic (S+; blue) and symbiont-free (S-; tan) plants from fitted vital rate model.



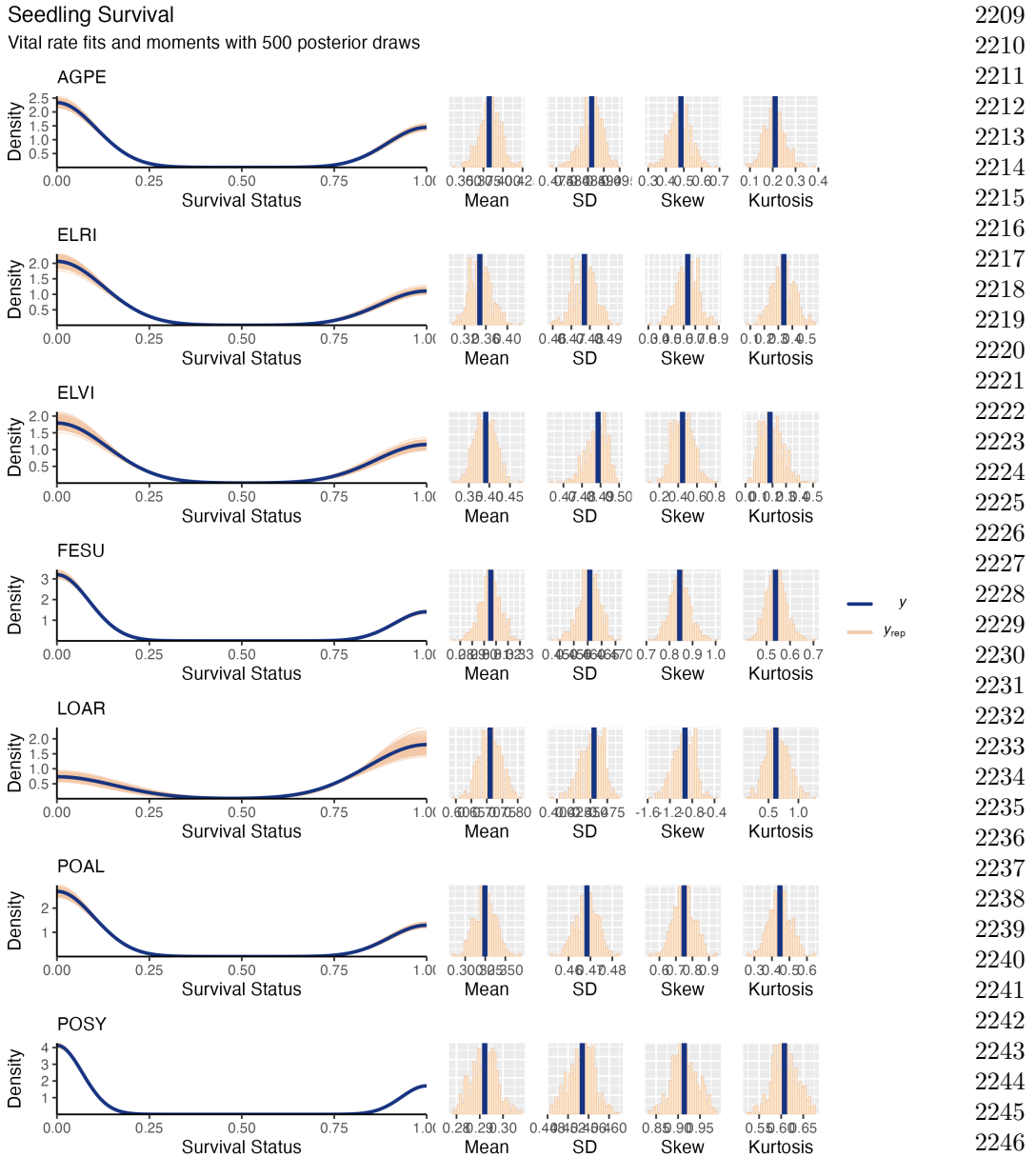
**Fig. S27** Posterior distributions of the standard deviations of inter-annual year effects for spikelets per inflorescence. Histograms include 7500 post-warmup MCMC samples for symbiotic (S+; blue) and symbiont-free (S-; tan) plants from fitted vital rate model.



**Fig. S28** Posterior distributions of the standard deviations of inter-annual year effects for recruitment. Histograms include 7500 post-warmup MCMC samples for symbiotic (S+; blue) and symbiont-free (S-; tan) plants from fitted vital rate model.

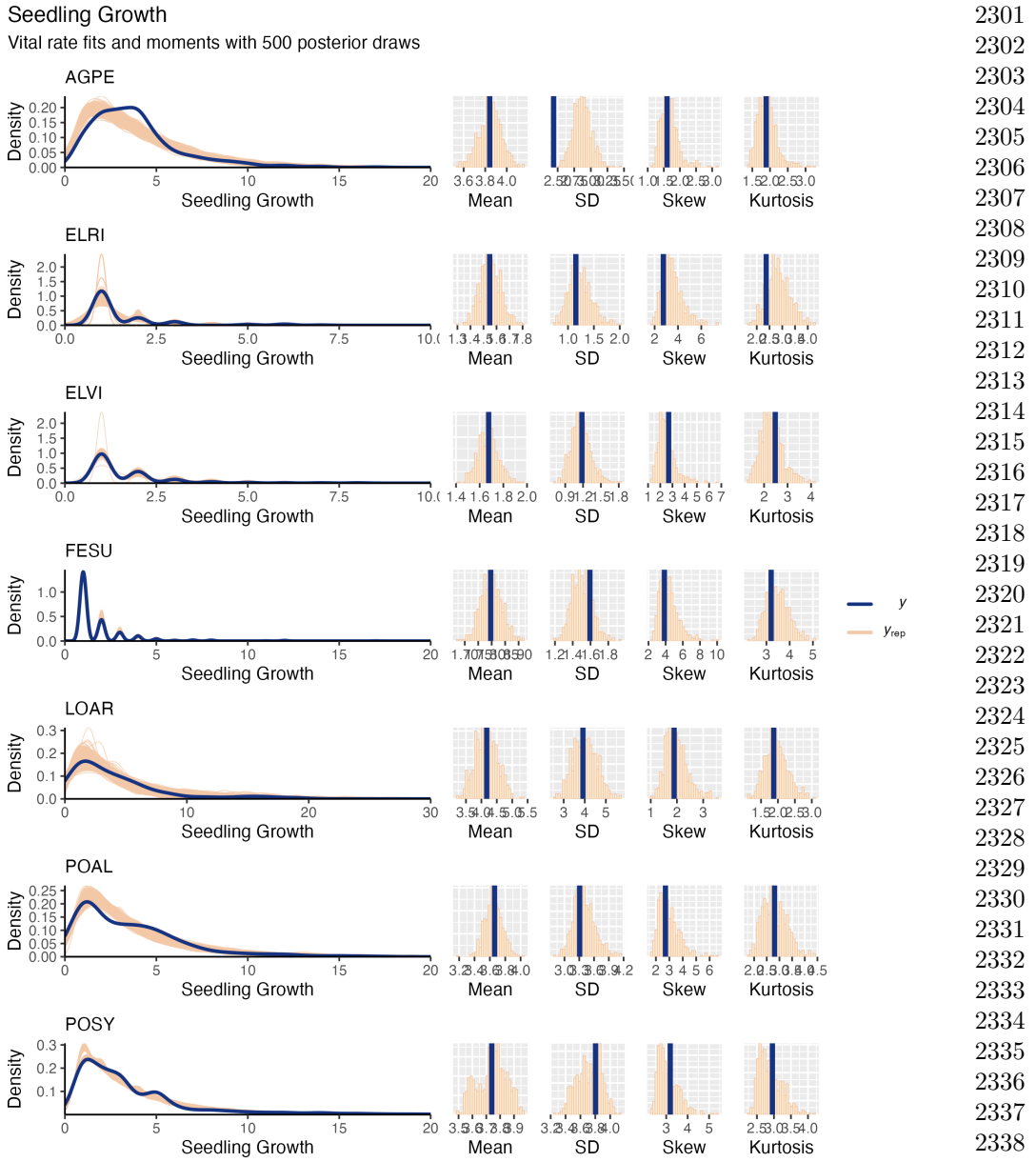


**Fig. S29** Posterior predictive check for statistical model of Adult Survival. Consistency between real data and simulated values indicates that fitted models describe the data well. Lines show density distributions of observed data (blue line) compared to data simulated from fitted models (tan lines) generated from 500 draws from posterior distributions of model parameters along with the distribution's moments.



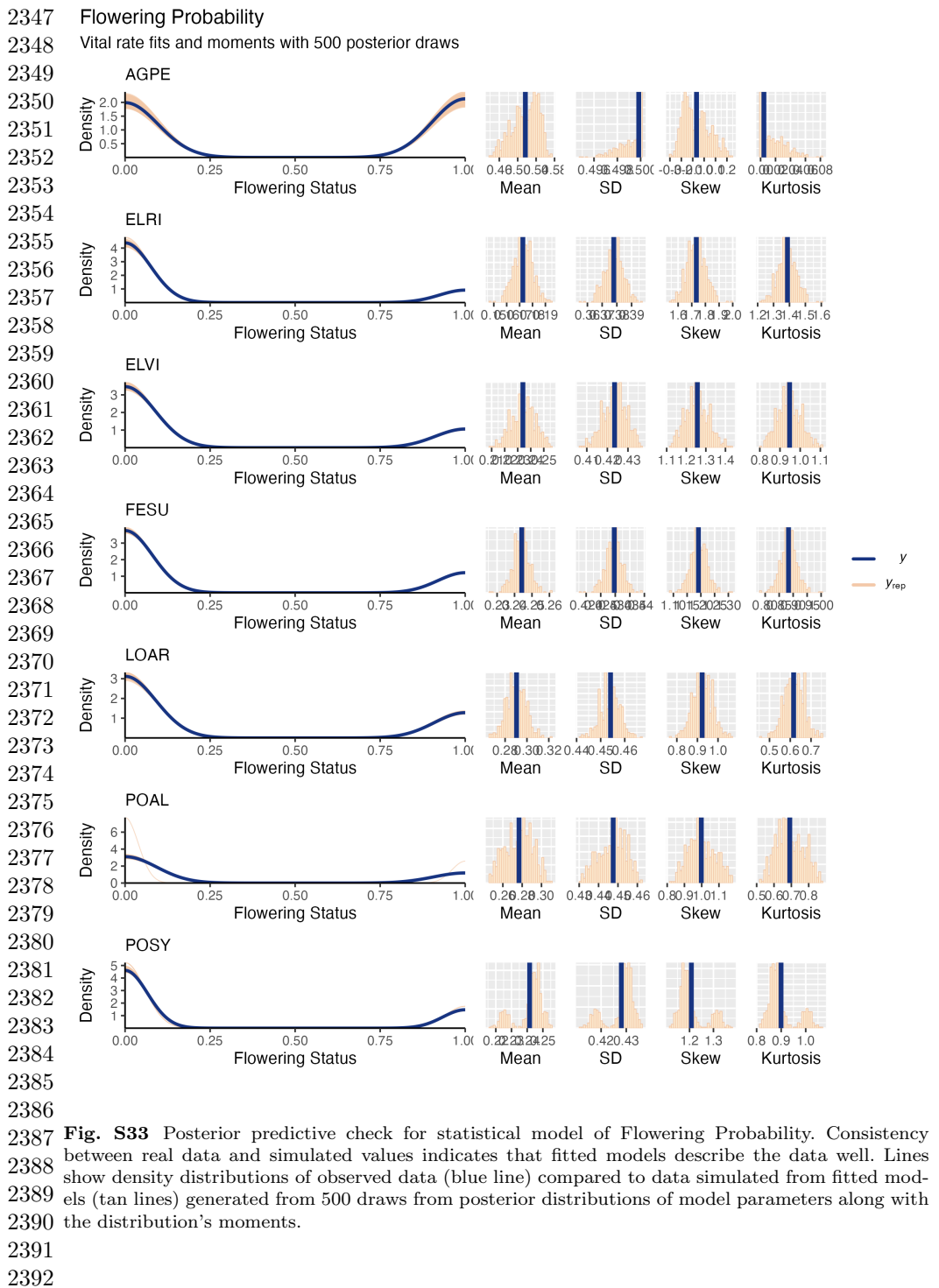
**Fig. S30** Posterior predictive check for statistical model of Seedling Survival. Consistency between real data and simulated values indicates that fitted models describe the data well. Lines show density distributions of observed data (blue line) compared to data simulated from fitted models (tan lines) generated from 500 draws from posterior distributions of model parameters along with the distribution's moments.

**Fig. S31** Posterior predictive check for statistical model of Adult Growth. Consistency between real data and simulated values indicates that fitted models describe the data well. Lines show density distributions of observed data (blue line) compared to data simulated from fitted models (tan lines) generated from 500 draws from posterior distributions of model parameters along with the distribution's moments.



**Fig. S32** Posterior predictive check for statistical model of Seedling Growth. Consistency between real data and simulated values indicates that fitted models describe the data well. Lines show density distributions of observed data (blue line) compared to data simulated from fitted models (tan lines) generated from 500 draws from posterior distributions of model parameters along with the distribution's moments.

2301  
2302  
2303  
2304  
2305  
2306  
2307  
2308  
2309  
2310  
2311  
2312  
2313  
2314  
2315  
2316  
2317  
2318  
2319  
2320  
2321  
2322  
2323  
2324  
2325  
2326  
2327  
2328  
2329  
2330  
2331  
2332  
2333  
2334  
2335  
2336  
2337  
2338  
2339  
2340  
2341  
2342  
2343  
2344  
2345  
2346



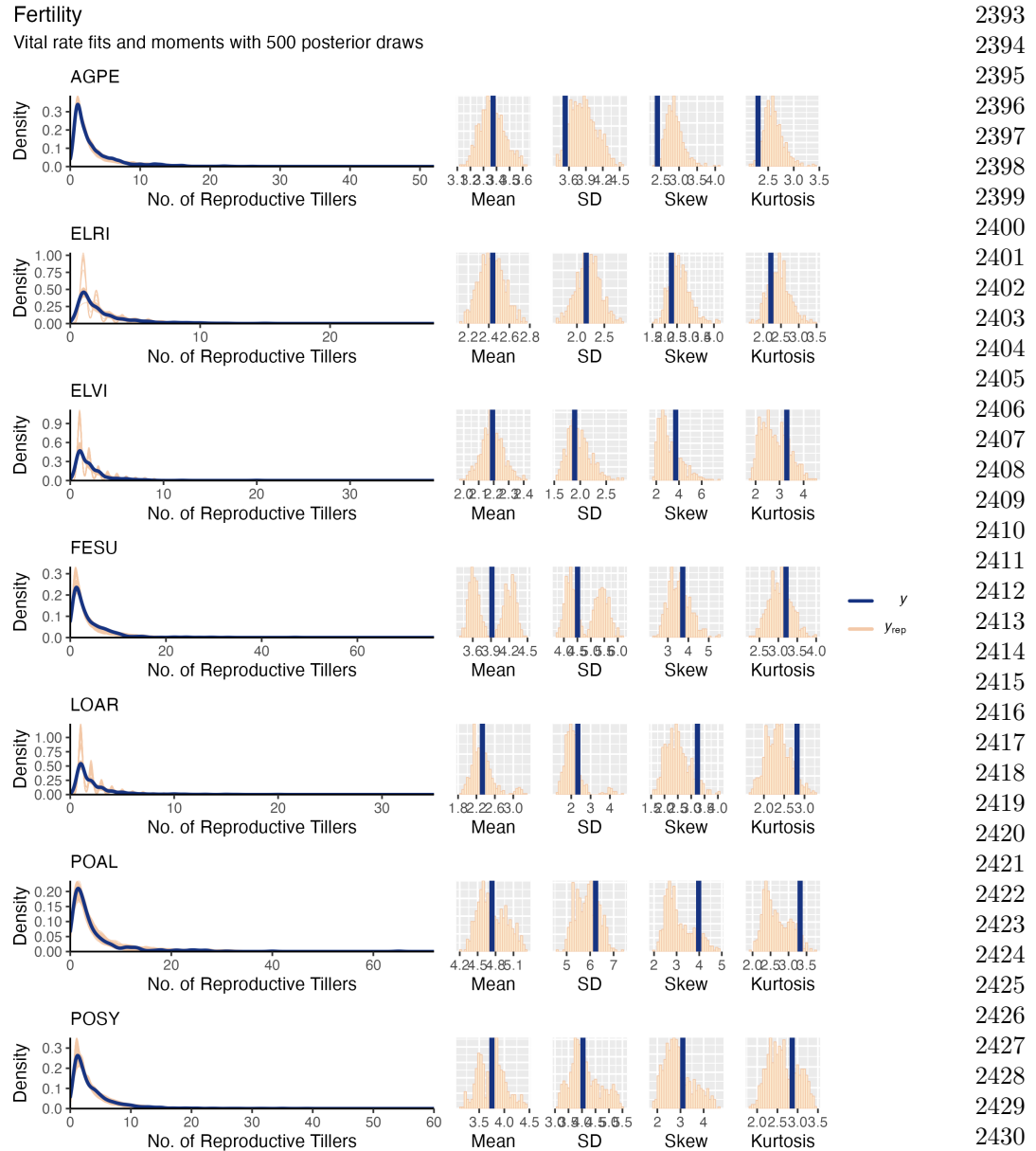


**Fig. S34** Posterior predictive check for statistical model of Flowering Tiller production. Consistency between real data and simulated values indicates that fitted models describe the data well. Lines show density distributions of observed data (blue line) compared to data simulated from fitted models (tan lines) generated from 500 draws from posterior distributions of model parameters along with the distribution's moments.

## 2439 Spikelet Production

2440 Vital rate fits and moments with 500 posterior draws

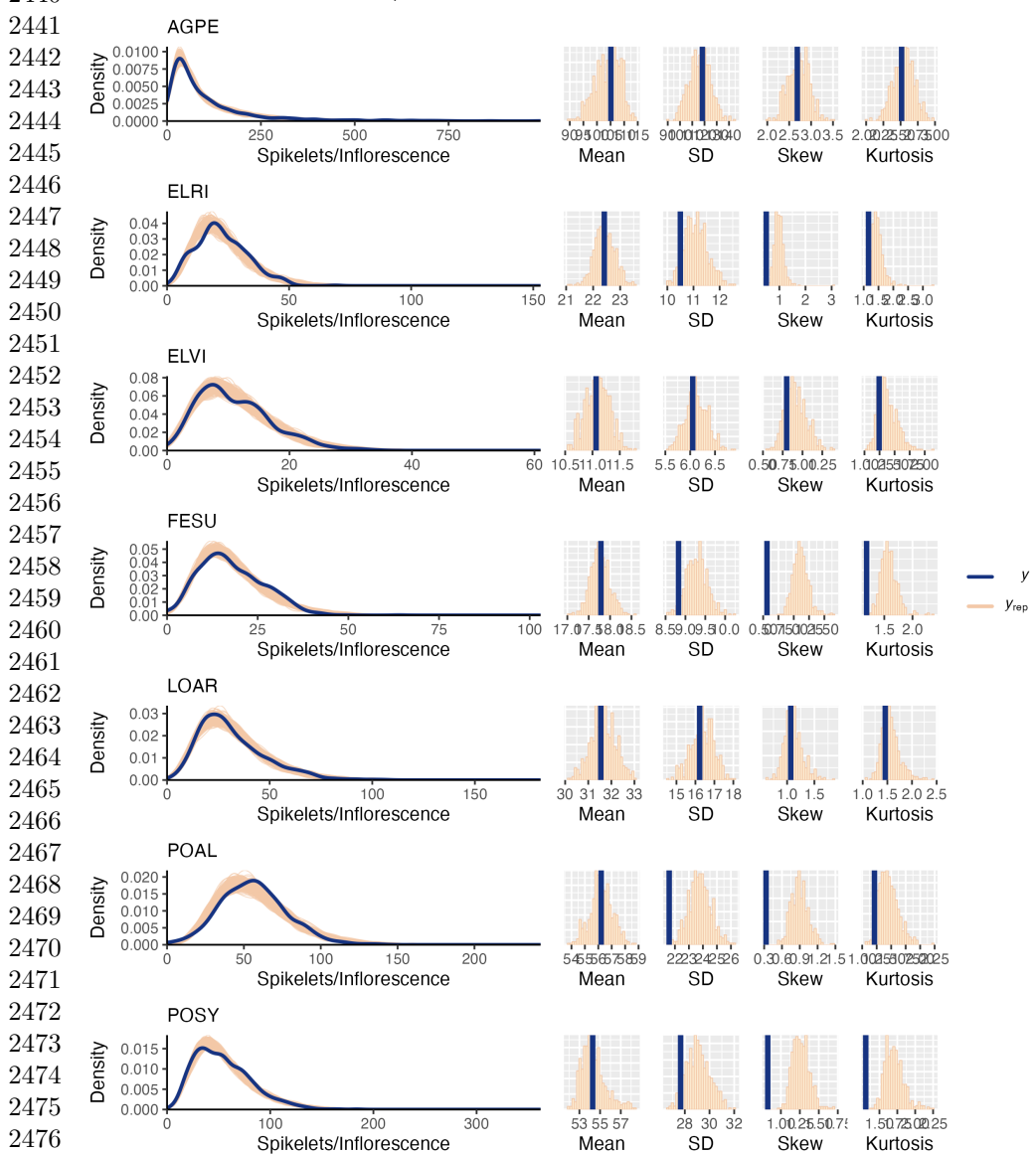


**Fig. S35** Posterior predictive check for statistical model of Spikelets/Inflorescence. Consistency between real data and simulated values indicates that fitted models describe the data well. Lines show density distributions of observed data (blue line) compared to data simulated from fitted models (tan lines) generated from 500 draws from posterior distributions of model parameters along with the distribution's moments.

2483

2484

Seed Production  
Vital rate fits and moments with 500 posterior draws

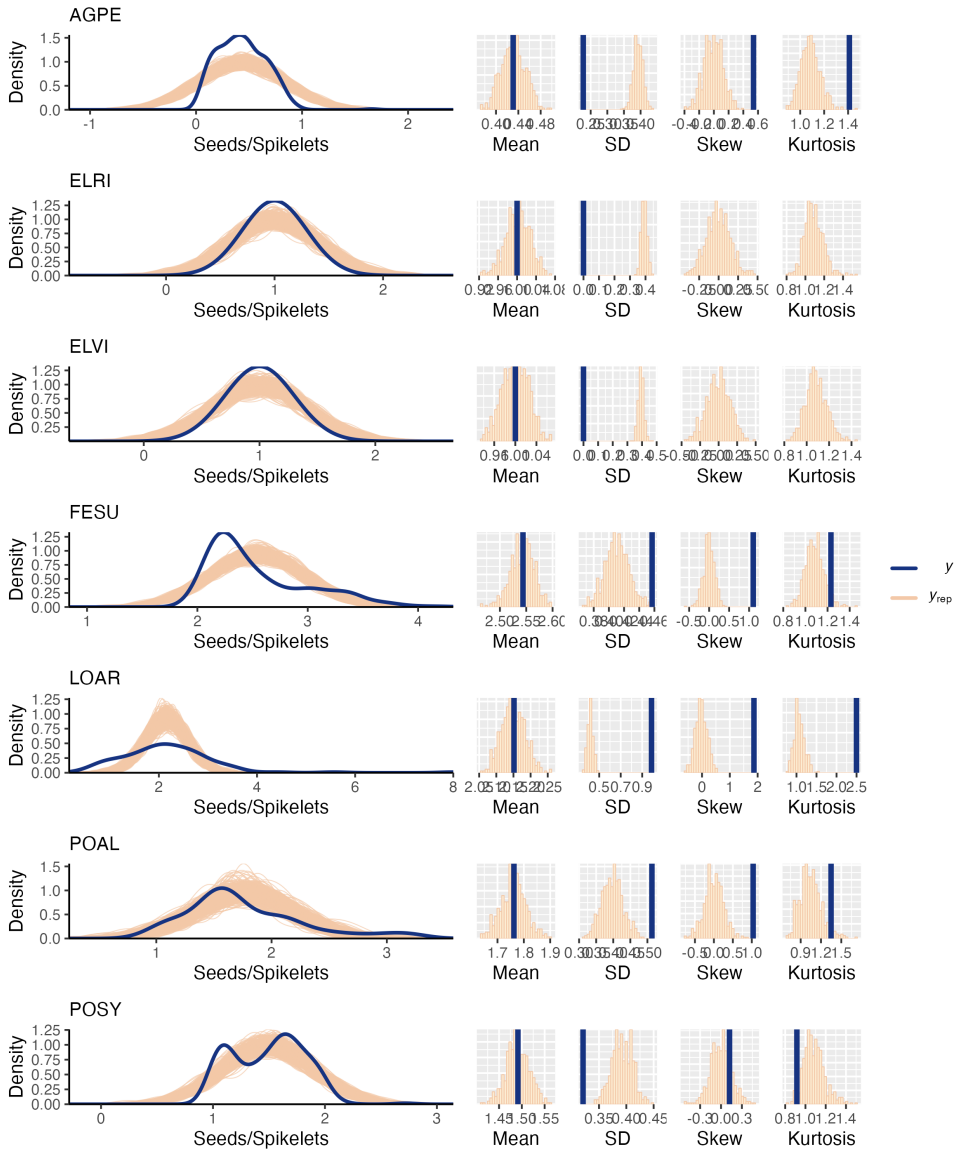


**Fig. S36** Posterior predictive check for statistical model of Mean Seeds/Spikelet. Consistency between real data and simulated values indicates that fitted models describe the data well. Lines show density distributions of observed data (blue line) compared to data simulated from fitted models (tan lines) generated from 500 draws from posterior distributions of model parameters along with the distribution's moments.

2485  
2486  
2487  
2488  
2489  
2490  
2491  
2492  
2493  
2494  
2495  
2496  
2497  
2498  
2499  
2500  
2501  
2502  
2503  
2504  
2505  
2506  
2507  
2508  
2509  
2510  
2511  
2512  
2513  
2514  
2515  
2516  
2517  
2518  
2519  
2520  
2521  
2522  
2523  
2524  
2525  
2526  
2527  
2528  
2529  
2530

2531 Recruitment

2532 Vital rate fits and moments with 500 posterior draws

2533 AGPE

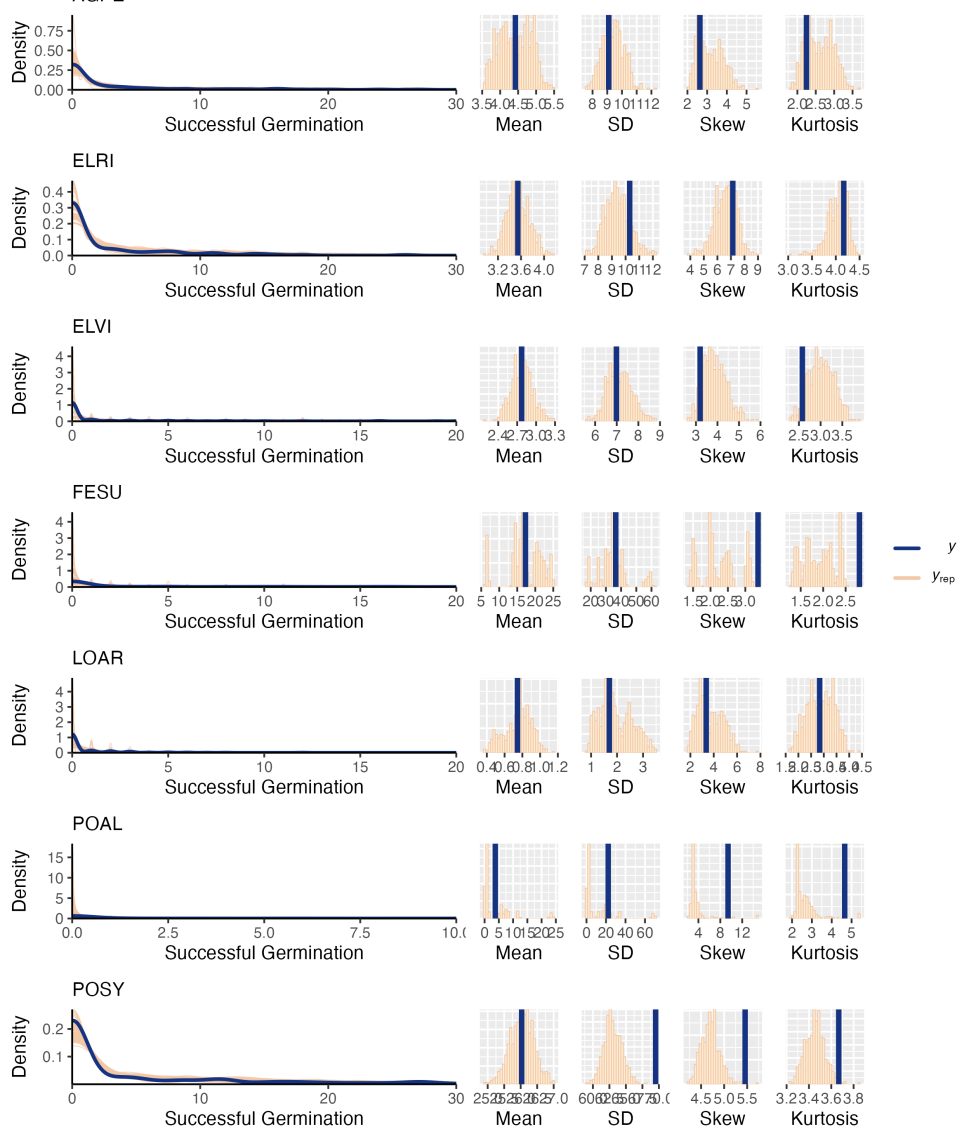


**Fig. S37** Posterior predictive check for statistical model of Recruitment. Consistency between real data and simulated values indicates that fitted models describe the data well. Lines show density distributions of observed data (blue line) compared to data simulated from fitted models (tan lines) generated from 500 draws from posterior distributions of model parameters along with the distribution's moments.

2575

2576

### Size specific vital rate moments

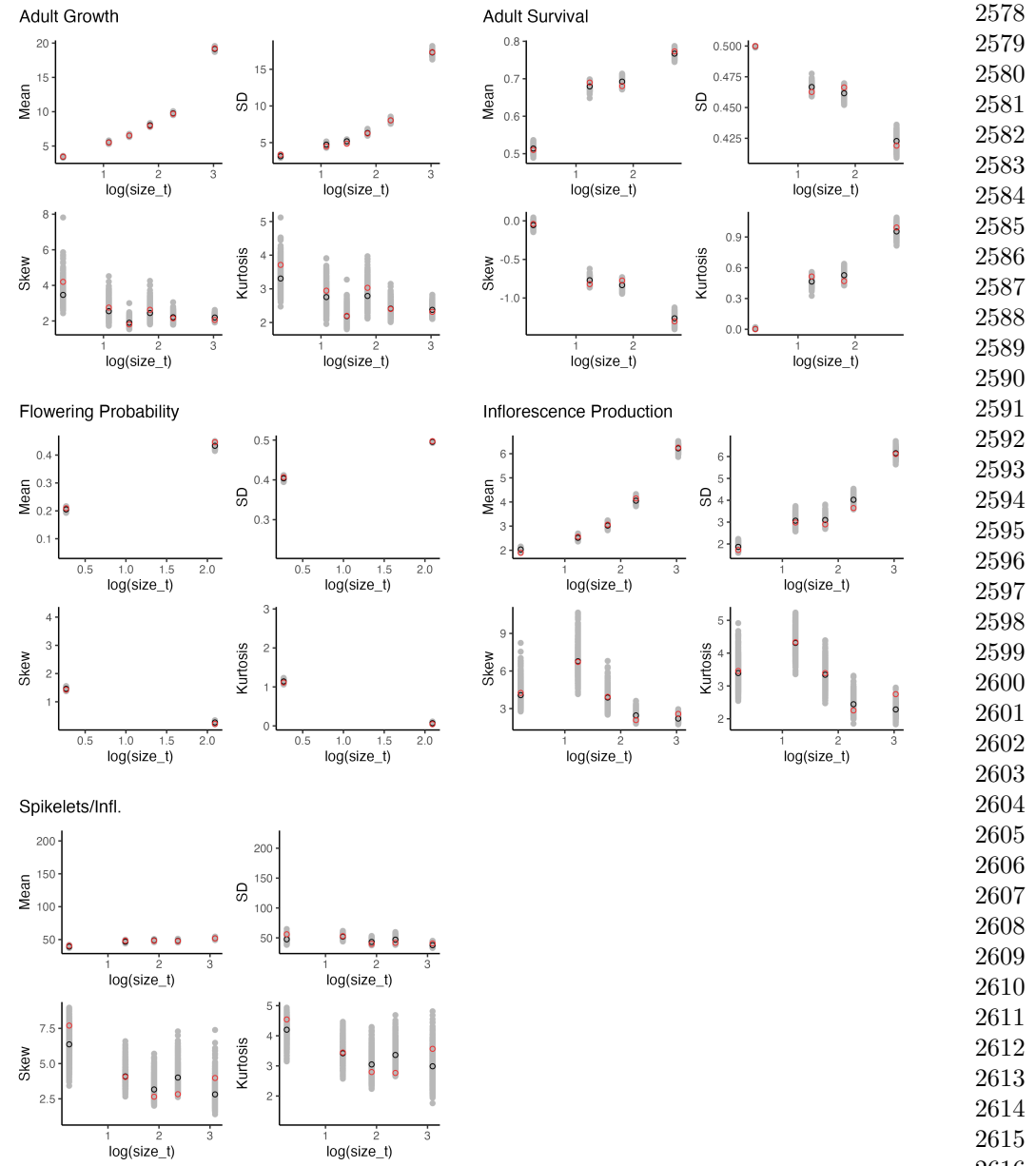
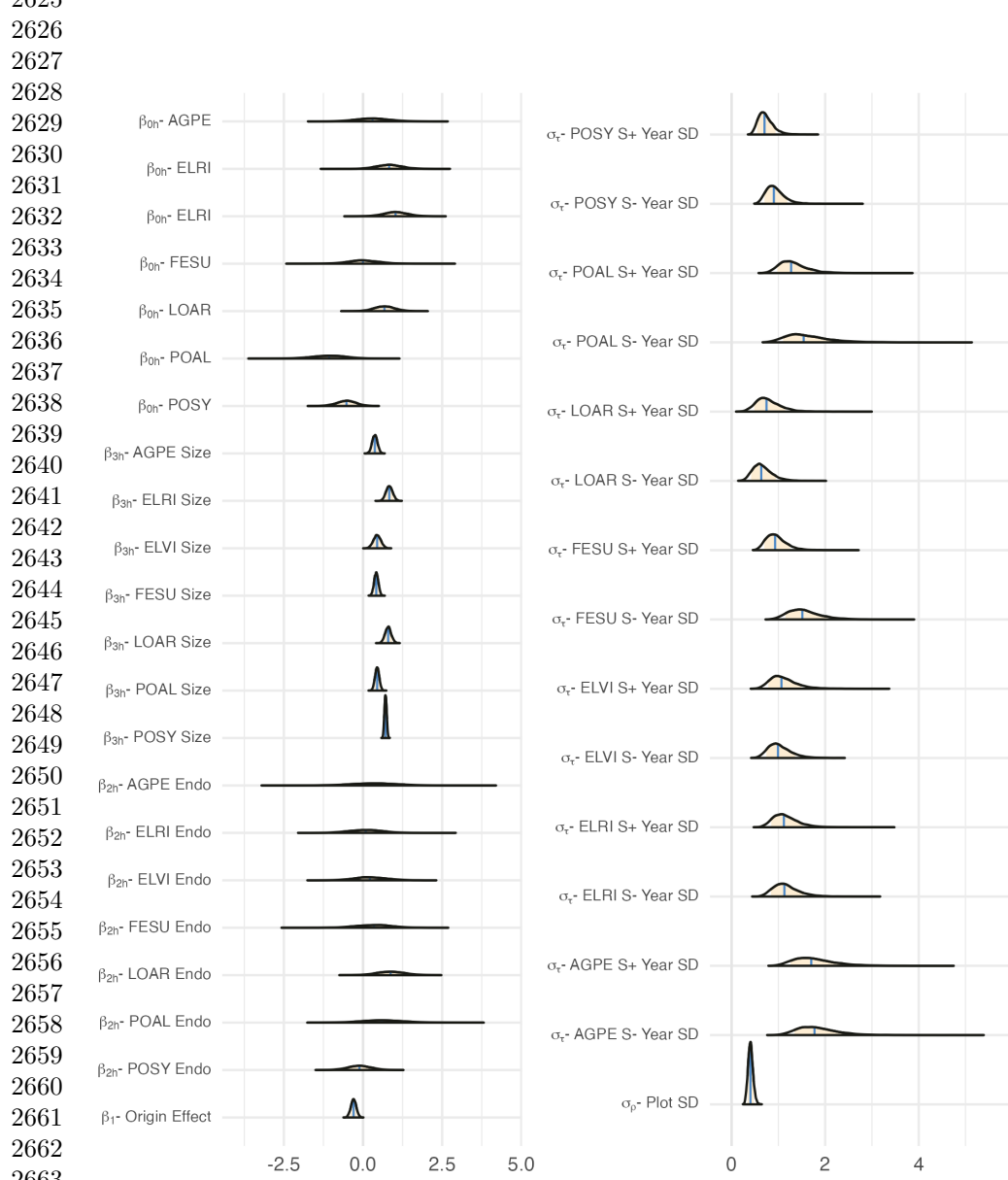
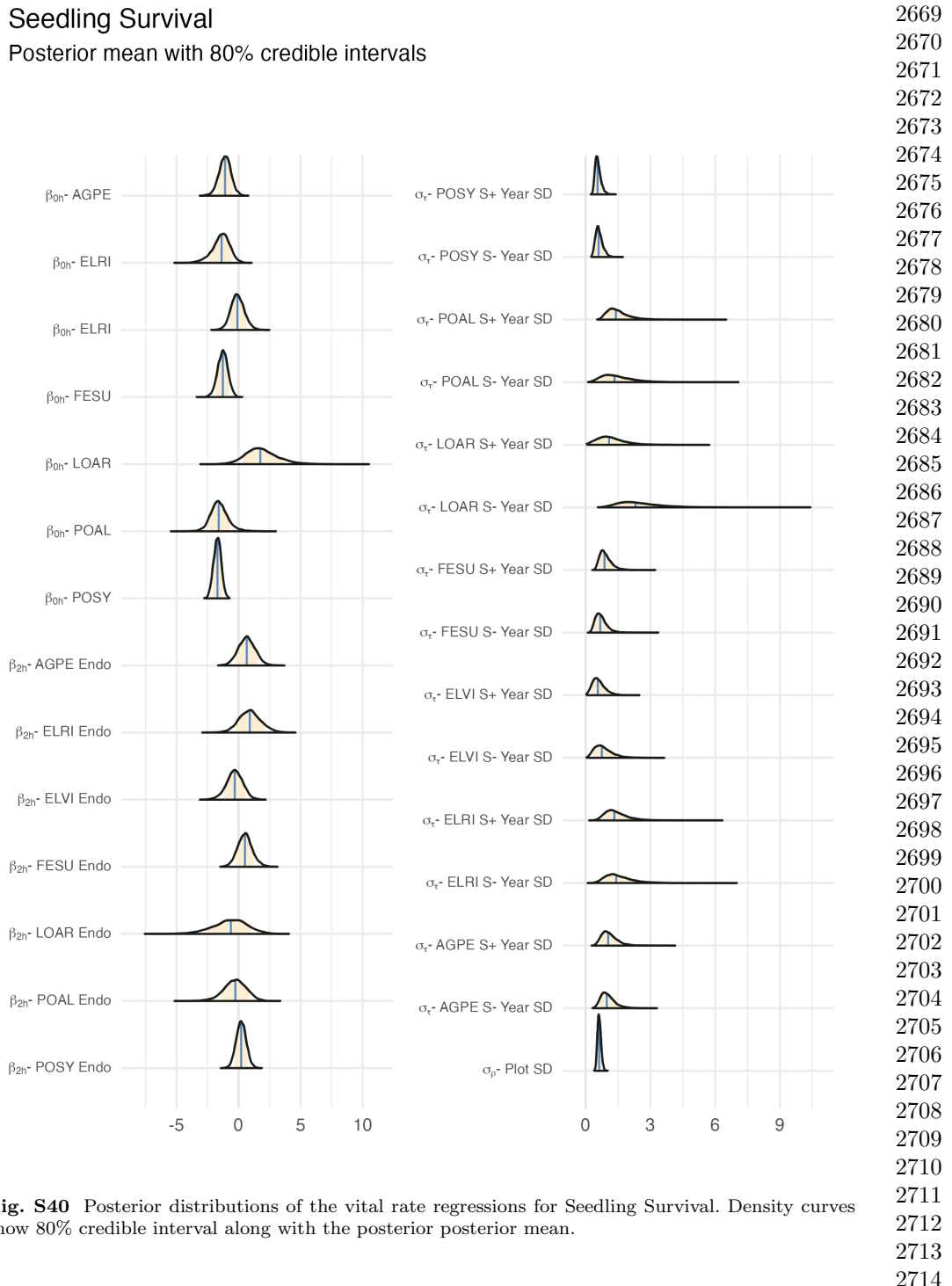


**Fig. S38** Consistency between real data and fitted values across sizes indicates that the vital rate models are accurately capturing size dependence. Graphs of posterior predictive check for mean and higher moments of the vital rate models across size. Points show the value of statistical moments binned across size for the observed data (red circles) compared to the simulated datasets (grey circles) and the median of the simulated values (black circles) generated from 500 posterior draws from the fitted model.

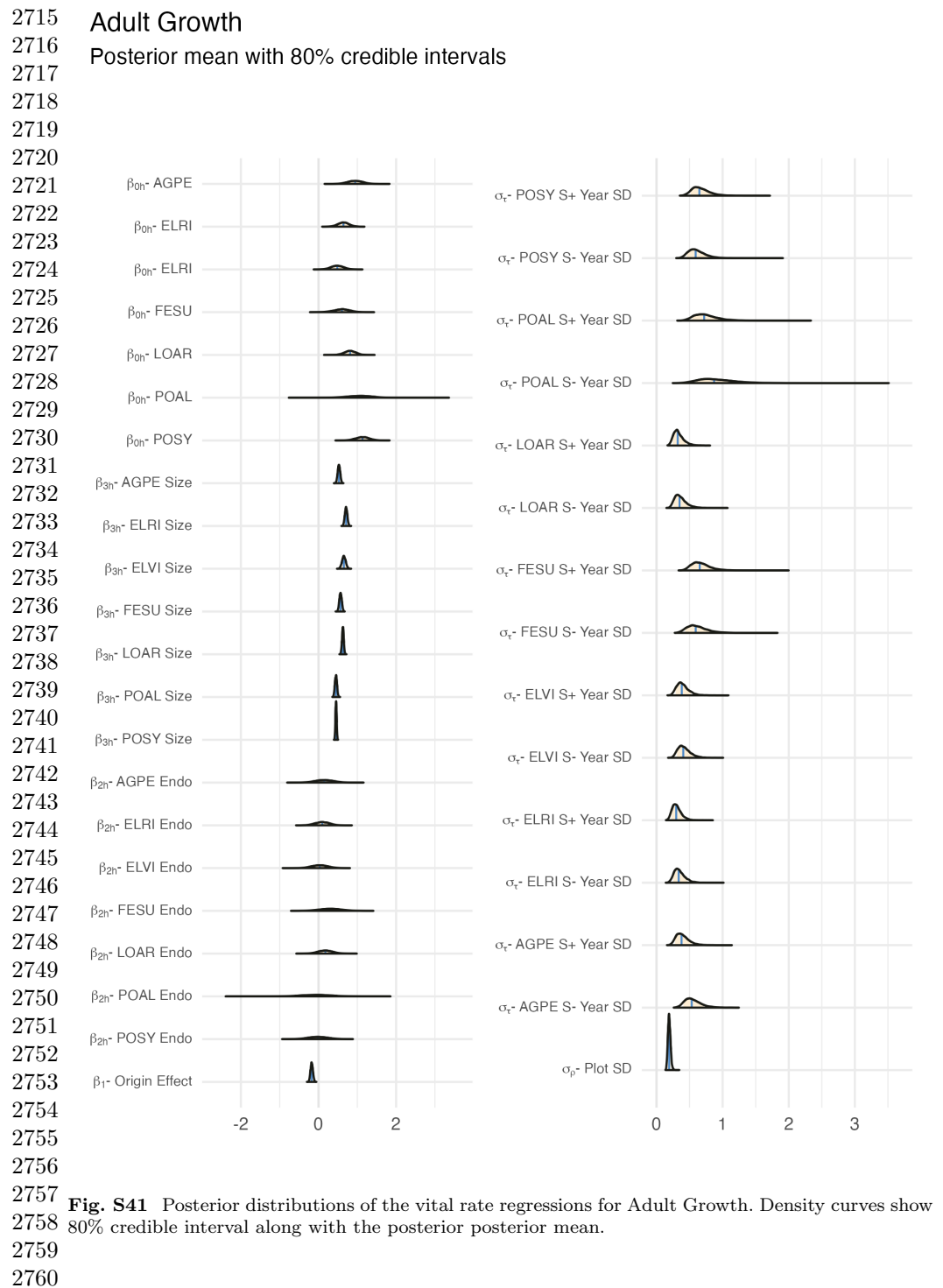
2623 Adult Survival  
 2624 Posterior mean with 80% credible intervals  
 2625

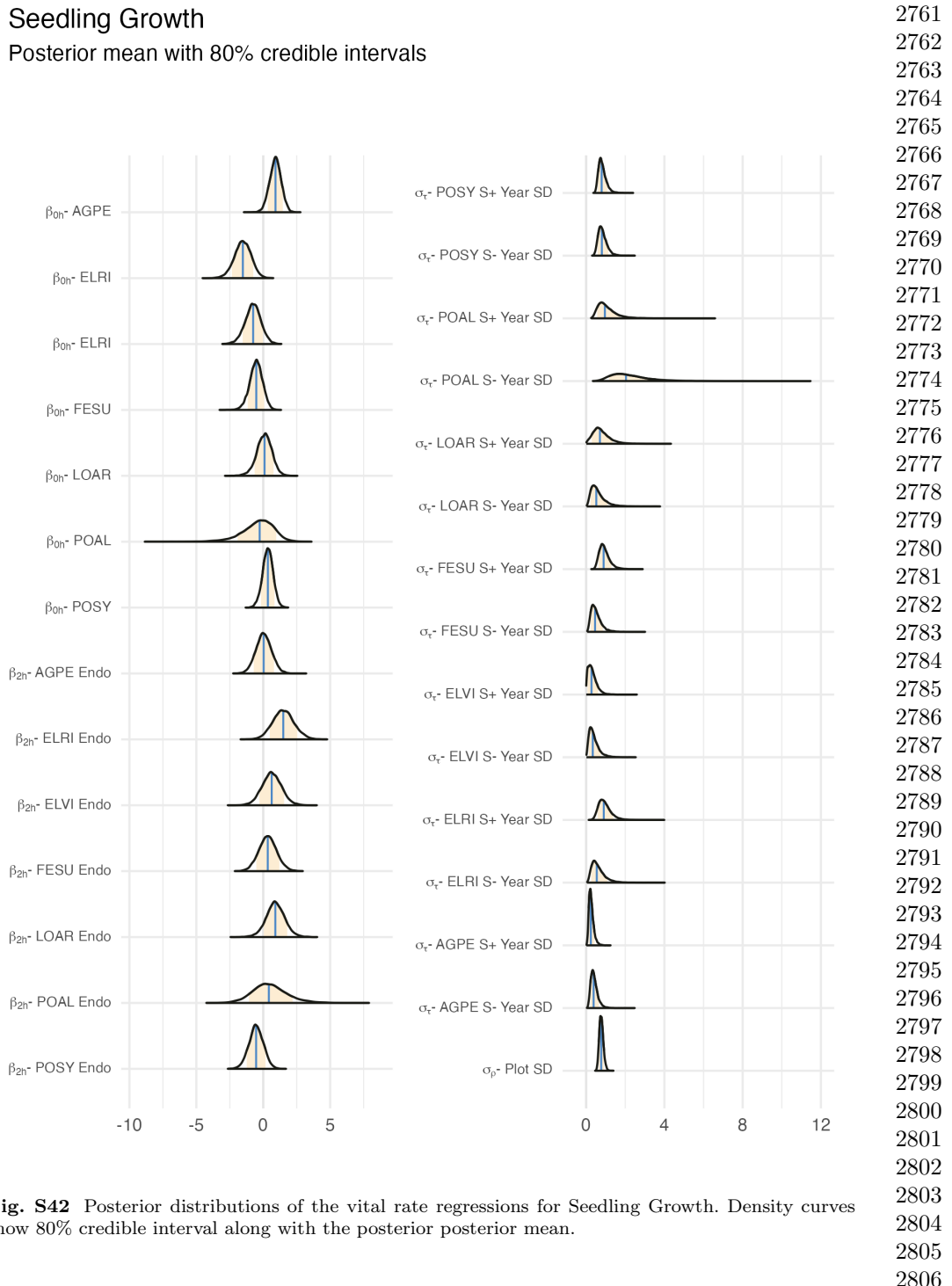


2665 Fig. S39 Posterior distributions of the vital rate regressions for Adult Survival. Density curves show  
 2666 80% credible interval along with the posterior posterior mean.  
 2667  
 2668

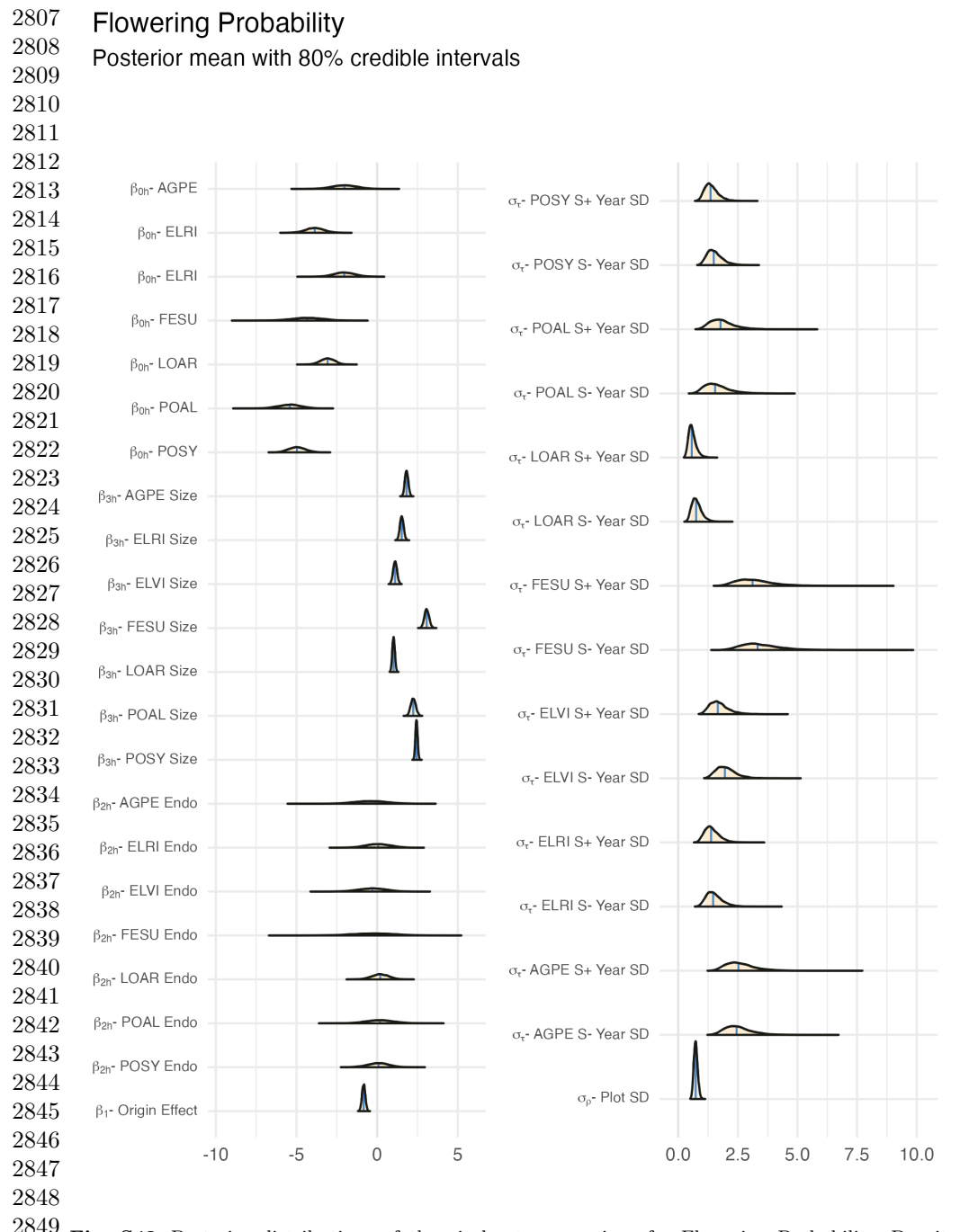


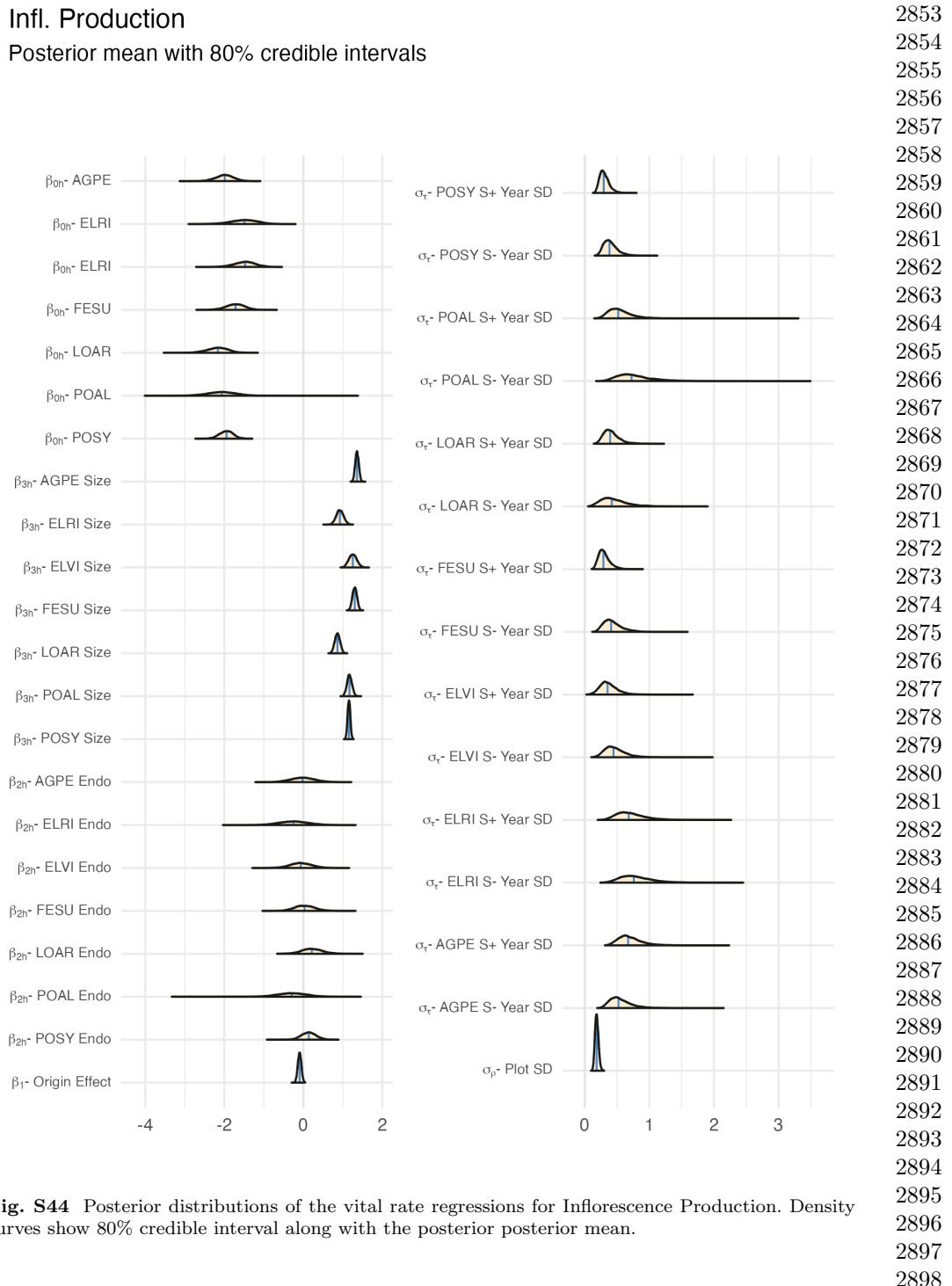
**Fig. S40** Posterior distributions of the vital rate regressions for Seedling Survival. Density curves show 80% credible interval along with the posterior posterior mean.



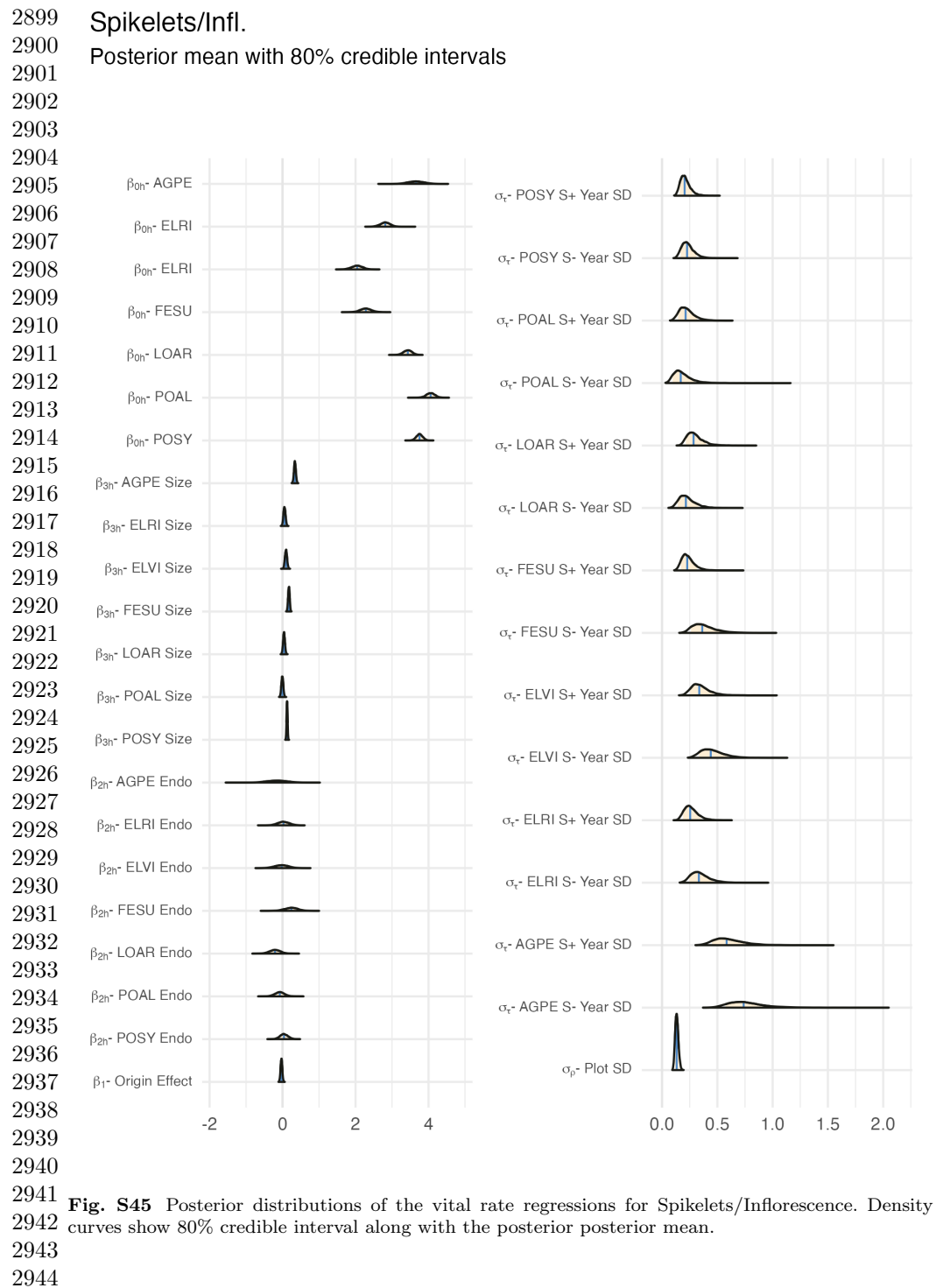


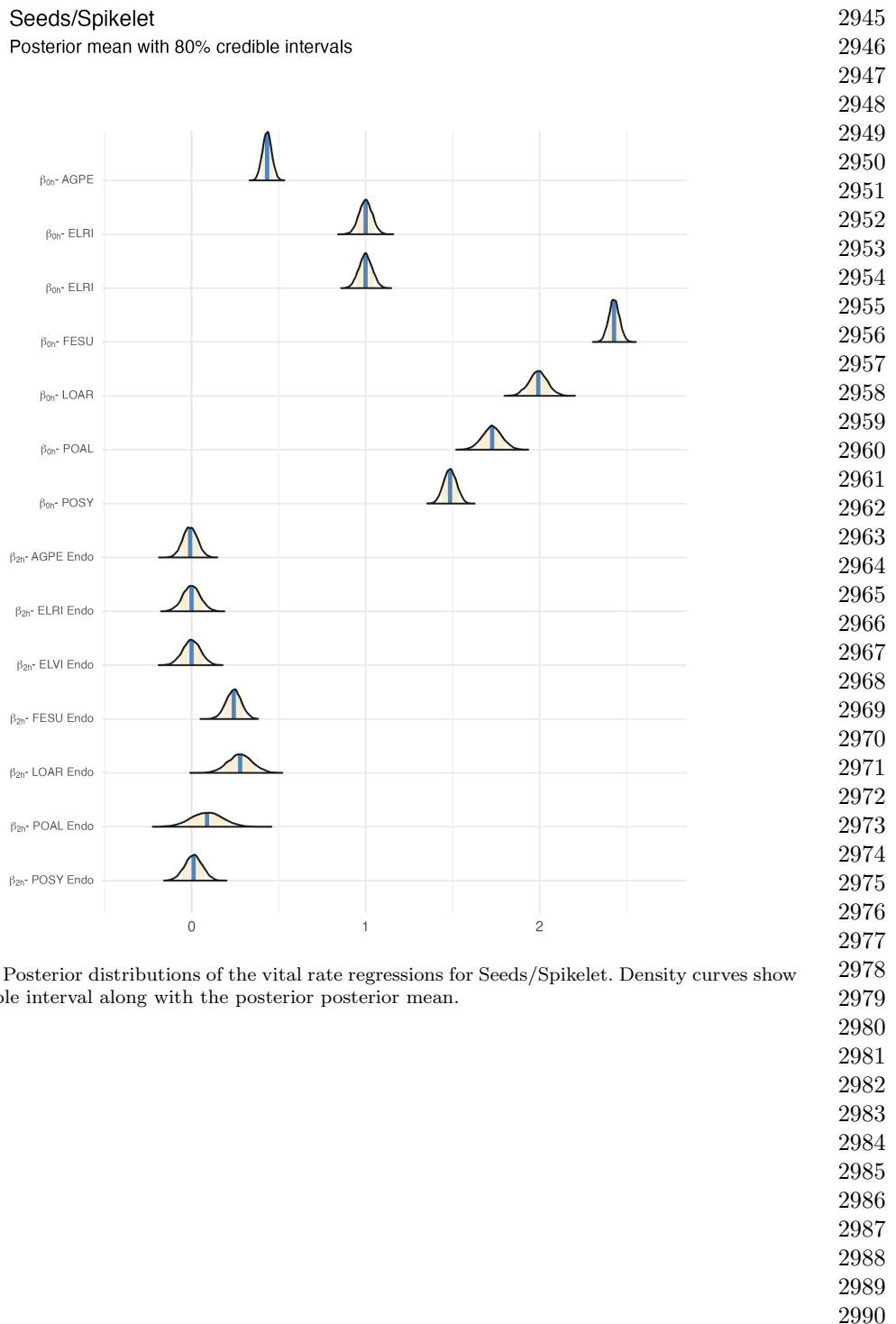
**Fig. S42** Posterior distributions of the vital rate regressions for Seedling Growth. Density curves show 80% credible interval along with the posterior posterior mean.



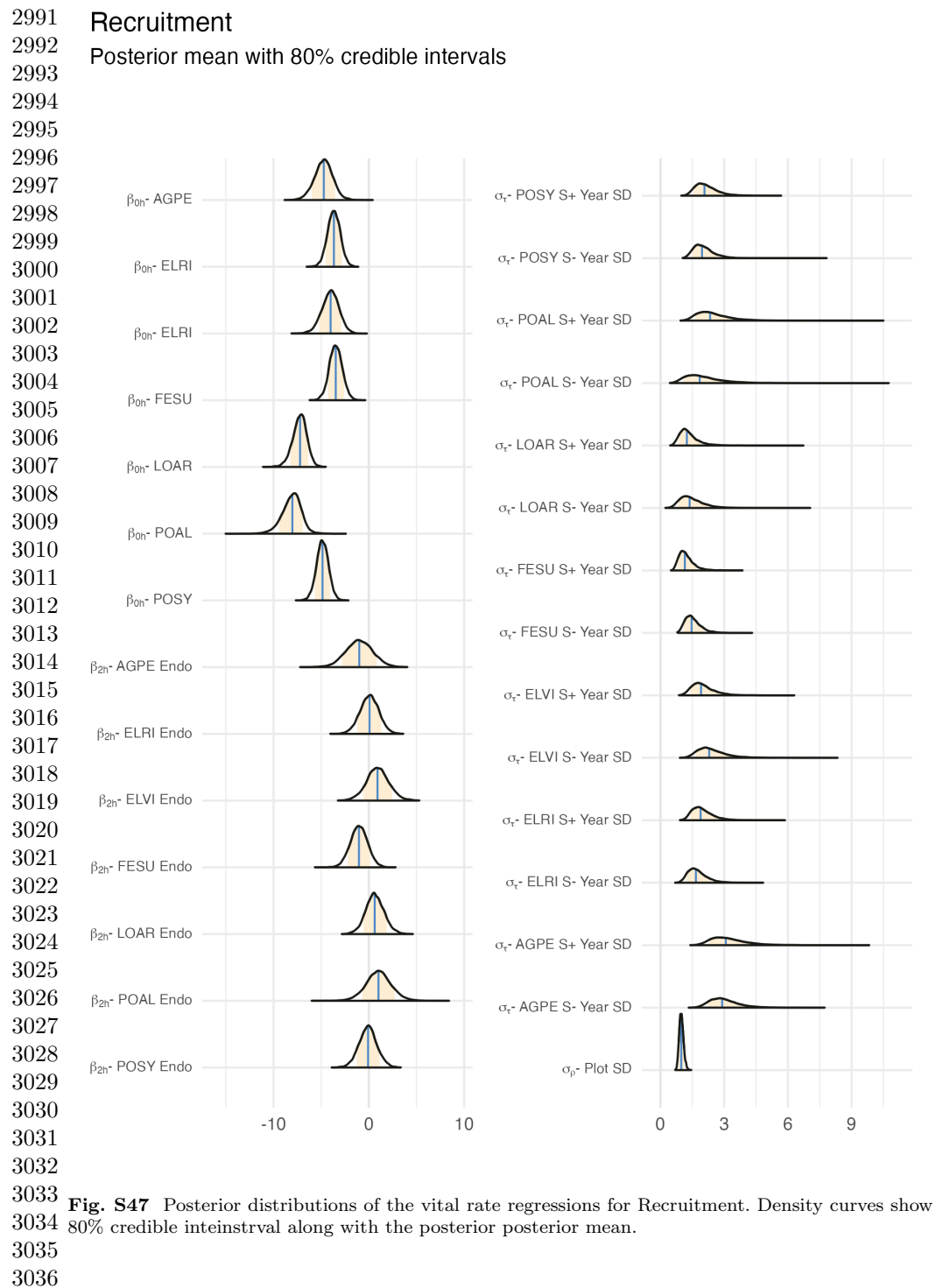


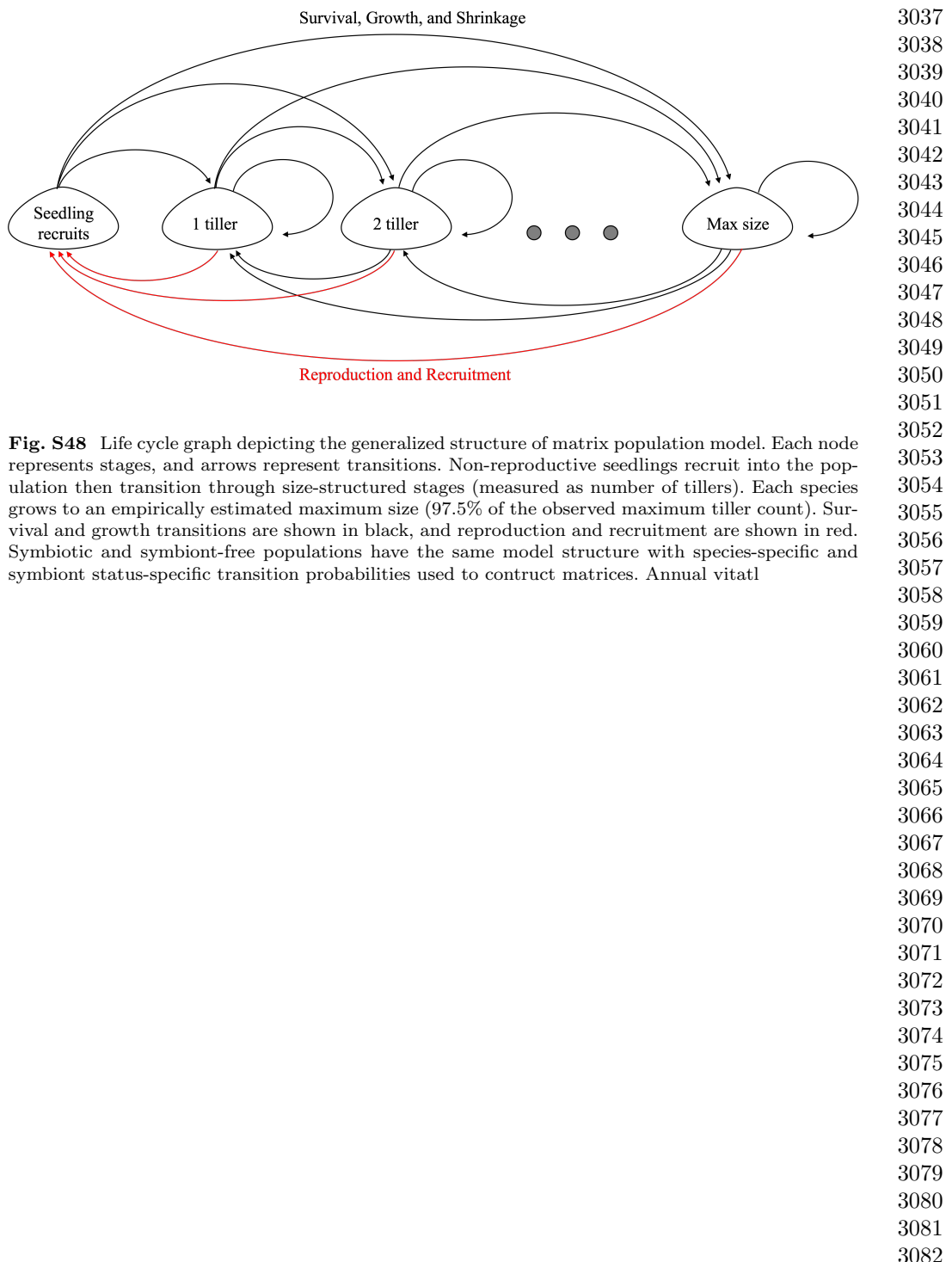
**Fig. S44** Posterior distributions of the vital rate regressions for Inflorescence Production. Density curves show 80% credible interval along with the posterior posterior mean.

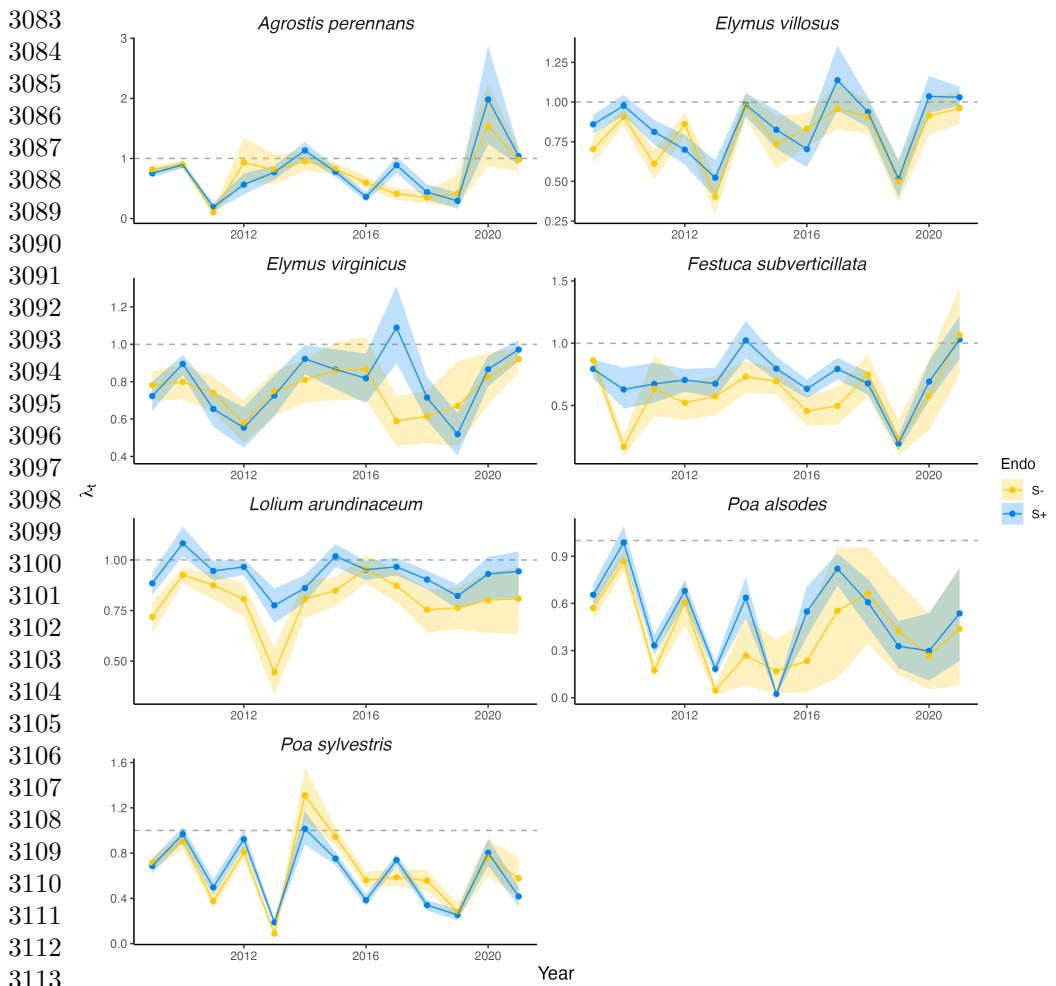




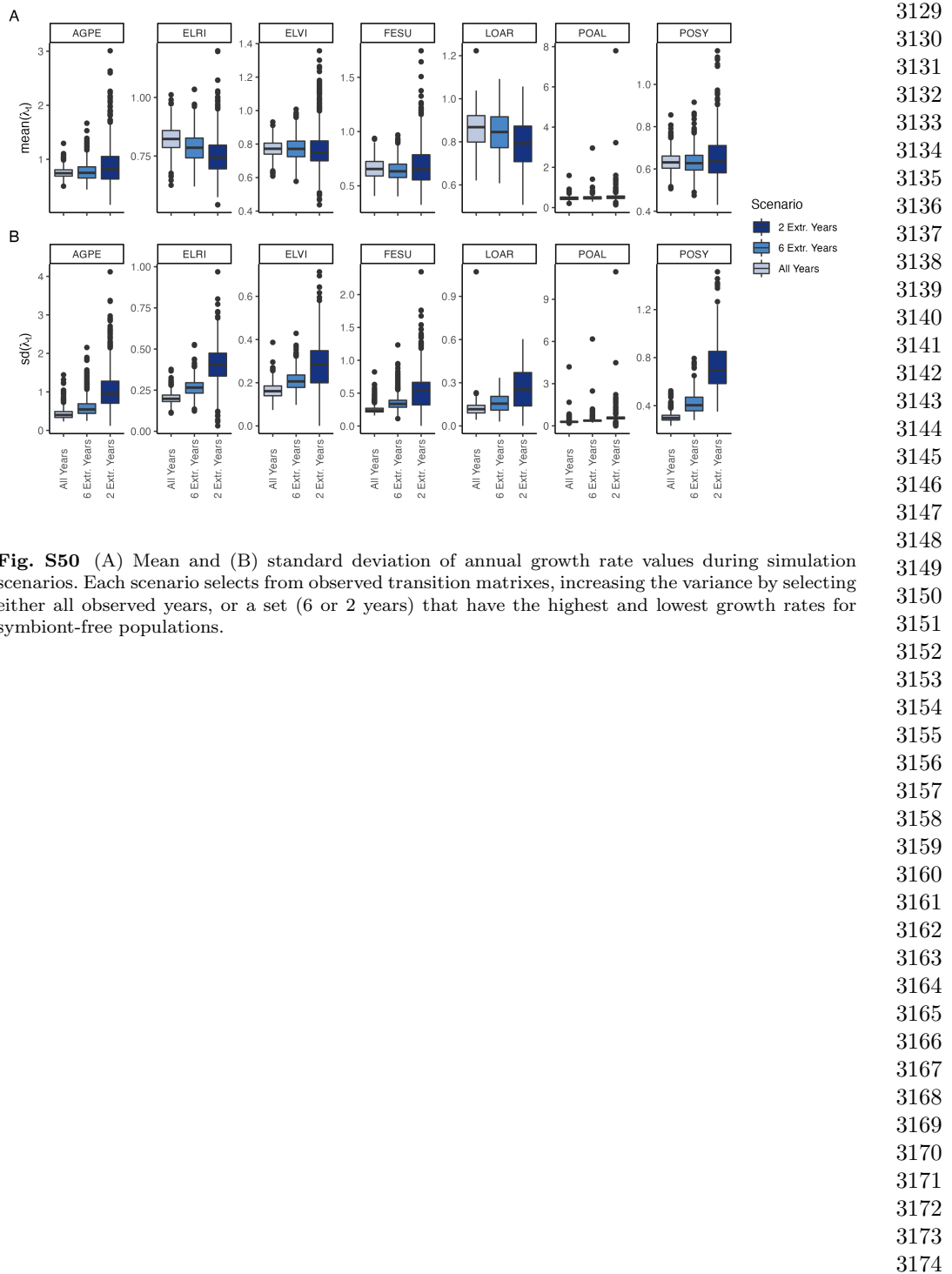
**Fig. S46** Posterior distributions of the vital rate regressions for Seeds/Spikelet. Density curves show 80% credible interval along with the posterior posterior mean.



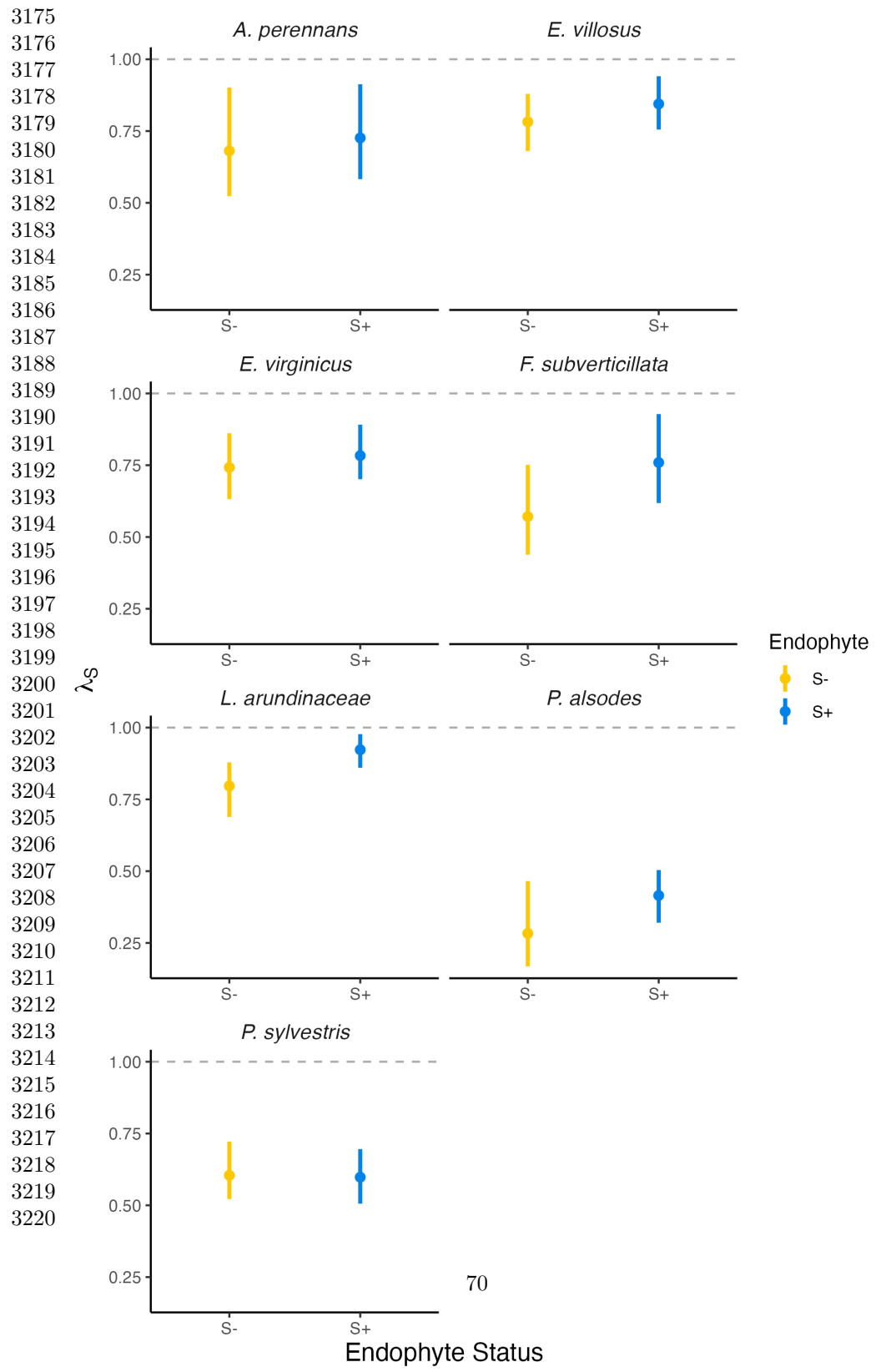




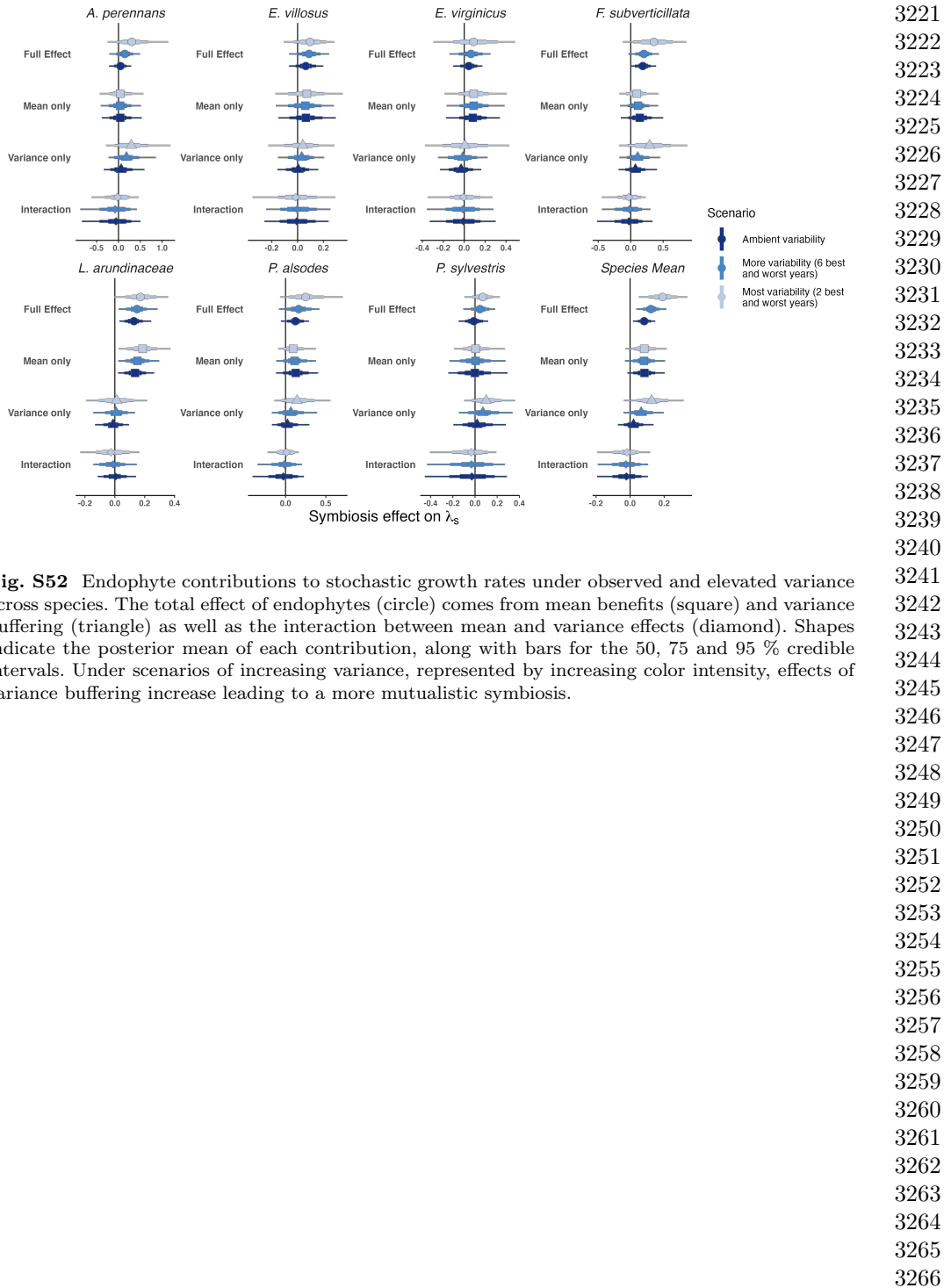
**3115 Fig. S49** Annual growth rate values ( $\lambda_t$ ) over thirteen years. Mean values for symbiotic (blue) and  
 3116 symbiont-free (yellow) population growth rates are shown along with 80% credible intervals. Dashed  
 3117 line at ( $\lambda_t = 1$ ) indicates stable population growth rate. All values are calculated from matrix models  
 3118 representing recruit plants.

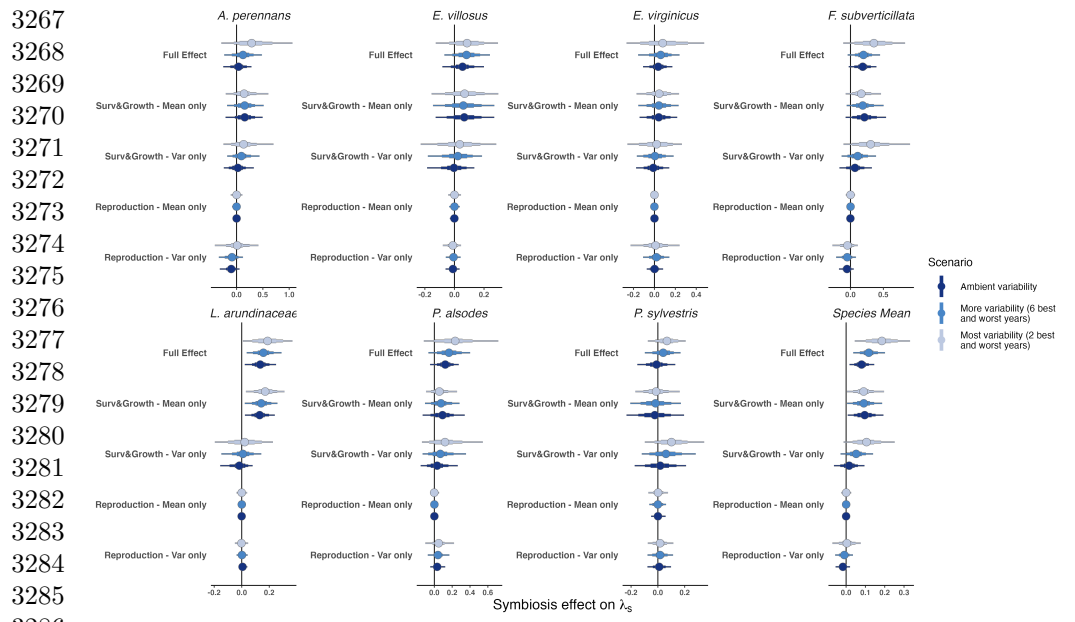


**Fig. S50** (A) Mean and (B) standard deviation of annual growth rate values during simulation scenarios. Each scenario selects from observed transition matrixes, increasing the variance by selecting either all observed years, or a set (6 or 2 years) that have the highest and lowest growth rates for symbiont-free populations.



**Fig. S51** Stochastic population growth rates ( $\lambda_s$ ) for symbiotic (blue) and symbiont-free (yellow) populations. Points show posterior medians along with the 95% credible interval 50% and posterior medians. All values are calculated from matrix models representing recruit plants.





### Endophyte Status Checks

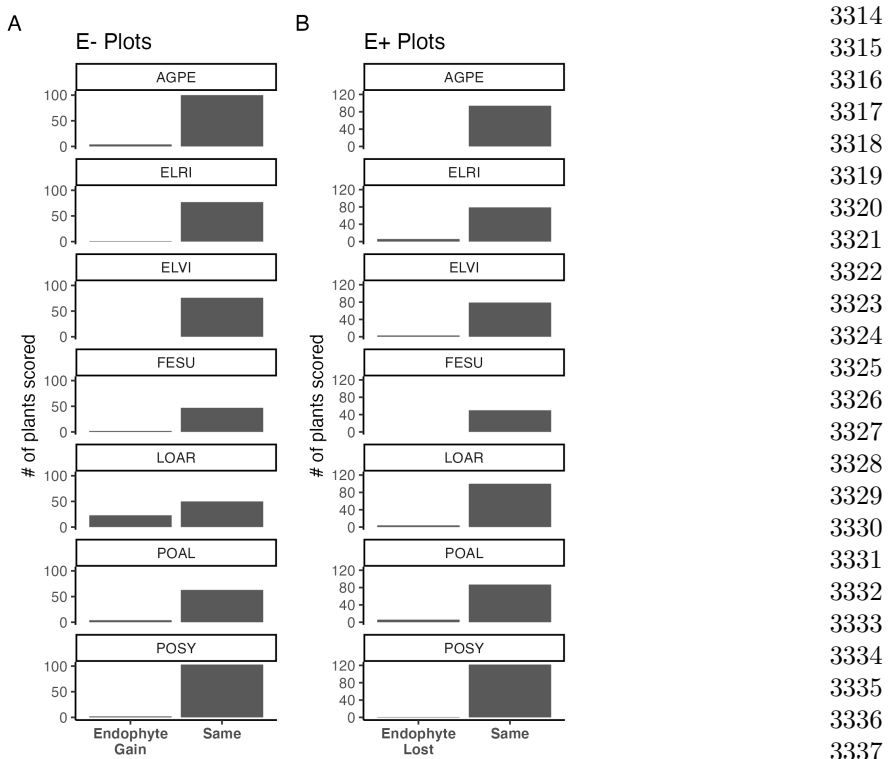
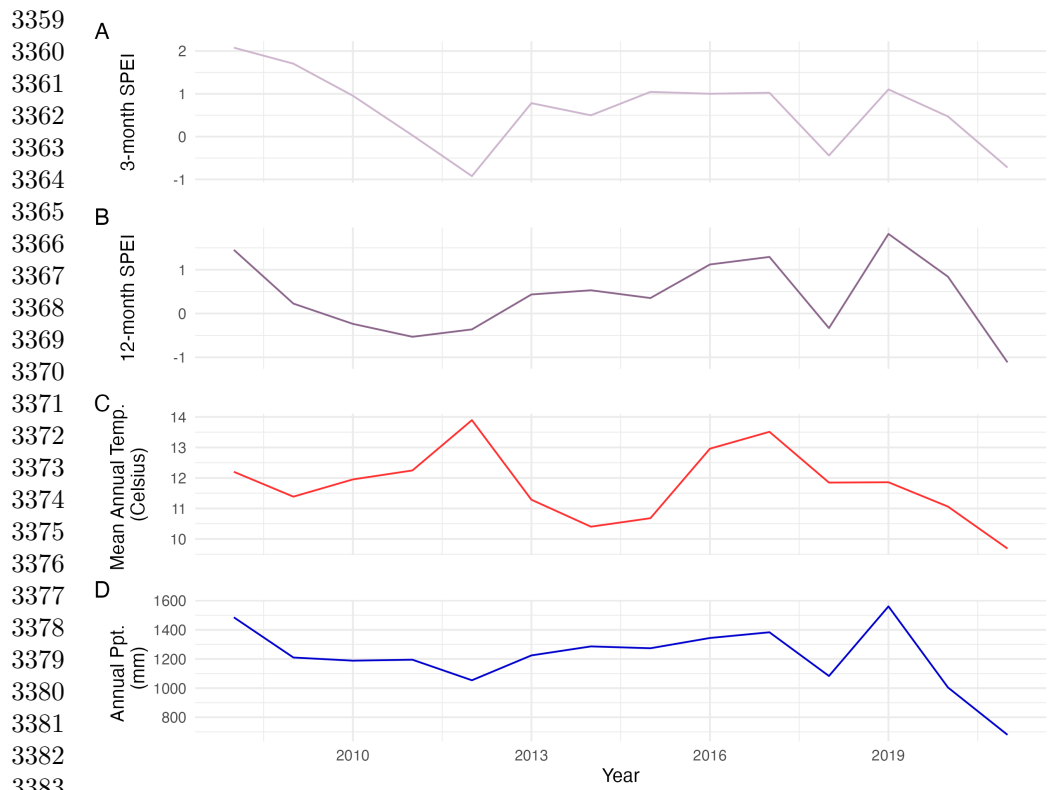


**Fig. S54** Faithfulness of experimental plots to assigned endophyte status. Counts of plants scored with leaf peels or seed squashes to check the faithfulness of recruits to the assigned plot-level endophyte status. (A) Endophytic plants may be gained in initially S- plots, or (B) lost in initially S+ plots.



3385 **Fig. S55** Weather station time-series for Bloomington, IN. The Seasonal Precipitation-  
 3386 Evapotranspiration Index (SPEI) calculated for the (A) three month growing season and (B) annually  
 3387 from daily weather station observations of (C) average temperatures and (D) cumulative precipita-  
 3388 tion. Climatic data shown are determined by the census year centered on the month of July.  
 3389  
 3390  
 3391  
 3392  
 3393  
 3394  
 3395  
 3396  
 3397  
 3398  
 3399  
 3400  
 3401  
 3402  
 3403  
 3404

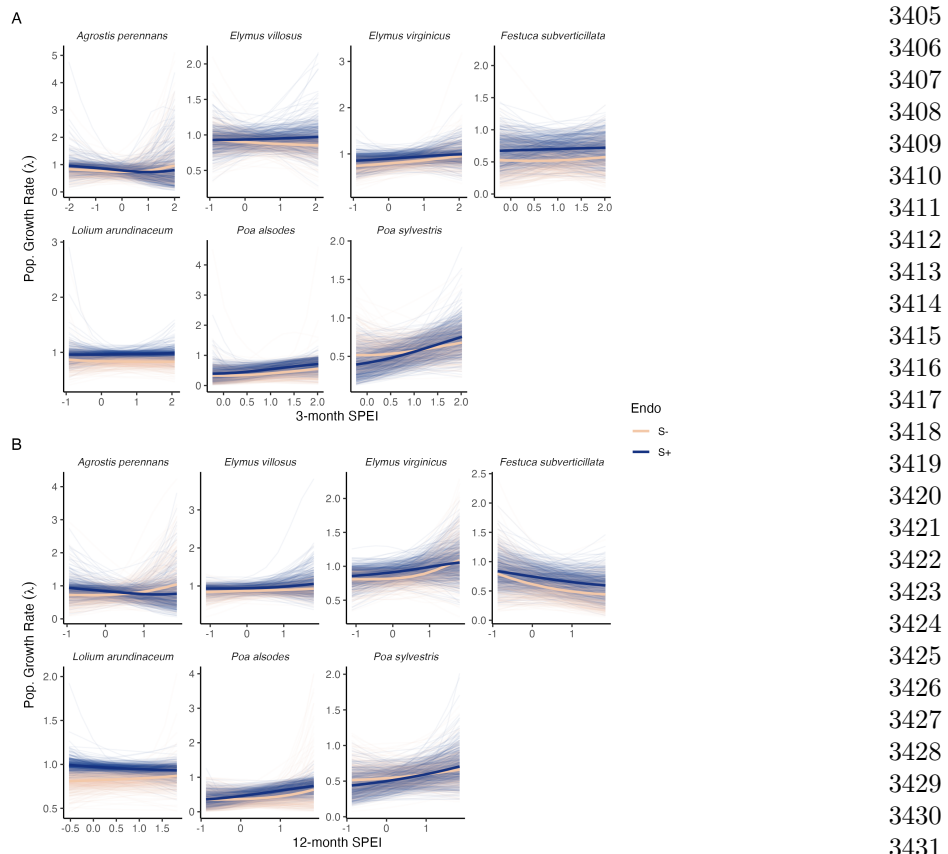


**Fig. S56** Predicted population growth rates across drought indices. Symbiotic (S+; blue) and symbiont-free (S-; tan) populations respond differently to climate as measured by the (A) 3-month SPEI and (B) 12-month SPEI. Thick lines represent the predicted mean growth rate and thin lines show 500 posterior draws.

3405  
3406  
3407  
3408  
3409  
3410  
3411  
3412  
3413  
3414  
3415  
3416  
3417  
3418  
3419  
3420  
3421  
3422  
3423  
3424  
3425  
3426  
3427  
3428  
3429  
3430  
3431  
3432  
3433  
3434  
3435  
3436  
3437  
3438  
3439  
3440  
3441  
3442  
3443  
3444  
3445  
3446  
3447  
3448  
3449  
3450

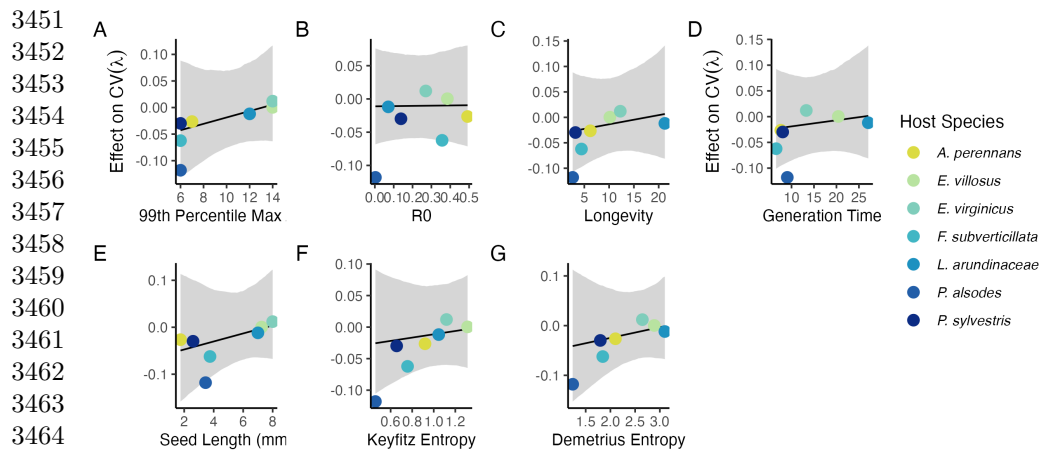


**Fig. S57** Relationship between variance buffering and life history traits describing the fast-slow life history continuum accounting for phylogenetic covariance between grass host species. Regressions between life history traits describing the fast-slow life history continuum ((A) 99th percentile maximum age observed during long term censuses in years; (B) Net reproductive rate; (C) Longevity; (D) Generation time in years; (G) Seed size) and the effect of endophyte symbiosis on the coefficient of variation in population growth rate ( $\lambda$ ). Each panel shows the fitted mean relationship (line) along with the 95% credible interval.

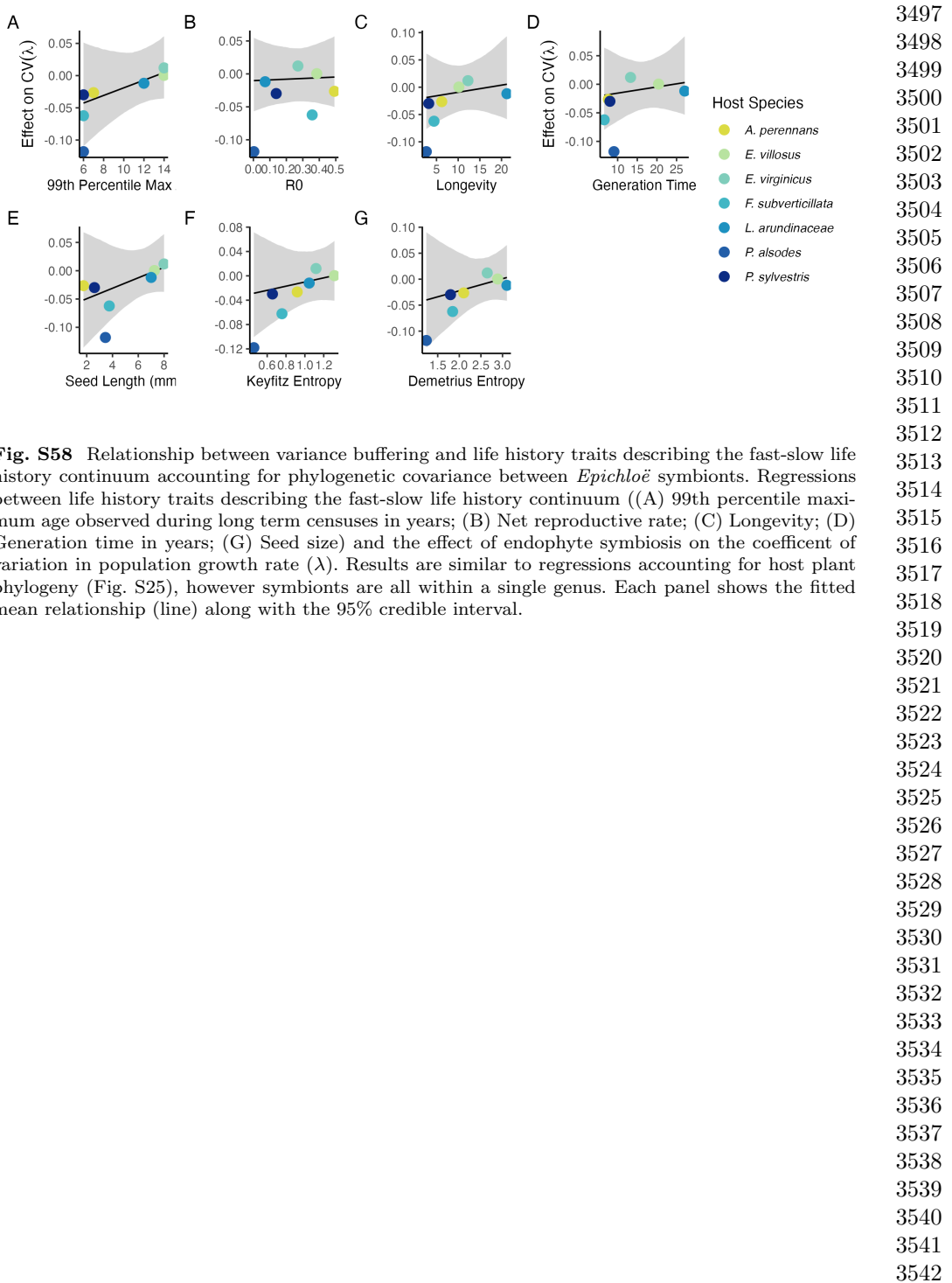
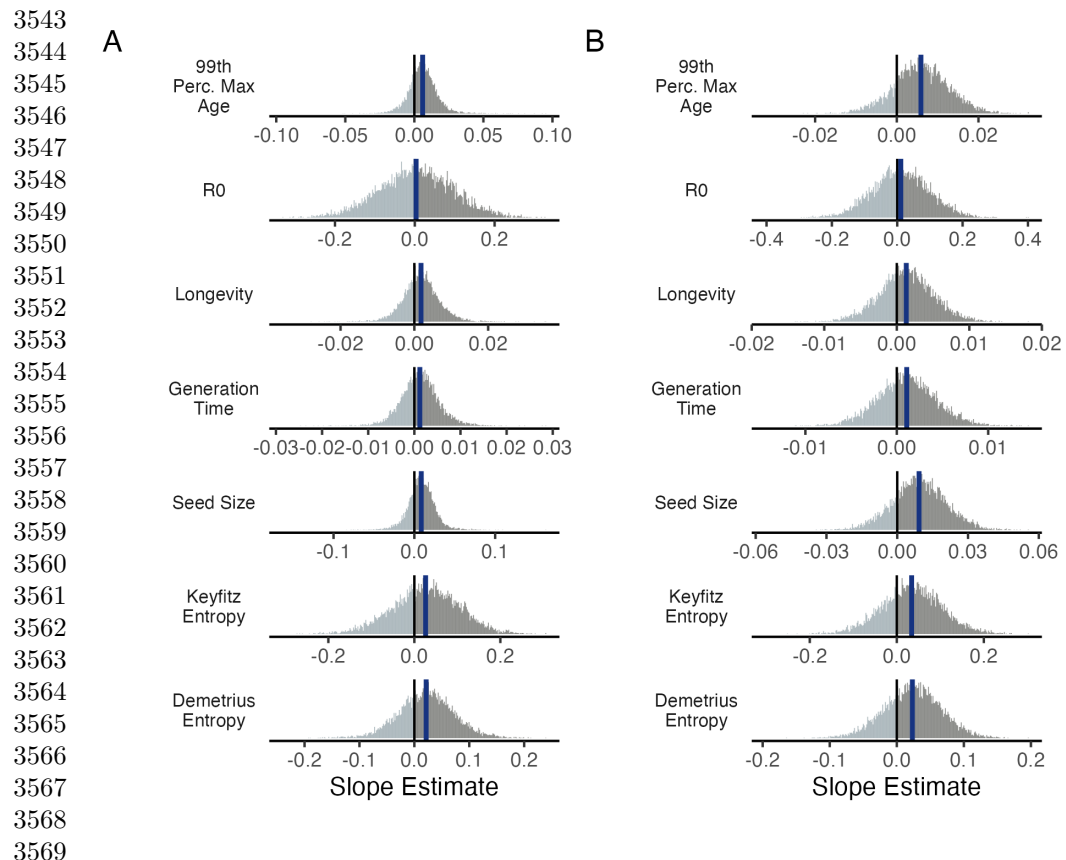


**Fig. S58** Relationship between variance buffering and life history traits describing the fast-slow life history continuum accounting for phylogenetic covariance between *Epichloë* symbionts. Regressions between life history traits describing the fast-slow life history continuum ((A) 99th percentile maximum age observed during long term censuses in years; (B) Net reproductive rate; (C) Longevity; (D) Generation time in years; (G) Seed size) and the effect of endophyte symbiosis on the coefficient of variation in population growth rate ( $\lambda$ ). Results are similar to regressions accounting for host plant phylogeny (Fig. S25), however symbionts are all within a single genus. Each panel shows the fitted mean relationship (line) along with the 95% credible interval.



3570 **Fig. S59** Posterior estimates of life history trait effects on variance buffering. Grey histograms  
3571 show the posterior distribution of the slope parameter from models incorporating (A) host plant  
3572 phylogenetic covariance and (B) symbiont phylogenetic covariance for each life history trait with blue  
3573 bars showing the posterior mean.

3573  
3574  
3575  
3576  
3577  
3578  
3579  
3580  
3581  
3582  
3583  
3584  
3585  
3586  
3587  
3588

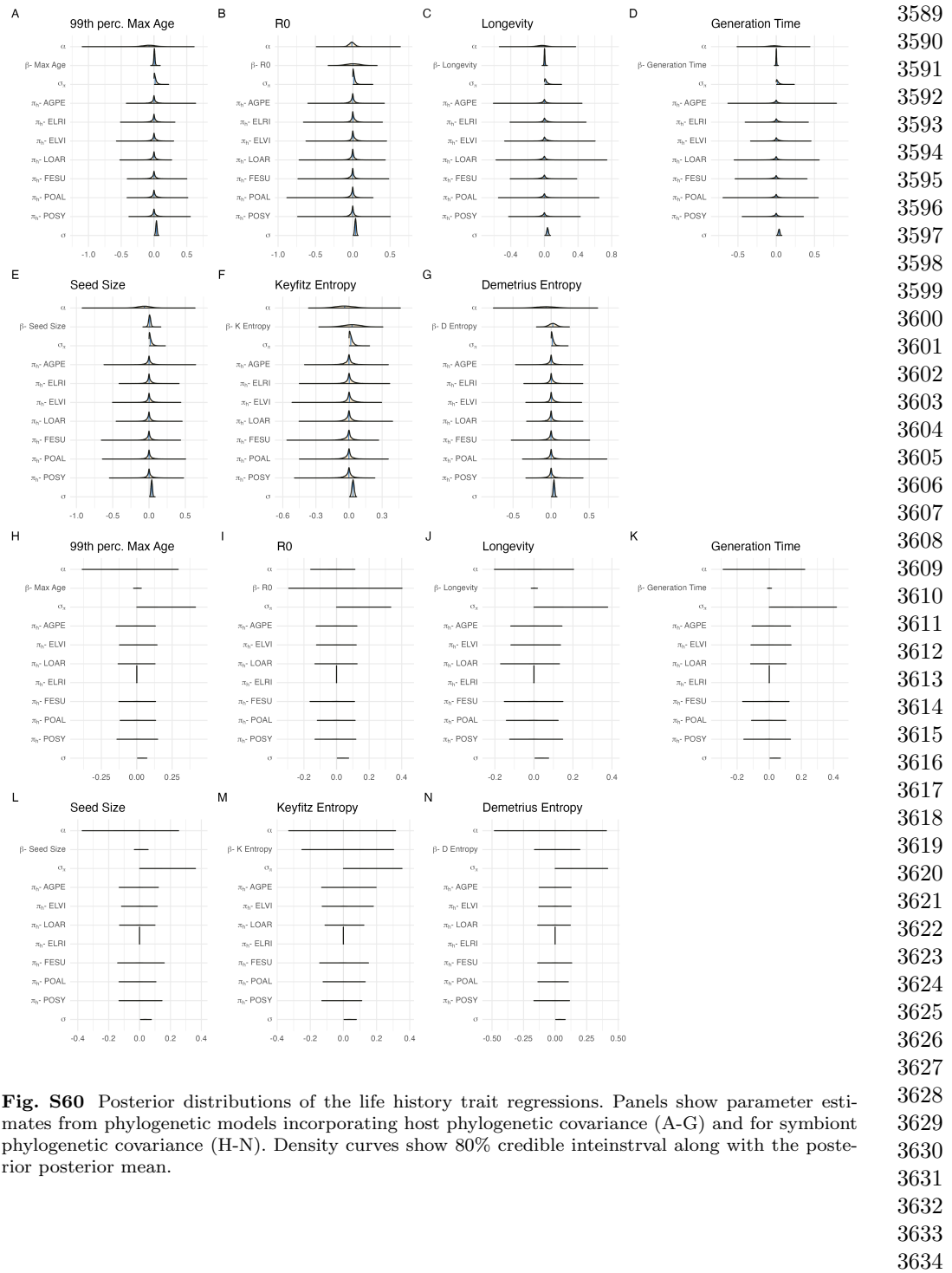


**Fig. S60** Posterior distributions of the life history trait regressions. Panels show parameter estimates from phylogenetic models incorporating host phylogenetic covariance (A-G) and for symbiont phylogenetic covariance (H-N). Density curves show 80% credible interval along with the posterior mean.

**3635 Supplemental Tables S1-S3**

3636

3637

3638

3639

3640

3641

3642

3643

3644

3645

3646

3647

3648

3649

3650

3651

3652

3653

3654

3655

3656

3657

3658

3659

3660

3661

3662

3663

3664

3665

3666

3667

3668

3669

3670

3671

3672

3673

3674

3675

3676

3677

3678

3679

3680

**Table S1** Summary of host-endophyte propagule and transplant methods

Host Species	Symbiont Species	Heat treatment duration (Temp.)	Transplant date
<i>Agrostis perennans</i>	<i>E. amarillans</i>	12 min. hot water bath (60 °C)	April 2008 (10 plots)
<i>Elymus villosus</i>	<i>E. elymi</i>	6 days drying oven (60 °C)	April 2008 (10 plots)
<i>Elymus virginicus</i>	<i>E. elymi</i> or <i>EviTG-1</i>	6 days drying oven (60 °C)	April 2008 (10 plots)
<i>Festuca subverticillata</i>	<i>E. starrii</i>	6 days drying oven (60 °C)	April 2008 (10 plots)
<i>Lolium arundinaceum</i>	<i>E. coenophiala</i>	6 days drying oven (60 °C)	Sept. 2007 (10 plots)
<i>Poa alsodes</i>	<i>E. alsodes</i>	7 days drying oven (60 °C)	Sept. 2007 (8 plots)/April 2008 (10 plots)
<i>Poa sylvestris</i>	<i>E. PsyTG-1</i>	7 days drying oven (60 °C)	Sept. 2007 (8 plots)/April 2008 (10 plots)
			3681
			3682
			3683
			3684
			3685
			3686
			3687
			3688
			3689
			3690
			3691
			3692
			3693
			3694
			3695
			3696
			3697
			3698
			3699
			3700
			3701
			3702
			3703
			3704
			3705
			3706
			3707
			3708
			3709
			3710
			3711
			3712
			3713
			3714
			3715
			3716
			3717
			3718
			3719
			3720
			3721
			3722
			3723
			3724
			3725
			3726

3727  
 3728  
 3729  
 3730  
 3731  
 3732  
 3733  
 3734  
 3735  
 3736  
 3737  
 3738  
 3739  
 3740  
 3741  
 3742  
 3743  
 3744  
 3745  
 3746  
 3747  
 3748  
 3749  
 3750  
 3751  
 3752  
 3753  
 3754  
 3755  
 3756  
 3757  
 3758  
 3759  
 3760  
 3761  
 3762  
 3763  
 3764  
 3765  
 3766  
 3767  
 3768  
 3769  
 3770  
 3771  
 3772

**Table S2** Summary of focal life history traits

Host Species	Observed max age (years)	99th percentile max age (years)	Generation time (years)	$R_0$	Longevity (years)	Seed length (mm.)	Keyfitz Entropy	Demetrius Entropy	Imperfect transmission rate (%)	Stromata Observed (% of individ. per species)
<i>Agrostis perennans</i>	11	7	7.6	0.58	6.4	1.75	0.9	2.1	69.8	0.0
<i>Elymus villosus</i>	14	14	20.7	0.35	9.8	7.25	1.3	2.9	100	4.6
<i>Elymus virginicus</i>	14	14	13.4	0.25	12.5	8	1.1	2.6	100	0.6
<i>Festuca subverticillata</i>	9	6	6.6	0.28	4.3	3.75	0.8	1.8	42.7	0.0
<i>Lolium arundinaceum</i>	12*	12*	27.4	0.08	21.3	7	1.1	3.1	100	0.0
<i>Poa alsodes</i>	8	6	9.2	0.003	2.6	3.45	0.5	1.2	99.9	0.0
<i>Poa sylvestris</i>	12	6	8.0	0.14	3.2	2.6	0.7	1.8	16.6	0.1
Page's $\lambda$ (host)	—	0.27	0.28	0.23	0.28	0.27	0.25	0.25	—	—
Page's $\lambda$ (symbiont)	—	0.63	0.63	0.63	0.63	0.62	0.62	0.62	—	—

\*Censuses for *L. arundinaceum* plots stopped after year 12 of the experiment.

Host Species	Effect on CV( $\lambda$ )	Effect on Mean( $\lambda$ )	$\frac{\Delta\lambda^-}{\Delta SPEI_3}$	$\frac{\Delta\lambda^+}{\Delta SPEI_3}$	3 month S- to S+ ratio	$\frac{\Delta\lambda^-}{\Delta SPEI_{12}}$	$\frac{\Delta\lambda^+}{\Delta SPEI_{12}}$	12 month S- to S+ ratio
<i>Agrostis perennans</i>	-0.0264	0.0441	0.03	-0.04	0.85	0.11	-0.06	1.82
<i>Elymus villosus</i>	0.0003	0.0509	-0.03	0.01	1.95	0.03	0.04	0.70
<i>Elymus virginicus</i>	0.0120	0.0578	0.07	0.05	1.50	0.10	0.07	1.42
<i>Festuca subverticillata</i>	-0.0622	0.1639	0.02	0.02	1.01	-0.13	-0.09	1.43
<i>Lolium arundinaceum</i>	-0.0118	0.1022	-0.01	0.01	1.32	0.03	-0.03	1.02
<i>Poa alsodes</i>	-0.1179	0.1282	0.10	0.14	0.71	0.11	0.14	0.73
<i>Poa sylvestris</i>	-0.0298	-0.0085	0.07	0.16	0.44	0.05	0.10	0.55

3819 **References**

- 3820 [1] Seneviratne, S. *et al.* *Changes in climate extremes and their impacts on the*  
3821 *natural physical environment* (Cambridge University Press, 2012).
- 3822 [2] Bathiany, S., Dakos, V., Scheffer, M. & Lenton, T. M. Climate models predict  
3823 increasing temperature variability in poor countries. *Science advances* **4**, eaar5809  
3824 (2018).
- 3825 [3] IPCC. Climate change 2021: The physical science basis (2021). URL <https://www.ipcc.ch/report/ar6/wg1/>.
- 3826 [4] Clark, J. S. Why environmental scientists are becoming bayesians. *Ecology letters*  
3827 **8**, 2–14 (2005).
- 3828 [5] Lewontin, R. C. & Cohen, D. On Population Growth in a Randomly Varying Envi-  
3829 ronment. *Proceedings of the National Academy of Sciences* **62**, 1056–1060 (1969).  
3830 URL <https://www.pnas.org/content/62/4/1056>. Publisher: National Academy of  
3831 Sciences Section: Biological Sciences: Zoology.
- 3832 [6] Tuljapurkar, S. D. Population dynamics in variable environments. III. Evolution-  
3833 ary dynamics of r-selection. *Theoretical Population Biology* **21**, 141–165 (1982).  
3834 URL <http://www.sciencedirect.com/science/article/pii/0040580982900107>.
- 3835 [7] Cohen, J. E. Comparative statics and stochastic dynamics of age-structured  
3836 populations. *Theoretical population biology* **16**, 159–171 (1979).
- 3837 [8] Tuljapurkar, S. *Population dynamics in variable environments* Vol. 85 (Springer  
3838 Science & Business Media, 2013).
- 3839 [9] Pfister, C. A. Patterns of variance in stage-structured populations: evolutionary  
3840 predictions and ecological implications. *Proceedings of the National Academy of  
3841 Sciences* **95**, 213–218 (1998).
- 3842 [10] Compagnoni, A. *et al.* The effect of demographic correlations on the stochastic  
3843 population dynamics of perennial plants. *Ecological Monographs* **86**, 480–494  
3844 (2016).
- 3845 [11] Ellis, M. M. & Crone, E. E. The role of transient dynamics in stochastic  
3846 population growth for nine perennial plants. *Ecology* **94**, 1681–1686 (2013).
- 3847 [12] Murphy, G. I. Pattern in life history and the environment. *The American  
3848 Naturalist* **102**, 391–403 (1968).
- 3849 [13] Davison, R., Stadman, M. & Jongejans, E. Stochastic effects contribute to  
3850 population fitness differences. *Ecological Modelling* **408**, 108760 (2019).
- 3851
- 3852
- 3853
- 3854
- 3855
- 3856
- 3857
- 3858
- 3859
- 3860
- 3861
- 3862
- 3863
- 3864

- [14] Compagnoni, A. *et al.* Herbaceous perennial plants with short generation time have stronger responses to climate anomalies than those with longer generation time. *Nature communications* **12**, 1–8 (2021). 3865  
3866  
3867  
3868  
3869  
3870  
3871  
3872  
3873  
3874  
3875  
3876  
3877  
3878  
3879  
3880  
3881  
3882  
3883  
3884  
3885  
3886  
3887  
3888  
3889  
3890  
3891  
3892  
3893  
3894  
3895  
3896  
3897  
3898  
3899  
3900  
3901  
3902  
3903  
3904  
3905  
3906  
3907  
3908  
3909  
3910
- [15] Le Coeur, C., Yoccoz, N. G., Salguero-Gómez, R. & Vindenes, Y. Life history adaptations to fluctuating environments: Combined effects of demographic buffering and lability. *Ecology Letters* **25**, 2107–2119 (2022). 3865  
3866  
3867  
3868  
3869  
3870  
3871  
3872  
3873  
3874  
3875  
3876  
3877  
3878  
3879  
3880  
3881  
3882  
3883  
3884  
3885  
3886  
3887  
3888  
3889  
3890  
3891  
3892  
3893  
3894  
3895  
3896  
3897  
3898  
3899  
3900  
3901  
3902  
3903  
3904  
3905  
3906  
3907  
3908  
3909  
3910
- [16] Morris, W. F. *et al.* Longevity can buffer plant and animal populations against changing climatic variability. *Ecology* **89**, 19–25 (2008). 3865  
3866  
3867  
3868  
3869  
3870  
3871  
3872  
3873  
3874  
3875  
3876  
3877  
3878  
3879  
3880  
3881  
3882  
3883  
3884  
3885  
3886  
3887  
3888  
3889  
3890  
3891  
3892  
3893  
3894  
3895  
3896  
3897  
3898  
3899  
3900  
3901  
3902  
3903  
3904  
3905  
3906  
3907  
3908  
3909  
3910
- [17] Rodríguez-Caro, R. C. *et al.* The limits of demographic buffering in coping with environmental variation. *Oikos* **130**, 1346–1358 (2021). 3865  
3866  
3867  
3868  
3869  
3870  
3871  
3872  
3873  
3874  
3875  
3876  
3877  
3878  
3879  
3880  
3881  
3882  
3883  
3884  
3885  
3886  
3887  
3888  
3889  
3890  
3891  
3892  
3893  
3894  
3895  
3896  
3897  
3898  
3899  
3900  
3901  
3902  
3903  
3904  
3905  
3906  
3907  
3908  
3909  
3910
- [18] Tuljapurkar, S. & Orzack, S. H. Population dynamics in variable environments i. long-run growth rates and extinction. *Theoretical Population Biology* **18**, 314–342 (1980). 3865  
3866  
3867  
3868  
3869  
3870  
3871  
3872  
3873  
3874  
3875  
3876  
3877  
3878  
3879  
3880  
3881  
3882  
3883  
3884  
3885  
3886  
3887  
3888  
3889  
3890  
3891  
3892  
3893  
3894  
3895  
3896  
3897  
3898  
3899  
3900  
3901  
3902  
3903  
3904  
3905  
3906  
3907  
3908  
3909  
3910
- [19] Fieberg, J. & Ellner, S. P. Stochastic matrix models for conservation and management: a comparative review of methods. *Ecology letters* **4**, 244–266 (2001). 3865  
3866  
3867  
3868  
3869  
3870  
3871  
3872  
3873  
3874  
3875  
3876  
3877  
3878  
3879  
3880  
3881  
3882  
3883  
3884  
3885  
3886  
3887  
3888  
3889  
3890  
3891  
3892  
3893  
3894  
3895  
3896  
3897  
3898  
3899  
3900  
3901  
3902  
3903  
3904  
3905  
3906  
3907  
3908  
3909  
3910
- [20] Menges, E. S. Applications of population viability analyses in plant conservation. *Ecological Bulletins* 73–84 (2000). 3865  
3866  
3867  
3868  
3869  
3870  
3871  
3872  
3873  
3874  
3875  
3876  
3877  
3878  
3879  
3880  
3881  
3882  
3883  
3884  
3885  
3886  
3887  
3888  
3889  
3890  
3891  
3892  
3893  
3894  
3895  
3896  
3897  
3898  
3899  
3900  
3901  
3902  
3903  
3904  
3905  
3906  
3907  
3908  
3909  
3910
- [21] Kuparinen, A., Boit, A., Valdovinos, F. S., Lassaux, H. & Martinez, N. D. Fishing-induced life-history changes degrade and destabilize harvested ecosystems. *Scientific reports* **6**, 22245 (2016). 3865  
3866  
3867  
3868  
3869  
3870  
3871  
3872  
3873  
3874  
3875  
3876  
3877  
3878  
3879  
3880  
3881  
3882  
3883  
3884  
3885  
3886  
3887  
3888  
3889  
3890  
3891  
3892  
3893  
3894  
3895  
3896  
3897  
3898  
3899  
3900  
3901  
3902  
3903  
3904  
3905  
3906  
3907  
3908  
3909  
3910
- [22] Hilde, C. H. *et al.* The Demographic Buffering Hypothesis: Evidence and Challenges. *Trends in Ecology & Evolution* **0** (2020). URL [https://www.cell.com/trends/ecology-evolution/abstract/S0169-5347\(20\)30050-1](https://www.cell.com/trends/ecology-evolution/abstract/S0169-5347(20)30050-1). Publisher: Elsevier. 3865  
3866  
3867  
3868  
3869  
3870  
3871  
3872  
3873  
3874  
3875  
3876  
3877  
3878  
3879  
3880  
3881  
3882  
3883  
3884  
3885  
3886  
3887  
3888  
3889  
3890  
3891  
3892  
3893  
3894  
3895  
3896  
3897  
3898  
3899  
3900  
3901  
3902  
3903  
3904  
3905  
3906  
3907  
3908  
3909  
3910
- [23] Dybala, K. E., Gardali, T. & Eadie, J. M. Dependent vs. independent juvenile survival: contrasting drivers of variation and the buffering effect of parental care. *Ecology* **94**, 1584–1593 (2013). 3865  
3866  
3867  
3868  
3869  
3870  
3871  
3872  
3873  
3874  
3875  
3876  
3877  
3878  
3879  
3880  
3881  
3882  
3883  
3884  
3885  
3886  
3887  
3888  
3889  
3890  
3891  
3892  
3893  
3894  
3895  
3896  
3897  
3898  
3899  
3900  
3901  
3902  
3903  
3904  
3905  
3906  
3907  
3908  
3909  
3910
- [24] Colchero, F., Eckardt, W. & Stoinski, T. Evidence of demographic buffering in an endangered great ape: Social buffering on immature survival and the role of refined sex-age classes on population growth rate. *Journal of Animal Ecology* **90**, 1701–1713 (2021). 3865  
3866  
3867  
3868  
3869  
3870  
3871  
3872  
3873  
3874  
3875  
3876  
3877  
3878  
3879  
3880  
3881  
3882  
3883  
3884  
3885  
3886  
3887  
3888  
3889  
3890  
3891  
3892  
3893  
3894  
3895  
3896  
3897  
3898  
3899  
3900  
3901  
3902  
3903  
3904  
3905  
3906  
3907  
3908  
3909  
3910
- [25] Rodriguez, R., White Jr, J., Arnold, A. E. & Redman, a. R. a. Fungal endophytes: diversity and functional roles. *New phytologist* **182**, 314–330 (2009). 3865  
3866  
3867  
3868  
3869  
3870  
3871  
3872  
3873  
3874  
3875  
3876  
3877  
3878  
3879  
3880  
3881  
3882  
3883  
3884  
3885  
3886  
3887  
3888  
3889  
3890  
3891  
3892  
3893  
3894  
3895  
3896  
3897  
3898  
3899  
3900  
3901  
3902  
3903  
3904  
3905  
3906  
3907  
3908  
3909  
3910
- [26] McFall-Ngai, M. *et al.* Animals in a bacterial world, a new imperative for the life sciences. *Proceedings of the National Academy of Sciences* **110**, 3229–3236 (2013). 3865  
3866  
3867  
3868  
3869  
3870  
3871  
3872  
3873  
3874  
3875  
3876  
3877  
3878  
3879  
3880  
3881  
3882  
3883  
3884  
3885  
3886  
3887  
3888  
3889  
3890  
3891  
3892  
3893  
3894  
3895  
3896  
3897  
3898  
3899  
3900  
3901  
3902  
3903  
3904  
3905  
3906  
3907  
3908  
3909  
3910

- 3911 [27] Funkhouser, L. J. & Bordenstein, S. R. Mom knows best: the universality of  
3912 maternal microbial transmission. *PLoS biology* **11**, e1001631 (2013).
- 3913
- 3914 [28] Fine, P. E. Vectors and vertical transmission: an epidemiologic perspective.  
3915 *Annals of the New York Academy of Sciences* **266**, 173–194 (1975).
- 3916
- 3917 [29] Russell, J. A. & Moran, N. A. Costs and benefits of symbiont infection in aphids:  
3918 variation among symbionts and across temperatures. *Proceedings of the Royal  
3919 Society B: Biological Sciences* **273**, 603–610 (2006).
- 3920
- 3921 [30] Kivlin, S. N., Emery, S. M. & Rudgers, J. A. Fungal symbionts alter plant  
3922 responses to global change. *American Journal of Botany* **100**, 1445–1457 (2013).
- 3923
- 3924 [31] Dunbar, H. E., Wilson, A. C. C., Ferguson, N. R. & Moran, N. A. Aphid thermal  
3925 tolerance is governed by a point mutation in bacterial symbionts. *PLoS biology*  
3926 **5**, e96 (2007).
- 3927
- 3928 [32] Reyna, R., Cooke, P., Grum, D., Cook, D. & Creamer, R. Detection and local-  
3929 ization of the endophyte *undifilum oxytropis* in locoweed tissues. *Botany* **90**,  
3930 1229–1236 (2012).
- 3931
- 3932 [33] Saikkonen, K., Gundel, P. E. & Helander, M. Chemical ecology mediated by  
3933 fungal endophytes in grasses. *Journal of chemical ecology* **39**, 962–968 (2013).
- 3934
- 3935 [34] Neyaz, M., Gardner, D. R., Creamer, R. & Cook, D. Localization of the  
3936 swainsonine-producing chaetothyriales symbiont in the seed and shoot apical  
3937 meristem in its host *ipomoea carnea*. *Microorganisms* **10**, 545 (2022).
- 3938
- 3939 [35] Chamberlain, S. A., Bronstein, J. L. & Rudgers, J. A. How context dependent  
3940 are species interactions? *Ecology letters* **17**, 881–890 (2014).
- 3941
- 3942 [36] Catford, J. A., Wilson, J. R., Pyšek, P., Hulme, P. E. & Duncan, R. P. Address-  
3943 ing context dependence in ecology. *Trends in Ecology & Evolution* **37**, 158–170  
3944 (2022).
- 3945
- 3946 [37] Jordano, P. Spatial and temporal variation in the avian-frugivore assemblage of  
3947 *prunus mahaleb*: patterns and consequences. *Oikos* 479–491 (1994).
- 3948
- 3949 [38] Leuchtmann, A. Systematics, distribution, and host specificity of grass endo-  
3950 phytes. *Natural toxins* **1**, 150–162 (1992).
- 3951
- 3952 [39] Cheplick, G. P., Faeth, S. & Faeth, S. H. *Ecology and evolution of the grass-*  
3953 *endophyte symbiosis* (OUP USA, 2009).
- 3954
- 3955 [40] Brem, D. & Leuchtmann, A. Epichloë grass endophytes increase herbivore resis-  
3956 tance in the woodland grass *brachypodium sylvaticum*. *Oecologia* **126**, 522–530  
3957 (2001).

- [41] Decunta, F. A., Pérez, L. I., Malinowski, D. P., Molina-Montenegro, M. A. & Gundel, P. E. A systematic review on the effects of epichloë fungal endophytes on drought tolerance in cool-season grasses. *Frontiers in plant science* **12**, 644731 (2021). 3957  
3958  
3959  
3960  
3961  
3962  
3963  
3964  
3965  
3966  
3967  
3968  
3969  
3970  
3971  
3972  
3973  
3974  
3975  
3976  
3977  
3978  
3979  
3980  
3981  
3982  
3983  
3984  
3985  
3986  
3987  
3988  
3989  
3990  
3991  
3992  
3993  
3994  
3995  
3996  
3997  
3998  
3999  
4000  
4001  
4002
- [42] Bacon, C. W. & White, J. F. in *Stains, media, and procedures for analyzing endophytes* 47–56 (CRC Press, 2018).
- [43] Rudgers, J. A. & Swafford, A. L. Benefits of a fungal endophyte in elymus virginicus decline under drought stress. *Basic and Applied Ecology* **10**, 43–51 (2009).
- [44] Bultman, T. L., White Jr, J. F., Bowdish, T. I., Welch, A. M. & Johnston, J. Mutualistic transfer of epichloë spermatia by phorbis flies. *Mycologia* **87**, 182–189 (1995).
- [45] Stan Development Team. RStan: the R interface to Stan (2022). URL <https://mc-stan.org/>. R package version 2.21.7.
- [46] Elderd, B. D. & Miller, T. E. Quantifying demographic uncertainty: Bayesian methods for integral projection models. *Ecological Monographs* **86**, 125–144 (2016).
- [47] Gabry, J., Simpson, D., Vehtari, A., Betancourt, M. & Gelman, A. Visualization in bayesian workflow. *Journal of the Royal Statistical Society Series A: Statistics in Society* **182**, 389–402 (2019).
- [48] Brooks, S. P. & Gelman, A. General methods for monitoring convergence of iterative simulations. *Journal of computational and graphical statistics* **7**, 434–455 (1998).
- [49] Gelman, A. & Hill, J. *Data analysis using regression and multilevel/hierarchical models* (Cambridge university press, 2006).
- [50] Williams, J. L., Miller, T. E. & Ellner, S. P. Avoiding unintentional eviction from integral projection models. *Ecology* **93**, 2008–2014 (2012).
- [51] Jones, O. R. *et al.* Rcompadre and rage—two r packages to facilitate the use of the compadre and comadre databases and calculation of life-history traits from matrix population models. *Methods in Ecology and Evolution* **13**, 770–781 (2022).
- [52] .
- [53] Bürkner, P.-C. brms: An R package for Bayesian multilevel models using Stan. *Journal of Statistical Software* **80**, 1–28 (2017).
- [54] Zanne, A. E. *et al.* Three keys to the radiation of angiosperms into freezing environments. *Nature* **506**, 89–92 (2014).

- 4003 [55] Leuchtmann, A., Bacon, C. W., Schardl, C. L., White Jr, J. F. & Tadych,  
4004 M. Nomenclatural realignment of neotyphodium species with genus epichloë.  
4005 *Mycologia* **106**, 202–215 (2014).
- 4006  
4007 [56] Metcalf, C. J. E. *et al.* Statistical modelling of annual variation for inference  
4008 on stochastic population dynamics using integral projection models. *Methods in*  
4009 *Ecology and Evolution* **6**, 1007–1017 (2015).
- 4010  
4011 [57] Caswell, H. Matrix population models: Construction, analysis, and interpretation.  
4012 2nd edn sinauer associates. Inc., Sunderland, MA (2001).
- 4013  
4014 [58] Rees, M. & Ellner, S. P. Integral projection models for populations in temporally  
4015 varying environments. *Ecological Monographs* **79**, 575–594 (2009).
- 4016  
4017 [59] Vandenkoornhuyse, P., Quaiser, A., Duhamel, M., Le Van, A. & Dufresne, A.  
4018 The importance of the microbiome of the plant holobiont. *New Phytologist* **206**,  
4019 1196–1206 (2015).
- 4020  
4021 [60] Rees, M. Evolutionary ecology of seed dormancy and seed size. *Philosophical*  
4022 *Transactions of the Royal Society of London. Series B: Biological Sciences* **351**,  
4023 1299–1308 (1996).
- 4024  
4025 [61] Moles, A. T. & Westoby, M. Seedling survival and seed size: a synthesis of the  
4026 literature. *Journal of Ecology* **92**, 372–383 (2004).
- 4027  
4028 [62] Afkhami, M. E. & Rudgers, J. A. Symbiosis lost: imperfect vertical transmission  
4029 of fungal endophytes in grasses. *The American Naturalist* **172**, 405–416 (2008).
- 4030  
4031 [63] Brown, A. & Akçay, E. Evolution of transmission mode in conditional mutualisms  
4032 with spatial variation in symbiont quality. *Evolution* **73**, 128–144 (2019).
- 4033  
4034 [64] Bruijning, M., Henry, L. P., Forsberg, S. K., Metcalf, C. J. E. & Ayroles, J. F.  
4035 Natural selection for imprecise vertical transmission in host–microbiota systems.  
*Nature ecology & evolution* **6**, 77–87 (2022).
- 4036  
4037 [65] Leuchtmann, A. & Clay, K. in *The population biology of grass endophytes* 185–202  
4038 (Springer, 1997).
- 4039  
4040 [66] Lange, C. *et al.* Impact of intraspecific variation in insect microbiomes on host  
4041 phenotype and evolution. *The ISME journal* **17**, 1798–1807 (2023).
- 4042  
4043 [67] Jeschke, J. M. & Kokko, H. The roles of body size and phylogeny in fast and  
4044 slow life histories. *Evolutionary Ecology* **23**, 867–878 (2009).
- 4045  
4046 [68] Quintana-Ascencio, P. F., Menges, E. S., Cook, G. S., Ehrlé, J. & Afkhami,  
4047 M. Drivers of demography: Past challenges and a promise for a changed future.  
*Demographic Methods across the Tree of Life; Salguero-Gómez, R., Gamelon, M.*,  
4048 *Eds* 115–129 (2021).

- [69] Evers, S. M. *et al.* Lagged and dormant season climate better predict plant vital rates than climate during the growing season. *Global Change Biology* **27**, 1927–1941 (2021). 4049  
4050  
4051  
4052  
4053  
4054  
4055  
4056  
4057  
4058  
4059  
4060  
4061  
4062  
4063  
4064  
4065  
4066  
4067  
4068  
4069  
4070  
4071  
4072  
4073  
4074  
4075  
4076  
4077  
4078  
4079  
4080  
4081  
4082  
4083  
4084  
4085  
4086  
4087  
4088  
4089  
4090  
4091  
4092  
4093  
4094